Perception and decision making in vehicle following: modelling, calibration, validation and simulation

Author:
Li, Chenyang

Publication Date:
2018

DOI:
https://doi.org/10.26190/unsworks/3539

Perception and Decision Making in Vehicle Following: Modelling, Calibration, Validation and Simulation

Chenyang Li

A thesis in fulfilment of the requirements for the degree of

Doctor of Philosophy

School of Civil and Environmental Engineering

Faculty of Engineering

September 2018

THE UNIVERSITY OF NEW SOUTH WALES

Thesis/Dissertation Sheet

Surname/Family Name	:	**Li**
Given Name/s	:	**Chenyang**
Abbreviation for degree as give in the University calendar	:	**CVEN1630**
Faculty	:	**Faculty of Engineering**
School	:	**School of Civil and Environmental Engineering**
Thesis Title	:	**Perception and Decision Making in Vehicle Following: Modelling, Calibration, Validation and Simulation**

Abstract 350 words maximum: (PLEASE TYPE)

Driving brings great convenience and efficiency to people's daily travel. On the other hand, possible road crashes while driving pose a great challenge to the safety of road users. More insights into human driving behaviour are needed to improve driving safety. As the key part of driving behaviour, vehicle following, characterised by the interaction between a vehicle and its leader in a single-lane roadway, has been extensively studied for more than sixty years. However, perception and decision making have seldom been mathematically incorporated in dominant methods of vehicle following modelling. The investigation of these two components is expected to expand the knowledge boundary regarding human driving behaviour. Specifically, perception of traffic dynamics and risk perception are introduced as the representation of perception while decision theory under risk and risk attitudes are incorporated for modelling decision making.

After the microscopic modelling of perception and decision making in single-lane vehicle following, the flow-density relation is also derived. Through macroscopic sensitivity analysis, a more risk-averse attitude, the perception of a more severe crash, a greater standard deviation of perceived time headway, a longer time interval for calculating the future speed and a longer vehicle length are found to lower the capacity of traffic facilities and cause more congestion in macroscopic traffic. The model calibration and validation are performed against the vehicle-trajectory data that were collected at a freeway section of I-80 Emeryville. It is found that drivers when following a car show a more accurate and stable time-headway perception than following a truck. Truck drivers tend to have a more stable time-headway perception and less risk aversion than car drivers. When following a different type of vehicle, drivers are shown to perceive a more severe crash. Subsequently, the comparison between the predicted space headway and the observed value of the validation validate the effectiveness of the proposed model and the relevant findings. The simulation based on the proposed vehicle following model is also presented. Based on the mixed error measurement, the simulation presents a reasonably accurate reproduction of the observed traffic dynamics of the study area.

ORIGINALITY STATEMENT

'I hereby declare that this submission is my own work and to the best of my knowledge it contains no materials previously published or written by another person, or substantial proportions of material which have been accepted for the award of any other degree or diploma at UNSW or any other educational institution, except where due acknowledgement is made in the thesis. Any contribution made to the research by others, with whom I have worked at UNSW or elsewhere, is explicitly acknowledged in the thesis. I also declare that the intellectual content of this thesis is the product of my own work, except to the extent that assistance from others in the project's design and conception or in style, presentation and linguistic expression is acknowledged.'

Signed ……………………………………………..............

Date ……………………18/09/2018……………..............

ABSTRACT

Driving is one of the most widely used human skills today. Most people who drive received their licence and began driving in their teens. Driving brings great convenience and efficiency to people's daily travel. On the other hand, possible road crashes while driving pose a great challenge to the safety of road users. More insights into human driving behaviour are needed to improve driving safety.

As the key part of driving behaviour, vehicle following, characterised by the interaction between a vehicle and its leader in a single-lane roadway, has been extensively studied for more than sixty years. However, perception and decision making have seldom been mathematically incorporated in dominant methods of vehicle following modelling, therefore without the corresponding calibration, validation and simulation exercises. In addition, the heterogeneity in drivers' perception and decision making under different types of vehicle following situations are rare to explore.

Since perception and decision making are two important components of the decision process of vehicle following, the investigation of these two components is expected to expand the knowledge boundary regarding human driving behaviour. Specifically, perception of traffic dynamics and risk perception are introduced as the representation of perception while decision theory under risk and risk attitudes are incorporated for modelling decision making.

Time headway is a traffic quantity that drivers usually rely on to measure the gap from the leading vehicle. Since time headway has been shown to be stable for an individual driver and heterogeneous among different drivers, time-headway perception is used by the study of this thesis to investigate drivers' heterogeneity in perception of traffic dynamics.

Risk perception is a human factor that depends upon individual characteristics and the type of risk. Slovic and Weber (2002) described risk perception as the representation of the probability and severity of risk in one's mind. Both the probability and severity of crash are shown to have an impact on drivers' speed choices (Humphrey, 1998, Ward et al., 1998, Christensen and Amundsen, 2005). To explore drivers' heterogeneity in risk perception under different vehicle following situations, the study of this thesis models risk perception from the two aspects: perceived crash probability and perceived crash severity. Since risk perception is essentially an internal activity of human brains, it is quite difficult for transport researchers to observe directly. The study of this thesis therefore derives the perceived crash probability from the probability distribution of perceived time headway and represents the perceived crash severity with the perceived crash severity factor that is embedded into the crash disutility function.

Decision making in vehicle following is hypothesised to be an individual decision making under risk within the scope of this thesis. As one of the classical theories for decision making under risk, state-dependent expected utility theory is used as a modelling framework for decision making in vehicle following. The existing literature of vehicle following modelling displays no application of state-dependent expected utility theory. State-dependent expected utility theory consists of two core concepts: subjective probability and state-dependent utility. The study of this thesis therefore utilises these two features to characterise probabilities and utility functions in two states of vehicle following, i.e., staying safe and crashing into the leading vehicle.

Risk attitudes refer to the subjective appraisal of the consequences of decisions under risk. Many transport studies have improved model predictions by successfully incorporating risk attitudes. However, risk attitudes have seen the limited application to modelling decision making in vehicle following. Hence, the vehicle following model that explicitly incorporates drivers' risk attitudes is developed. Moreover, the constant relative risk aversion model is used for measuring individual risk attitudes.

After the microscopic modelling of perception and decision making in single-lane vehicle following, the flow-density relation is also derived. Through macroscopic sensitivity analysis, a more risk-averse attitude, the perception of a more severe crash, a greater standard deviation of perceived time headway, a longer time interval for calculating the future speed and a longer vehicle length

are found to lower the capacity of traffic facilities and cause more congestion in macroscopic traffic.

The model calibration and validation are performed against the vehicle-trajectory data that were collected at a freeway section of I-80 Emeryville, California, the U.S. To investigate the proposed model in four types of vehicle following, the vehicle-trajectory data are segmented into four corresponding sub-datasets: Car follows Car, Car follows Truck, Truck follows Car, and Truck follows Truck. Each sub-dataset is randomly separated into a calibration set (70%) and a validation set (30%). The calibration results are obtained by using a nonlinear least-squares method written in Stata (statistical analysis software). It is found that drivers when following a car show a more accurate and stable time-headway perception than following a truck. Truck drivers tend to have a more stable time-headway perception and less risk aversion than car drivers. When following a different type of vehicle, drivers are shown to perceive a more severe crash. Subsequently, the predicted space headway is compared with the observed value of the validation sets in terms of RMSE, R-squared of y=x fit, kernel density, and deviation histogram. The comparison results validate the effectiveness of the proposed model and the relevant findings.

The simulation based on the proposed vehicle following model is also presented. The comparison of the simulated and observed traffic dynamics of the study area is conducted in terms of flow, space mean speed and time mean speed. The

input-output flow of the simulation and the field observation is also compared. Based on the mixed error measurement, the simulation presents a reasonably accurate reproduction of the observed traffic dynamics of the study area. The simulated traffic states of the before- and after-on-ramp section of the study area are analysed through fundamental diagrams. It is found that lane 1 (HOV lane) for both sections is in free-flow traffic state while lane 2-6 are in distinct congested state during 5:15 p.m. to 5:30 p.m. In addition, the before-on-ramp section displays a smooth transition from the free-flow state to the congested state in the fundamental diagrams. As for the after-on-ramp section, some scattered points emerge in the fundamental diagrams. The occurrence of these scattered points results from traffic disruption caused by the merging vehicles originating from the on-ramp.

Within the scope of vehicle following research, the study of this thesis bridges the gap in the existing literature that shows a lack of attention to perception and making in the decision process of vehicle following. Within the scope of transport research, the study of this thesis develops a fundamental modelling framework for unifying traffic operations and safety analysis both microscopically and macroscopically. Besides the accurate reproduction of traffic dynamics, the proposed model has the potential of interpreting risky driving behaviour and identifying dangerous driving spots when utilised for safety analysis. In addition, the proposed model provides an opportunity to evaluate the impacts of traffic management and road environment on drivers' perception and decision making.

Apart from transport, the study of this thesis has a promising application to insurance field. Real-time insurance which changes the insurance premiums based on driver performance does affect driving behaviour. The modelling framework proposed in the study of this thesis therefore would facilitate the evaluation of such real-time insurance policies.

ACKNOWLEDGEMENTS

First of all, I would like to express my gratitude to my main supervisor Dr Vinayak Dixit for his academic and financial support throughout my research. Many thanks to him for trusting me and providing all the research resources I needed. Furthermore, the insightful guidance and the research freedom he provided are highly appreciated.

Secondly, I am grateful to my co-supervisor Dr Taha Rashidi for his precious advice to my research. I would also like to thank people from rCITI, including Dr Zhitao Xiong, Dr Sisi Jian, Dr Xiang Zhang, Dr Neeraj Saxena, Dr David Arbis, Dr Kasun Wijayaratna, Dr Tao Wen, Xun Li, Edward Robson, Nan Nathen Chen, Navreet Virdi, Amarin Siripanich and R.K.M. Prasanga, for their valuable assistance to my research and study. I also want to thank my friends Dr Lifu Sheng, Huan He, Dr De Zhao, Jin Dang and Hao Luo for their help and company.

Lastly, I would like to dedicate my greatest gratitude to my parents and grandmother. Thank them for their selfless devotion and teaching me never give up even in the tough time. Huge thanks to my wife Ying Han for her constant support and encouragement since we first met in 2008.

TABLE OF CONTENTS

LIST OF TABLES

LIST OF FIGURES

CHAPTER 1. INTRODUCTION

1.1 Background Review

More people have realised the enormous impacts of road crashes on economy and society as the government becomes more proactive in raising public awareness of road safety. An example of such is the Australian “Towards Zero” campaign. In Australia, road crashes lead to the economic cost of around 27 billion AUD per annum as well as the devastating social impacts that are hard to estimate (Australian Government, 2017).

A predominant proportion of road traffic accidents are motor vehicles involved. According to road crash statistics for the year 2016 in New South Wales, Australia (Transport for NSW, 2017), there are 15026 car-involved crashes, accounting for 84.5% of total casualty crashes and overwhelmingly outnumbering other crash types. This is followed by 3494 crashes with light truck involved. A significant proportion of road traffic casualties are likewise attributed to the involvement of motor vehicles. Of 22593 total crash casualties in 2016 within New South Wales of Australia, 19403 casualties are caused by the car-involved crash, accounting for 85.9%. The successor is still light-truck-involved crash causing 4634 casualties. Unsurprisingly, car-involved and light-truck-involved crashes lead to the first and second largest numbers of fatalities with 249 and 101 killed, respectively.

1.2 Motivations

The degree of the motor vehicle involvement in road traffic accidents motivates scientific investigation into driving safety. As the key part of driving behaviour, vehicle following (also known as car following) behaviour is at the core of driving safety research. Vehicle following behaviour, characterised by the interaction between a vehicle and its leader in a single-lane roadway, has been studied extensively for more than sixty years ever since the study by Pipes (1953). However, drivers' perception of traffic dynamics has seldom been mathematically specified in dominant methods of vehicle following modelling. There is also rare empirical calibration and validation against field observations. The study by Hamdar et al. (2008) introduces a novel direction by incorporating the heterogeneity of perception of the leading vehicle's speed in modelling vehicle following. It leaves considerable research potential for exploring drivers' perception of other aspects of traffic dynamics, such as distance and time headway.

Human decision-making research has made substantial progress ever since the ground-breaking work by Bernoulli (1738). Decision theory provides a solid foundation for studying human decision in many domains such as economics, psychology and insurance. In recent years, decision theory has drawn growing attention in driving safety studies (Dixit, 2013, Dixit et al., 2014, Talebpour et al., 2011, Hamdar et al., 2015). As the core part of driving safety research, vehicle following behaviour describes how drivers make choices of speed while following a vehicle, hence is worth studying from the decision-theoretic perspective. Nevertheless, vehicle following behaviour has seen insufficient modelling effort within the decision-theoretic framework. Furthermore, Hamdar et al. (2008) identified that the modelling of the decision process is missing from existing vehicle following studies. This is exactly where decision theory would play a significant role. State-dependent expected utility theory proposed by Karni et al. (1983) and refined by Karni (1985) is a powerful decision-theoretic framework for weighing alternatives under risk. State-dependent expected utility theory includes two core concepts: subjective probability and state-dependent utility. The subjective probability measures the degree of drivers' belief with regard to the likely states while the state-dependent utility represents the degree of satisfaction with respect to consequences in certain states.

Vehicle following is inherently a risky driving task. Drivers need to anticipate the risk of crashing even in safe situations as road crashes may occur at any time. Therefore, studying vehicle following behaviour in the presence of crashing risk is of more practical significance. Specifically, drivers' attitudes and perception of crashing risks would affect their vehicle following behaviour in terms of speed choices. Such risk attitudes and risk perception are influenced by both drivers and road characteristics (Ulleberg and Rundmo, 2003, Farrow and Brissing, 1990, Jonah, 1986, Dixit, 2013, Tarko, 2009). A better understanding of risk attitudes and risk perception would help interpret risky vehicle following behaviours (e.g., tailgating) and identify dangerous vehicle following situations (e.g., following a truck). The studies by Dixit et al. (2011) and Arbis et al. (2016) are the two pioneers that jointly estimate risk attitudes and risk perception from simulator-based driving experiments. Specifically, Dixit et al. (2011) studied turning gap choice behaviour while Arbis et al. (2016) investigated an intersection-crossing game between two drivers. To the best of the author's knowledge, risk attitudes and risk perception in real-life vehicle following have not yet been fully studied.

Risk perception is a mental representation of the potential threat associated with an action, activity or situation (Bijkerk, 2007). Slovic and Weber (2002) stated that two key factors of risk perception are the extent to which a potential danger is dreadful (i.e., the severity of risk) and the extent to which it is unknown (i.e., the probability of risk). The risk associated with vehicle following refers to the rear-end crash that may occur. According to the statement of Humphrey (1998) with the support of Ward et al. (1998) along with Christensen and Amundsen (2005), both the probability and severity of a crash have an impact on drivers' speed choices.

Risk attitudes (namely risk aversion in the context of economics) refer to the subjective appraisal of the consequences of decisions under risk. People with different risk attitudes view the consequences in different ways. Specifically, an agent possesses: risk aversion if his/her utility function is concave (i.e., the payoff associated with a risky alternative is considered to be less valuable by this person); risk-seeking attitude if the utility function is convex (i.e., the payoff of a risky alternative is considered to be more valuable); and risk neutrality if he/she has a linear utility function (i.e., risk of an alternative doesn't affect the subjective appraisal of its payoff). The constant relative risk aversion model, proposed by Friedman and Savage (1948), is one of the most commonly used tools for capturing individual risk attitudes. The constant relative risk aversion model has been shown to be a more plausible specification of individual risk attitudes than any other types of utility functions (Blanchard and Fischer, 1989, Wakker, 2008, Camerer and Ho, 1994), and been widely applied to various fields of study such as behavioural economics (Holt and Laury, 2002, Palacios-Huerta and Serrano, 2006, Harrison and Rutström, 2009, Tversky and Kahneman, 1992, Andersen et al., 2009), financial option (Henderson and Hobson, 2002), sociology (Harrison et al., 2007), psychology (Luce and Krumhansl, 1988) and health science (Bleichrodt et al., 1999). Many transport studies have successfully investigated the effect of risk attitudes on travel time variability (Hensher et al., 2011, Li et al., 2012), turning gap choices (Dixit et al., 2014, Dixit et al., 2011), intersection manoeuvre choices (Arbis et al., 2016), route choices (Dixit et al., 2015, Dixit et al., 2013), public transit choices (Rey et al., 2016) and evacuation departure choices (Dixit et al., 2012) by using the constant relative risk aversion model. Despite the vast amount of the application of risk attitudes within transport research and beyond as well as its significance of improving model prediction against reality, the existing literature lacks the introduction of risk attitudes into modelling the decision process of vehicle following.

1.3 Aims

The study of this thesis aims to:

- develop a vehicle following model incorporating perception of traffic dynamics, risk perception, decision theory under risk, and risk attitudes;

- introduce the time-headway perception as the subjective representation of traffic dynamics;

- utilise perceived crash probability and perceived crash severity to account for risk perception;

- take state-dependent expected utility theory as the modelling framework, and utilise subjective probability and state-dependent utility to characterise probabilities and utility functions in two states of vehicle following, i.e., staying safe and crashing into the leading vehicle;

- adopt the constant relative risk aversion model to model drivers' risk attitudes;

- process the real-life vehicle trajectory data using the techniques of smoothing, filling, filtering and segmentation;

- calibrate the vehicle following model using a nonlinear least-squares method written in Stata (statistical software) by Danuso (1992) and Royston (1993) and 70% of the entire processed data;

- validate the vehicle following model using the rest of the entire processed data (i.e. 30%); and

- implement simulation exercise in Aimsun (traffic simulation software) based on the vehicle following model and the parameter estimates of the calibration.

1.4 Contributions

Rothery (1992) presented a complete decision process of the single-lane vehicle following illustrating the sub-processes and their interrelation, as shown in Figure 1.1. The decision process provides a comprehensive framework for the discussion of this thesis and for locating the contributions of this thesis within the research of vehicle following.

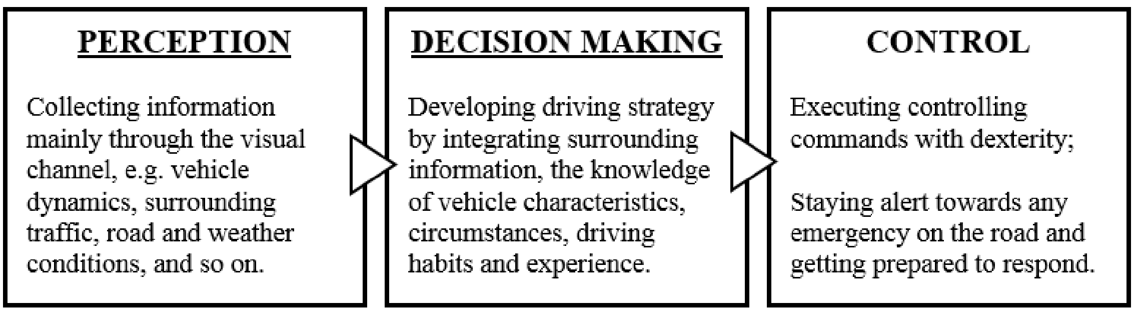

Figure 1.1 Decision process of single-lane vehicle following (Rothery, 1992)

Perception and decision making, underlined in Figure 1.1, are two sub-processes that the study of this thesis focuses on. The research gap in perception of vehicle following is the insufficient mathematical specification and empirical calibration of drivers' perception (especially perception of traffic dynamics). Another lacuna lies in the decision making of vehicle following, showing the lack of theoretic variation in decision-theoretic modelling. The author of this thesis believes investigating advancements to these two components would bring novel research insights to decision-theoretic modelling of vehicle following.

The presence of crash risk is critical in characterising the decision process of vehicle following. The consideration of risk in perception and decision making brings about the inclusion of risk perception and risk attitudes, respectively. These two risk attributes are the subjective appraisal of the probabilities and consequences of risks. They advance decision theoretic modelling by taking into account the presence of risk and quantifying the impact of risk on human perception and decision making. The literature on risk perception and risk attitudes demonstrates their significance within various research areas of decisions under risk and their absence in the vehicle-following context. The author of this thesis thus expects they are of the similar significance in modelling the decision process of vehicle following.

The study of this thesis mainly deals with two components in the decision process of vehicle following underlined in Figure 1.1, which are perception and decision making. It should be noted that perception and decision making are interrelated instead of being independent of each other. While following the leader, a driver will perceive the surroundings to collect information (e.g. space headway, time headway and speed), then make a speed decision based on the information. Therefore, perception is the first step of the decision process of vehicle following. Following that, it comes to decision making. Drivers' perception is studied through the perception of traffic dynamics and risk perception while decision making is incorporated by using decision theory under risk and risk attitudes. This is the domain of this thesis illustrated in Figure 1.2 for a better overview.

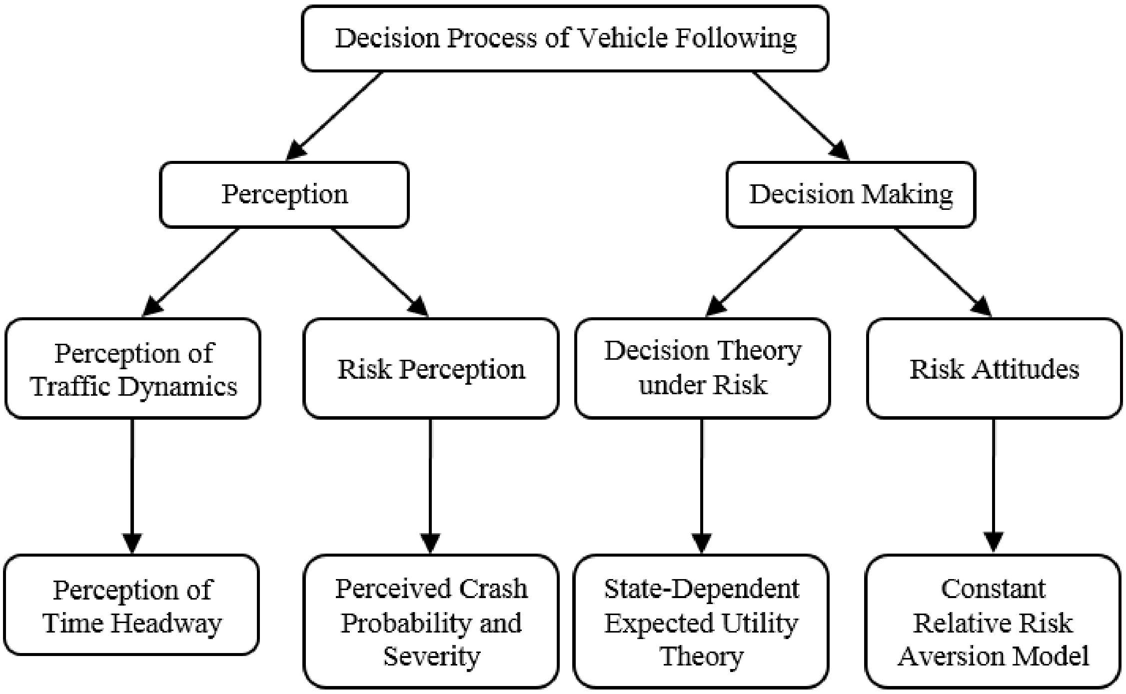

Figure 1.2 Overview of the domain of this thesis

1.5 Thesis Organisation

The rest of this thesis is organised as follows.

Chapter 2 reviews previous vehicle following literature and identifies the research gap in perception and decision making. Literature regarding the perception of traffic dynamics, risk perception, risk attitudes and decision theory under risk displays a lack of application to modelling vehicle following.

Chapter 3 presents the theoretical framework of modelling perception and decision making in vehicle following, introduces the underlying assumptions of the modelling, mathematically formulates the vehicle following model incorporating perception and decision making, and derives the corresponding flow-density relation. Macroscopic sensitivity analysis of model parameters and variable is also performed.

Chapter 4 describes the vehicle-trajectory data used for calibration and validation, introduces the techniques used for processing the original data, calibrates the model parameters in different vehicle following situations by using the vehicle-trajectory data, and validates the proposed model by comparing the predicted space headway with the observed counterpart in terms of RMSE, R-squared of y=x fit, kernel density, and deviation histogram.

Chapter 5 describes the simulation exercise based on the proposed vehicle following model implemented in Aimsun, and analyses the simulated and observed traffic dynamics of the study area in terms of flow, space mean speed and time mean speed. The input-output flow of the simulation and the field observation is also compared. The simulated traffic states of the before- and after-on-ramp sections of the study area are discussed through fundamental diagrams.

Chapter 6 summarises the work of this thesis, elaborates the key findings and conclusions for each main chapter, highlights the academic contributions and the promising application of the research of this thesis, and discusses the future research directions.

CHAPTER 2. LITERATURE REVIEW

2.1 Introduction

Most literature on the decision process of driving adopts decision theory under risk, in which an agent must make decisions in an uncertain environment, and the outcome would be either gains or losses. The hypothesis is likewise suitable for vehicle following behaviour as drivers make choices of the following speed and end up staying safe or crashing. A better understanding of decision making in vehicle following enhances safety evaluations of road user and infrastructure. As an inherent part in driving behaviour, decision process performs an important role in driving safety analysis. In recent years, decision-theoretic modelling has received growing focus in driving safety literature (Dixit, 2013, Dixit et al., 2014, Talebpour et al., 2011, Hamdar et al., 2015).

However, prior research has seen limited developments in decision-theoretic modelling of vehicle following. In particular, Hamdar et al. (2008) pointed out the investigation of drivers' decision process is missing from previous studies. It provides a promising direction for improving driving behavioural models and analysis of driving safety. The author of this thesis believes explicitly modelling the decision process is the key to enhancing safety analysis of vehicle following.

Perception and decision making, underlined in Figure 1.1, are the two decision sub-processes of vehicle following that the study of this thesis puts emphasis on. They are thus used as the subheadings of literature review.

2.2 Perception in Vehicle Following

In the decision process of vehicle following by Rothery (1992), shown in Figure 1.1, there are two critical components that decision-theoretic modelling relies on: perception and decision making. Each of the two plays an important role in model formulation and research findings obtained. Perception in vehicle following has become an indispensable component as human factors have seen increasing attention from driving safety research. In particular, the perception of traffic dynamics and risk perception have developed from being overlooked in the early studies, to receiving a wide range of investigations.

2.2.1 Perception of Traffic Dynamics

On reviewing road traffic accidents occurred in the United Kingdom during 1987, Brown (1990) summarised perceptual problems (e.g., misperception of speed and headway) are one of the most contributory human factors, accounting for about 25% of accidents. It necessitates the consideration of human perception in driving behavioural modelling.

The incorporation of perception of traffic dynamics has been rare in the early vehicle following literature (Chandler et al., 1958, Herman et al., 1959, Gazis et al., 1959, Gazis et al., 1961, Herman and Rothery, 1965, Kometani and Sasaki, 1959, Newell, 1961). In the late of 1950s, for instance, the General Motor models by Chandler et al. (1958), Gazis et al. (1959) and Herman et al. (1959) assume driving responses in vehicle following are closely associated with the stimulus (e.g. difference in speeds or headways) stemming from the leading vehicle. With this hypothesis, they proposed the stimulus-response relationship describing vehicle following behaviour, as shown in Equation [2.1] (Saifuzzaman and Zheng, 2014).

$$Response = Sensitivity \times Stimulus \qquad [2.1]$$

In the stimulus-response relationship, Chandler et al. (1958) and Herman et al. (1959) defined stimulus as the actual speed difference between the leading vehicle and the following vehicle, in which possible errors due to human perception are unrecognised.

As vehicle following modelling gains the influence of behavioural realism, many studies got started to recognise the perceptual dimension. Wiedemann (1994) proposed 'psychophysical' models by introducing the concept of 'perceptual threshold' to vehicle following modelling. The perceptual threshold is used to determine the perceptual minimum of drivers with regard to the stimulus (e.g., speed difference and spacing relative to the leading vehicle). Michaels (1963) stated drivers' perception of stimuli while following the leader is identified with the changes in the visual angles towards the leading vehicle. He calculated the visual angle and angular velocity to substitute spacing and relative speed in the conventional stimulus-response models, respectively. Subsequently, Andersen and Sauer (2007) and Jin et al. (2011) adopted visual angle to modify desired spacing model (Helly, 1959) and full velocity difference model (Jiang et al., 2001) that both follow the stimulus-response hypothesis, respectively.

However, drivers' perception of traffic dynamics has not been mathematically specified in decision-theoretic modelling of vehicle following, let alone empirical calibration and validation against field observations.

Until the seminal study by Hamdar et al. (2008), drivers' perception of the leaders' velocity is assumed to follow a normal distribution with the actual speed of the leading vehicles as the mean value. Subsequent studies inheriting the theoretical framework by Hamdar et al. (2008) have performed empirical calibration and practical validation against observations of vehicle following behaviour (Hamdar et al., 2009, Hamdar et al., 2015). The study by Hamdar et al. (2008) introduces a novel direction by incorporating the heterogeneity of drivers' perception in modelling vehicle following. It also leaves considerable research potential for exploring drivers' perception of other aspects of traffic dynamics, such as distance and time headway.

This thesis thus introduces the time-headway perception as the subjective representation of traffic dynamics in decision-theoretic modelling of vehicle following. The deviation of perception from the reality is statistically revealed by calibration against field trajectory data.

2.2.2 Risk Perception

Risk perception is a mental representation of the potential threat associated with an action, activity or situation (Bijkerk, 2007). Risk perception is also a human factor that depends upon individual characteristics and the type of danger. Risk perception in the driving context has been extensively investigated in previous research (Finn and Bragg, 1986, DeJoy, 1992, Brown and Groeger, 1988, Matthews and Moran, 1986), and been shown to have an influence on driving behaviour (Grayson and Groeger, 2000, Grayson et al., 2003).

Literature exhibits two approaches to investigating risk perception which stem from different theoretical backgrounds. Under the theories of risk homeostasis (Wilde, 1982a, Wilde, 1982b, Trimpop, 1996, Vrolix, 2006, Malnaca, 2008, Lu et al., 2012, Lu et al., 2013), risk compensation (Dulisse, 1997, Taylor, 1964), behavioural adaptation (Hoedemaeker and Brookhuis, 1998, Jonah et al., 2001, Reinhardt-Rutland, 2001, Charlton and Lewis-Evans, 2006, Lewis-Evans and Charlton, 2006) and risk adaption (Koornstra, 2009), risk perception is used as an index that measures the magnitude of the risk perceived by people. Risk perception in the driving context is usually quantified by surrogate indicators such as stated concern about traffic accidents (Rundmo and Iversen, 2004), stated crash probability (Arbis et al., 2016), safety margin (Lu et al., 2012), time-to-collision and time headway (Kondoh et al., 2008). With this method, researchers have studied risk perception among elderly drivers (Siren and Kjær, 2011), adolescent drivers (Ulleberg and Rundmo, 2003, Rundmo and Iversen, 2004), SUV and car drivers (Thomas and Walton, 2007) as well as French and Dutch drivers (Bijkerk, 2007). Despite the significance of this approach, the following one is developed to interpret risk perception from the decision-making perspective explicitly.

The second approach describes risk perception as the representation of the probability and severity of risk in one's mind. This complies with the statement by Slovic and Weber (2002) that two key factors of risk perception are the extent to which a potential danger is dreadful (i.e., the severity of risk) and the extent to which it is unknown (i.e., the probability of risk). To be specific, the risk associated with vehicle following refers to the rear-end crash that may occur. According to the statement of Humphrey (1998) with the support of Ward et al. (1998) along with Christensen and Amundsen (2005), both the probability and severity of crash have an impact on drivers' speed choices. The study of this thesis thus takes risk perception into account from the following two aspects: the perceived probability and perceived severity of a crash.

Many transport studies have practised the inclusion of the perceived probability and perceived severity of crash into driving behavioural modelling. Hamdar et al. (2008) derived the perceived crash probability (i.e., the subjective crash probability in Hamdar et al.'s statement) from the stochasticity of drivers' perception of traffic dynamics which has been covered in Section 2.2.1. As for the perceived crash severity, Hamdar et al. (2008) assumed that it corresponds to a crash seriousness term weighted by the coefficient of sensitivity to crash loss which is embedded into the crash disutility function. In the latest version of their model, Hamdar et al. (2015) replaced it with the crash severity weighting factor. Dixit et al. (2014) explored drivers' risk perception using the data collected from standard lottery choices (Holt and Laury, 2002) and the gap-selection-and-turning experiment in a controlled virtual-reality lab environment. The gap-choice experiment is to let the subject choose a gap in ten gaps of oncoming traffic in ascending order of size and then make a turn. There are two possible outcomes which are mutually exclusive and collectively exhaustive: crashing or turning successfully. Risk perception is represented by the perceived crash probability which is assumed to follow the Weibull distribution as a function of gap size in seconds. They found that drivers who crash perceive less crash risk (i.e., smaller perceived crash probability) than those who do not crash regardless of driving skills. With the similar methodology to Dixit et al. (2014), Arbis et al. (2016) investigated the interaction between two drivers at a signalised intersection from a game-theoretic perspective. The experimental setup is that one driver is approaching the intersection when the signal is going to turn red, while the other is stopping in front of the intersection waiting for the green signal. In this conflicting situation, there are two options for each driver: drive or wait. The perceived crash probability is formulated as a function of crash likelihood parameter in a standard logistic form. The parameter of crash likelihood is estimated using the data collected from the Holt and Laury lottery choice task (Holt and Laury, 2002) and the intersection-manoeuvre experiment. Their finding is in accordance with that reported by Dixit et al. (2014): drivers who crash ignore more crash risk than those who drive safely. Tarko (2009) incorporated crash risk perception, together with subjective time value and speed enforcement, into the trip disutility function. There is a trade-off between a higher speed (i.e., less travel time and more time saved) and the perceived risks of crashing and receiving a speeding ticket. On the basis of the meta-analysis of actual risks by Elvik et al. (2004), Tarko (2009) defined crash risk perception as a function of road characteristics and speed. With the presence of wide pavements, truck drivers are shown to perceive less crash risk than car drivers. Residential areas and wide lateral clearance have no effect on drivers' crash risk perception. It should be noted that Tarko (2009) didn't specify the so-called perceived crash risk as probability or severity. A subsequent study by Dixit (2013) takes Tarko's perceived crash risk as the measurement of perceived crash severity. Apart from that, he assumed that the perceived probability of a crash is related to the proportion of the average running time per mile in the average travel time per mile. The perceived crash probability monotonically increases with the average running time per mile of vehicles in the urban network. He also assigned parameters to represent the perceived crash likelihood factor (i.e., how a driver perceives the crash likelihood) and the perceived crash severity factors (i.e., the crash impact factor and the crash disutility weighting factor in Dixit's statement). The perceived crash likelihood factor is embedded into the perceived crash probability function, while both the crash impact factor and the crash disutility weighting factor are integrated into the crash disutility function. By using the data of urban traffic network characteristics for various cities from Ardekani et al. (1992), Dixit (2013) analysed the effects of different network features on risk perception. It is found that more one-way streets would lower drivers' perception of crash likelihood, while drivers' perceived crash severity would increase due to less one-way streets, higher signal density, more lanes per street and actuated signals.

Since risk perception is essentially an internal activity of human brains, it is quite difficult for transport researchers to observe directly. Alternatively, risk perception can be either derived from observable transport quantities (e.g., velocity and time headway) or represented by parameters that can be calibrated empirically. The study of this thesis thus derives the perceived crash probability from actual time headway (a probability distribution also assumed) and represents the perceived crash severity with the perceived crash severity factor that is embedded into the crash disutility function.

2.3 Decision Making in Vehicle Following

The field of decision making can be classified according to whether the decision maker is an individual or a group of people (Luce and Raiffa, 2012). The key difference between an individual and a group of people is not a matter of the number of decision makers involved, but all about how decisions are finally made. In the context of vehicle following, drivers are assumed to be an independent decision-maker. In other words, drivers are able to make any speed choices on his/her perception and decision making without caring about what others think. Therefore, the decision making in vehicle following is an individual decision making.

Besides the classification by decision maker, a decision making can also be categorised according to whether decisions are made under conditions of certainty, risk or uncertainty. The certainty-risk-uncertainty classification will be elaborated through some examples.

A decision making is under certainty if one is fully confident about the outcomes of decisions. For instance, one can buy any priced merchandise when shopping. If he/she can afford it, the probability of a successful purchase is 100%. If not, the probability of the purchase is 0%.

A decision making is under risk if a decision does not necessarily result in a certain outcome, which is the reality most of the time. Fortunately, one knows all of the possible outcomes and all of the probabilities related to each outcome. Most of the decision making under risk occurs in the analysis of gambling. For example, in a roulette game, the probability of a ball falling into each number is known even though one cannot tell the winning number before the wheel stops spinning. Another example is randomly tossing a coin with a 50% chance of getting a head or tail.

A decision making is under uncertainty if one does not even know the probability of each possible outcome. Taking an example proposed by Luce and Raiffa (2012), one has already broken five good eggs into a bowl to make an omelette. He/she will break the sixth egg into the bowl. If the egg is in a good state, he/she would manage to make a six-egg omelette. If the egg is rotten and he/she cannot tell it from the appearance, it would end up destroying other five eggs and having no omelette made. In this case, one knows two possible outcomes (good egg or rotten egg). However, how likely each outcome would occur is uncertain. In fact, most of the real-life decision makings are under uncertainty.

Neither decision making under certainty nor decision making under uncertainty is suitable to define the decision making in vehicle following. In contrast, decision making under risk offers the promising potential of modelling vehicle following mathematically, which makes more sense from the research perspective. Hence, the decision making in vehicle following is hypothesised to be an individual decision making under risk within the scope of this thesis.

2.3.1 Decision Theory under Risk

Decision theory under risk is to describe individual decision making under risk. The expected utility hypothesis tracing back to Cramer (1728) and Bernoulli (1738) is the pioneer of decision theory under risk. The Bernoullian expected utility model determines the basic mathematical form of decision theory under risk, i.e., $EU_i = \sum_j^n P_j\, U_j$. For a certain alternative i, n includes all possible outcomes. P_j and U_j denote the probability and the utility associated with each outcome j, respectively. The decision maker would end up choosing the alternative that yields the maximum expected utility EU.

2.3.1.1 Prospect Theory

As a major variant of the Bernoullian expected utility model (Schoemaker, 1982), prospect theory by Kahneman and Tversky (1979) has received a small but growing interest in transport behavioural research (Hamdar et al., 2008, Li and Hensher, 2011, Hamdar et al., 2015, Avineri and Prashker, 2005, Senbil and Kitamura, 2005, Avineri, 2006, Connors and Sumalee, 2009, Talebpour et al., 2011).

Prospect theory evolves the Bernoullian expected utility model by incorporating two functions: value function and probability weighting function. The value function of prospect theory is a utility function that shows concave in the gain domain and convex in the loss domain, reflecting decreasing marginal utility over both gains and losses (i.e., diminishing sensitivity). The asymmetry of the value function between gains and losses is defined as loss aversion which means a loss brings more disutility than the utility of an equivalent gain. The features of diminishing sensitivity and loss aversion can be found in Figure 2.1. The probability weighting function is an inversely S-shaped probability function that underestimates the original probability near certainty and overestimates the original probability near impossibility, reflecting the subjective probability under extreme situations (Figure 2.2). Gains and losses in prospect theory are measured relative to a reference point which serves as the zero point of prospect theoretic utility. Kahneman and Tversky, however, provided little clarification on how the reference point is determined (Barberis, 2013). Kőszegi and Rabin (2006, 2007, 2009) argued the reference point refers to expectations or beliefs of the outcome people held in the recent past.

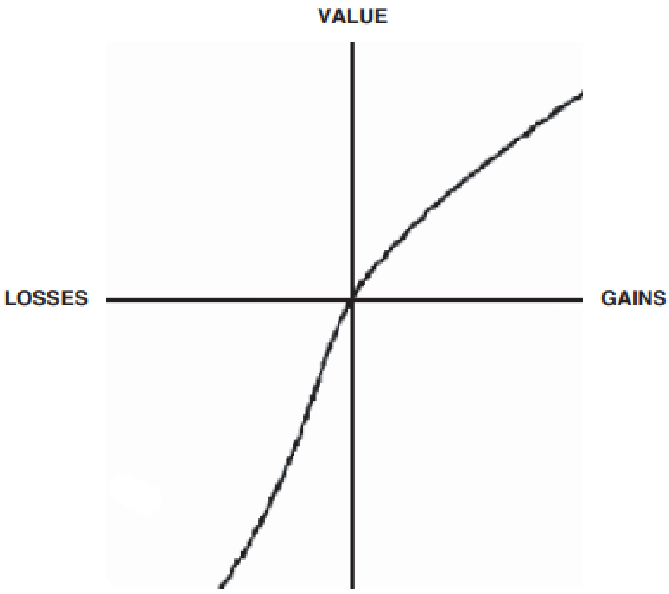

Figure 2.1 Typical value function in prospect theory (Tversky and Kahneman, 1986)

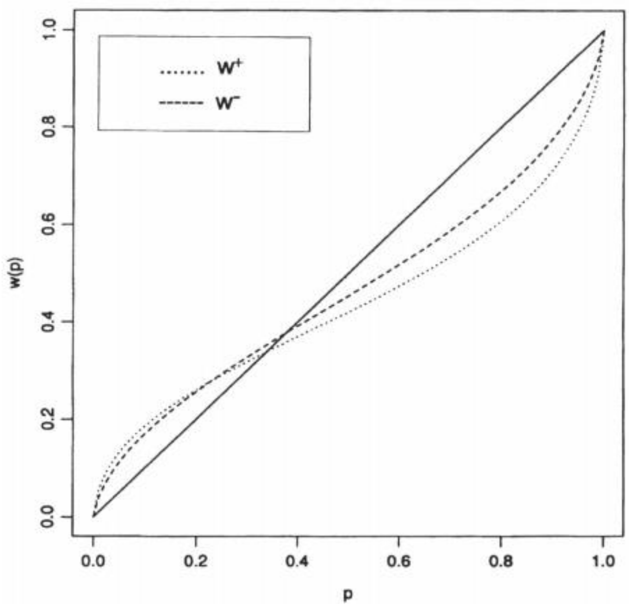

Figure 2.2 Probability weighting functions for gains (w^{+}) and losses (w^{-}) (Tversky and Kahneman, 1992)

Hamdar et al. (2008, 2015) initiated the first application of prospect theory to vehicle following modelling. They developed a value function to evaluate drivers' utility/disutility over gains/losses of acceleration. The concept of probability weighting function is not adopted in the two studies. Hamdar et al. (2008) assumed driver could receive the utility of acceleration gains only if no collision occurs, while Hamdar et al. (2015) relaxed the restriction. Additionally, Talebpour et al. (2011) enriched the value function by proposing a value function for the congested traffic condition and inheriting the value function by Hamdar et al. (2008) for the uncongested condition.

The key assumption within prospect theory is that people derive their utility only from gains and losses (Barberis, 2013). That is, the equal gains/losses under different circumstances still yield the same utility. Following this assumption, Hamdar et al. (2008) defined drivers' utility/disutility over acceleration gains/losses regardless of the speed level. The implication is, for instance, that the utility/disutility of an acceleration gain/loss at the speed of $10\ km/h$ is the same as the one of the equivalent acceleration gain/loss at the speed of $50\ km/h$, which is surely unrealistic. As a result, prospect theory falls short for the analysis of decision process in vehicle following in which the effect of the speed level on utility matters.

2.3.1.2 State-Dependent Expected Utility Theory

State-dependent expected utility theory proposed by Karni et al. (1983) and elaborated by Karni (1985) is another powerful tool for modelling decision process under risk, which defines utility over the final state, including gains/losses and the initial state. In consideration of drivers' diminishing marginal utility of speed, state-dependent expected utility theory is therefore a more plausible approach for modelling decision process in vehicle following than prospect theory.

Karni et al. (1983) developed state-dependent expected utility theory to include two core concepts: subjective probability and state-dependent utility. In the early studies of decision theory by Bernoulli (1738) and Von Neumann and Morgenstern (1947), probability is interpreted as the frequency that a random outcome occurs in repeated trials, which can be discovered empirically or mathematically (Anscombe and Aumann, 1963). This definition, regarded as the objective probability (Hacking, 1984), is not suitable for unique events that cannot be observed in the past (e.g., a third world war and someone being guilty) although it fits well for repetitive events such as spinning a roulette wheel, tossing a coin, rolling a die and winning a prize in a lottery. The notion of the subjective probability comes into being as a necessary complement to the definition of probability, which is advocated by Ramsey (1926), De Finetti (1937, 1974), Koopman (1940), Good (1950), Savage (1954), Davidson and Suppes (1956), Kraft et al. (1959), Pratt et al. (1964) and Suppes (1969). From their perspective, the subjective probability refers to a measure of the degree of one's belief in the likely occurrence of events. Drawing upon the subjective probability and Von Neumann-Morgenstern utility (1947), Savage (1954) proposed a standard analytical framework for decision theory under risk, known as subjective expected utility theory. It consists of three sets: acts, states and consequences. Acts are the alternatives when making decision. States are the states of the world, which are mutually exclusive and jointly exhaustive. Consequences are something that happens to a person in certain states due to the conduct of certain acts. Mathematically, acts are mappings (i.e., functions) that map each state to each consequence. Within this framework, Savage successfully proved the existence of the subjective probability and the Von Neumann-Morgenstern utility function such that the agent's preference among acts can be represented by the maximum subjective expected utility (i.e., the maximum product of the subjective probability and the Von Neumann-Morgenstern utility). Subsequently, Anscombe and Aumann (1963) introduced the state-independence utility function (i.e., the utility function that doesn't vary with the states of the world) to subjective expected utility theory in order to guarantee that the agent's preference among acts is immune from the states of the world. However, it would fall short when the states of the world have an impact on people's preference among acts. For example, one's health condition (i.e., the states of the world) takes an important role in his/her purchase of life insurance policy (i.e., selecting the act preferable to the others). To handle this problem, Karni et al. (1983) proposed a framework for proving that the agent's preference among acts can also be uniquely represented by the maximum product of the state-dependent utility and the subjective probability, namely state-dependent expected utility theory in my statement. The subjective probability measures the degree of belief with respect to the likely states while the state-dependent utility represents the degree of satisfaction with respect to consequences in certain states. Karni (1985, 1987, 1990, 1993a, 1993b) subsequently provided a complete elaboration on state-dependent expected utility theory.

The early application of state-dependent expected utility theory mainly corresponds to the choice of health and life insurance (Karni, 1985, Viscusi and Evans, 1990, Dionne and Harrington, 1992, Kelsey, 1992, Wakker and Zank, 1999, Kremslehner and Muermann, 2009), in which the preference among insurance policies is dependent on health status. It has also received a few interests from transport behavioural research in recent years. Dixit et al. (2012) modelled the evacuation departure choice under hurricane threat to investigate the effect of household demographic characteristics on evacuees' risk attitude, the evacuation time and the preparation time for fighting the storm. He assumed that the set of acts and the set of states are {stay, leave} and {hit, miss} respectively, so that the set of consequences is {stay when hit, stay when miss, leave when hit, leave when miss}. Dixit (2013) proposed a behavioural framework based on state-dependent expected utility model to interpret the classical two-fluid model proposed by Prigogine and Herman (1971) that describes urban traffic flow (Ardekani, 1984, Vo et al., 2007). The utility functions over speed are dependent on two states {crash, no crash}. It should be noted that Section 2.2.2 gives a detailed literature review on the subjective probability (i.e., the perceived probability) in driving behavioural modelling. The existing literature displays no application of state-dependent expected utility model to modelling the decision process of vehicle following, which provides additional motivation for the study of this thesis.

2.3.2 Risk Attitudes

An important property of expected utility hypothesis is risk attitudes (namely risk aversion in the context of economics). It is initially used to describe one's preference between a guaranteed gain and a risky bet with the equivalent expected value. The person is said to be: risk-averse if the guaranteed payoff is preferred; risk-taking if the risky bet is selected; and risk-neutral if he/she is indifferent to the two alternatives. Under expected utility theory, risk attitudes refer to the personal appraisal of the consequences of decisions under risk. People with different risk attitudes view the consequences in different ways. Specifically, an agent possesses: risk aversion if his/her utility function is concave as shown in Figure 2.3a (i.e., the payoff associated with a risky alternative is considered to be less valuable by this person); risk seeking if the utility function is convex as shown in Figure 2.3b (i.e., the payoff of a risky alternative is considered to be more valuable); and risk neutrality if he/she has a linear utility function as shown in Figure 2.3c (i.e., risk of an alternative doesn't affect the subjective appraisal of its payoff).

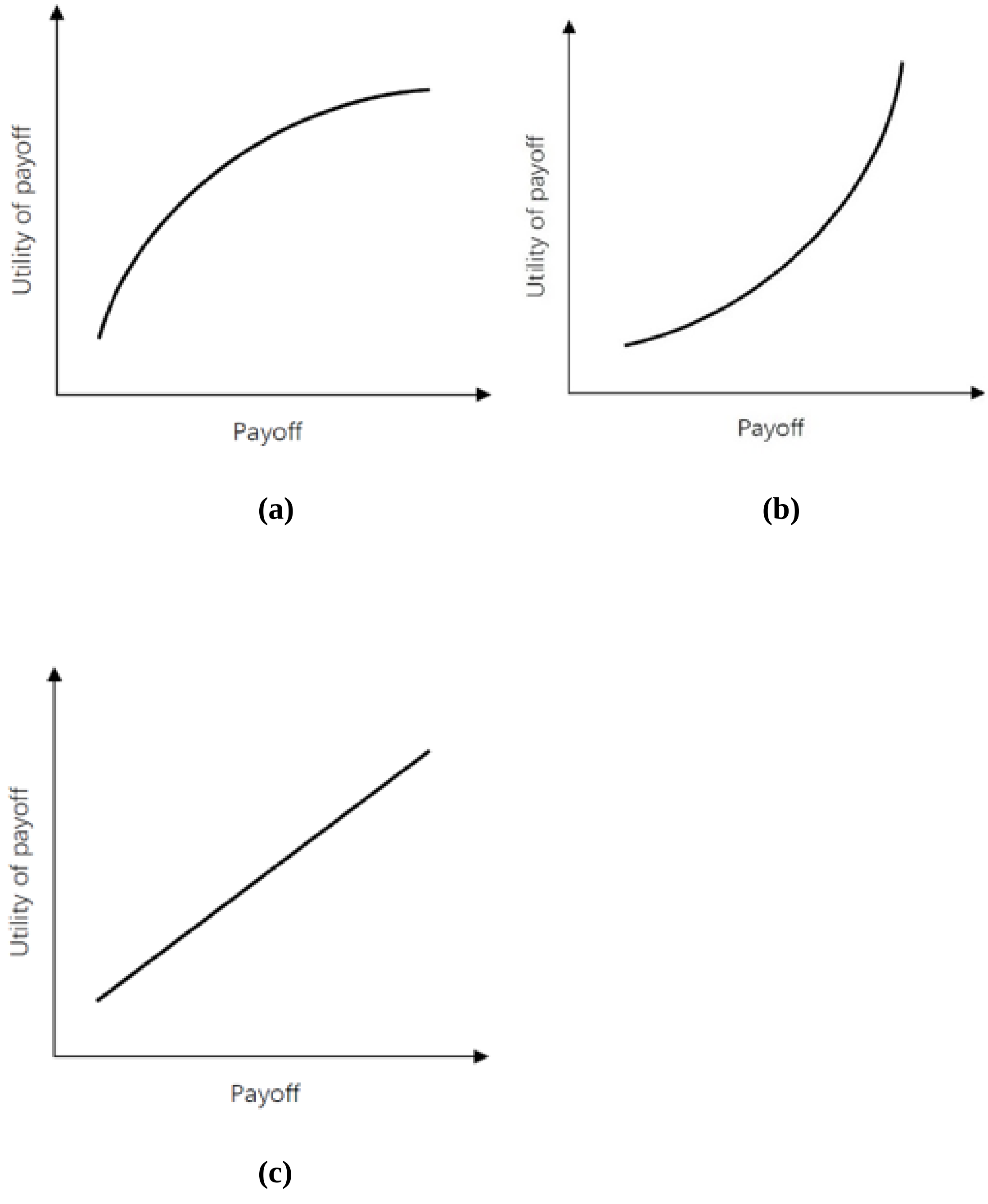

Figure 2.3 Utility functions of three risk attitudes: (a) risk aversion, (b) risk seeking, and (c) risk neutrality

To determine the exact value of risk attitudes, Pratt (1964) and Arrow (1965) proposed two measures of risk attitudes: Arrow-Pratt measure of absolute risk aversion ($-\frac{U''(x)}{U'(x)}$) and Arrow-Pratt measure of relative risk aversion ($-\frac{x*U''(x)}{U'(x)}$), where x is a payoff and $U(x)$ is the utility function of that payoff, along with $U'(x)$ and $U''(x)$ denoting the first and second derivate of the utility function respectively. Each type of risk attitudes measure has three sub-classes: increasing, constant and decreasing absolute/relative risk aversion. From the perspective of forming a portfolio with a risky asset and a riskless asset, the increasing/constant/decreasing absolute risk aversion indicates that one would increase/maintain/decrease the actual amount of the wealth in the risky asset as the wealth increases. Similarly, the increasing/constant/decreasing relative risk aversion suggests that one would increase/maintain/decrease the proportion of the wealth in the risky asset with the wealth increasing. The measure of relative risk aversion is still valid even if the utility function is not strictly concave or convex, which offers an advantage over the measure of absolute risk aversion. Notably, the Arrow-Pratt measures of risk attitudes facilitate the comparison of risk attitudes across individuals with different forms of utility function (i.e., positive affine transformation).

Of numerous utility functions, the constant relative risk aversion model, proposed by Friedman and Savage (1948), is one of the most commonly used tools for capturing individual risk attitudes. Since it is generally formulated as a power function, the study of this thesis takes the form, $U(x) = \frac{x^{1-r}}{1-\gamma}$, which is now in common use (e.g., Holt and Laury (2002) and Andersen et al. (2009)).

Unsurprisingly, it has a constant relative risk aversion (i.e., $-\frac{x*U''(x)}{U'(x)} = \gamma$) based on the Arrow-Pratt measure, which implies one's risk attitude stays constant throughout the range of his/her payoff. The constant relative risk aversion model has been shown to be a more plausible specification of individual risk attitudes than any other types of utility functions (Blanchard and Fischer, 1989, Wakker, 2008, Camerer and Ho, 1994), and been widely applied to various fields of study such as behavioural economics (Holt and Laury, 2002, Palacios-Huerta and Serrano, 2006, Harrison and Rutström, 2009, Tversky and Kahneman, 1992, Andersen et al., 2009), financial option (Henderson and Hobson, 2002), sociology (Harrison et al., 2007), psychology (Luce and Krumhansl, 1988) and health science (Bleichrodt et al., 1999).

Many transport studies have successfully investigated the effect of risk attitudes on travel time variability (Hensher et al., 2011, Li et al., 2012), turning gap choices (Dixit et al., 2014, Dixit et al., 2011), intersection manoeuvre choices (Arbis et al., 2016), route choices (Dixit et al., 2015, Dixit et al., 2013), public transit choices (Rey et al., 2016) and evacuation departure choices (Dixit et al., 2012) by using the constant relative risk aversion utility function. Despite the wealth of the application of risk attitudes within transport research and beyond as well as the importance of improving model prediction against reality, the existing literature displays a rare introduction of risk attitudes into modelling the decision process of vehicle following. This motivates the author of this thesis to develop vehicle following models that explicitly incorporate drivers' risk attitudes.

2.4 Conclusions

Literature concerning modelling vehicle following behaviour is reviewed, showing two gaps in the existing research. The first one is the insufficient mathematical specification and empirical calibration of drivers' perception (especially perception of traffic dynamics) in the decision process of vehicle following. Another lacuna lies in the lack of theoretic variation in modelling decision making of vehicle following. Due to the vital significance of perception and decision making in the decision process of vehicle following (Rothery, 1992), exploring research enhancements to these two components would provide novel insights into human decision associated with vehicle following.

As an important attribute of driving, risk is indispensable in characterising the decision process of vehicle following. The consideration of risk in perception and decision making brings about the inclusion of risk perception and risk attitudes, respectively. These two risk attributes are the subjective appraisal of the probabilities and consequences of risks. They advance decision theoretic modelling by taking into account the presence of risk and quantifying the impact of risk on human perception and decision making. The literature on risk perception and risk attitudes has also been reviewed, demonstrating their significance within various areas of decisions under risk and their absence in the vehicle-following context. The author of this thesis thus expects they are of the similar significance in modelling the decision process of vehicle following.

CHAPTER 3. MODEL FORMULATION

3.1 Introduction

Vehicle following which describes the interaction between a vehicle and its leader in a single-lane roadway has been extensively studied for more than sixty years. Vehicle following models are the core part of modern traffic flow theory and traffic microsimulation, which give insights into the interplay between individual driving behaviour and macroscopic traffic flow. A vehicle following model that could reproduce the real-life traffic dynamics is necessitated to give people a better understanding of latent factors that affect driving behaviour and road safety.

3.2 Theoretical Framework

Among many dimensions of vehicle following that are worth attention, the decision process is within the scope of this thesis. Rothery (1992) presented a research framework, as shown in Figure 1.1, which suggests that the decision process of the single-lane vehicle following is made up of perception, decision making and control. In particular, perception and decision making are under the major consideration of this thesis.

3.2.1 Perception of Traffic Dynamics

Hamdar et al. (2008) assumed that drivers' perception of the leaders' velocity follows a normal distribution with the actual speed of the leading vehicles as the mean value, which introduces a novel direction by incorporating the heterogeneity of drivers' perception in modelling vehicle following. It provides considerable research potential for exploring drivers' perception of other aspects of traffic dynamics, such as distance and time headway. The study of this thesis thus introduces the time-headway perception as the subjective representation of traffic dynamics in modelling the decision process of vehicle following.

3.2.2 Risk Perception

Risk perception is a mental representation of the potential threat associated with an action, activity or situation (Bijkerk, 2007). Slovic and Weber (2002) stated that two key factors of risk perception are the extent to which a potential danger is dreadful (i.e., the severity of risk) and the extent to which it is unknown (i.e., the probability of risk). The risk associated with vehicle following refers to the rear-end crash that may occur. According to the statement of Humphrey (1998) with the support of Ward et al. (1998) along with Christensen and Amundsen (2005), both the probability and severity of crash have an impact on drivers' speed choices. The study of this thesis takes risk perception into account from the two aspects: perceived crash probability and perceived crash severity.

Since risk perception is essentially an internal activity of human brains, it is quite difficult for transport researchers to observe directly. Alternatively, risk perception can be either derived from observable transport quantities (e.g., velocity and time headway) or represented by parameters that can be calibrated empirically. The study of this thesis therefore derives the perceived crash probability from actual time headway (a probability distribution also assumed) and represents the perceived crash severity with the perceived crash severity factor that is embedded into the crash disutility function.

3.2.3 Decision Theory under Risk

Decision theory under risk is an effective tool for mathematically modelling decision making under risk. As one of the classical decision theories under risk, state-dependent expected utility theory proposed by Karni et al. (1983) is used for modelling the decision making in vehicle following. State-dependent expected utility theory includes two core concepts: subjective probability and state-dependent utility. The subjective probability measures the degree of drivers' belief with regard to the likely states while the state-dependent utility represents the degree of satisfaction with respect to consequences in certain states. The study of this thesis therefore utilises these two features to characterise probabilities and utility functions in two states of vehicle following, i.e., staying safe and crashing into the leading vehicle.

3.2.4 Risk Attitudes

Risk attitudes refer to the subjective appraisal of the consequences of decisions under risk. People with different risk attitudes view the consequences in different ways. Specifically, an agent possesses: risk aversion if his/her utility function is concave (i.e., the payoff associated with a risky alternative is underestimated by this person); risk-seeking attitude if the utility function is convex (i.e., the payoff of a risky alternative is overestimated); and risk neutrality if he/she has a linear utility function (i.e., risk of an alternative doesn't affect the subjective appraisal of its payoff). The constant relative risk aversion model, proposed by Friedman and Savage (1948), is one of the most commonly used tools for capturing individual risk attitudes. The constant relative risk aversion model has been shown to be a more plausible specification of individual risk attitudes than any other types of utility functions (Blanchard and Fischer, 1989, Wakker, 2008, Camerer and Ho, 1994). The study of this thesis thus incorporates the parameter of risk attitudes by deriving utility functions from the constant relative risk aversion model.

3.3 Main Assumptions

Some basic assumptions of the proposed vehicle following model are specified before introducing the mathematical modelling. First of all, single-lane vehicle following behaviour is the focus of this thesis, which describes that a vehicle (car or truck) immediately follows the predecessor (car or truck) in the same lane. Secondly, vehicle following would end if any interruptions happen such as other vehicles merging into the gap, rear-end crashing and lane changing. Another assumption is that the driver of the following vehicle aims to reach the destination as quickly as possible under the condition of driving safety. For this purpose, the driver needs to maximise the expected utility by doing a speed-safety balance. The last hypothesis is that the time period of a complete vehicle following consists of a series of equal time intervals. At the beginning of each time interval, the driver of the following vehicle makes a choice of speed that is expected to reach at the end (i.e., the beginning of the next time interval). The following vehicle travels at a constant acceleration/deceleration to reach the selected speed. If a crash happened to the following vehicle during a time interval, the crashing speed is assumed to be the speed at the beginning of this time interval. During each time interval, the leading vehicle is assumed to travel constantly at the initial speed.

3.4 Microscopic Formulation

As depicted in Figure 3.1, consider at the moment t driver n is evaluating the speed $v_n(t+\tau)$ for the next moment $t+\tau$ where τ is the time interval. This speed is to be obtained by a constant acceleration/deceleration $\frac{v_n(t+\tau)-v_n(t)}{\tau}$ where $v_n(t)$ is the current speed.

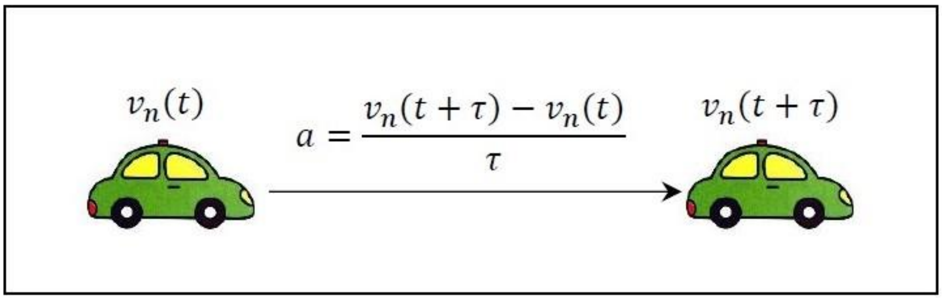

Figure 3.1 Constant acceleration/deceleration taken by the vehicle n

Driver n cannot anticipate the acceleration/deceleration of the leading vehicle $n-1$, thereby assuming that the leading vehicle $n-1$ continues to travel at the current speed $v_{n-1}(t)$, as shown in Figure 3.2.

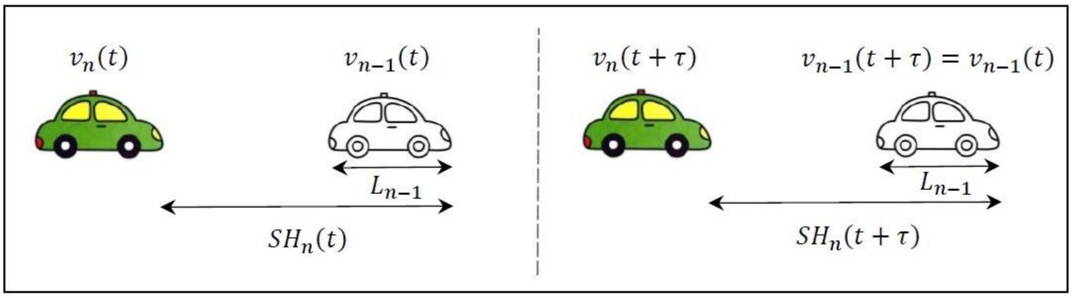

Figure 3.2 Constant speed of the leader $n-1$ assumed by the vehicle n

Then the distance that the leader $n-1$ travels during the time interval τ can be calculated as:

$$DIST_{n-1}(\tau) = v_{n-1}(t) \times \tau \qquad [3.1]$$

The distance that the vehicle n passes during τ can be written as:

$$DIST_n(\tau) = v_n(t) \times \tau + \frac{1}{2} \times \left(\frac{v_n(t+\tau) - v_n(t)}{\tau}\right) \times \tau^2 \quad [3.2]$$

With the vehicle n's current space headway denoted as $SH_n(t)$, the space headway for the next moment $t + \tau$ can be expressed as:

$$SH_n(t+\tau) = SH_n(t) + DIST_{n-1}(\tau) - DIST_n(\tau) \quad [3.3]$$

With Equations [3.1] and [3.2], Equation [3.3] can be rewritten as:

$$SH_n(t+\tau) = SH_n(t) + v_{n-1}(t) \times \tau - \left(v_n(t) \times \tau + \frac{1}{2} \times \left(\frac{v_n(t+\tau) - v_n(t)}{\tau}\right) \times \tau^2\right) \quad [3.4]$$

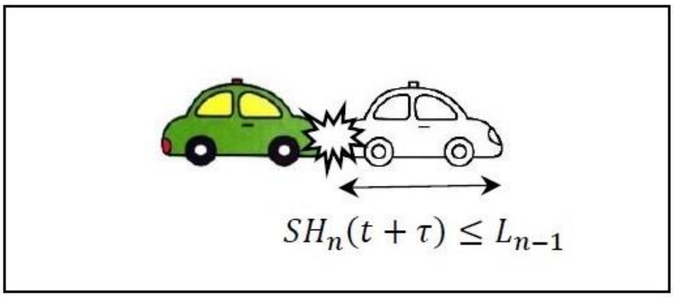

Figure 3.3 Rear-end crash between the vehicle n and its leader $n-1$

Let L_{n-1} denote the length of the leader $n-1$. As shown in Figure 3.3, a rear-end crash occurs when the space headway of the vehicle n at $t+\tau$ is equal to or less than the leading vehicle's length:

$$SH_n(t+\tau) \leq L_{n-1} \tag{3.5}$$

Combining Equations [3.4] and [3.5], we can obtain that:

$$SH_n(t) + v_{n-1}(t) \times \tau - \left(v_n(t) \times \tau + \frac{1}{2} \times \left(\frac{v_n(t+\tau) - v_n(t)}{\tau}\right) \times \tau^2\right) \leq L_{n-1} \tag{3.6}$$

With the assumption of $v_n(t) \neq 0$, Equation [3.6] can be written as:

$$\frac{SH_n(t)}{v_n(t)} \leq \frac{L_{n-1} - v_{n-1}(t) \times \tau + \left(v_n(t) \times \tau + \frac{1}{2} \times \left(\frac{v_n(t+\tau) - v_n(t)}{\tau}\right) \times \tau^2\right)}{v_n(t)} \tag{3.7}$$

In Equation [3.7], the left side is equal to the vehicle n's time headway at time t denoted by $TH_n(t)$, so we can get:

$$TH_n(t) = \frac{SH_n(t)}{v_n(t)} \tag{3.8}$$

And the right side is defined as:

$$TH_n^{critical}(t) = \frac{L_{n-1} - v_{n-1}(t) \times \tau + \left(v_n(t) \times \tau + \frac{1}{2} \times \left(\frac{v_n(t+\tau) - v_n(t)}{\tau}\right) \times \tau^2\right)}{v_n(t)} \qquad [3.9]$$

where $TH_n^{critical}(t)$ represents the critical time headway of the vehicle n at time t, which is a crash indicator for the next moment $t + \tau$.

Equation [3.7] indicates that there would be a crash happening at the next moment $t + \tau$ when the current time headway is equal to or smaller than the critical time headway, i.e., $TH_n(t) \leq TH_n^{critical}(t)$.

Driver n would compare the perceived time headway with the critical time headway for crash-risk perception. Therefore, driver n perceives a crash for the next moment $t + \tau$ when the perceived time headway at t is equal to or less than the critical time headway:

$$TH_n^*(t) \leq TH_n^{critical}(t) \qquad [3.10]$$

The probability of perceiving a crash for the next moment $t + \tau$ is expressed as:

$$P_c = P\left(TH_n^*(t) \leq TH_n^{critical}(t)\right) \qquad [3.11]$$

The study of this thesis assumes that driver n's perceived time headway at t is not the same as the actual time headway, but normally distributed with the actual time headway $TH_n(t)$ as the mean and σ as the standard deviation:

$$TH_n^*(t) \backsim N(TH_n(t), \sigma^2) \qquad [3.12]$$

As one of the model parameters to be calibrated, σ indicates how drivers' perception of time headway deviates from the reality.

The perceived time headway at t can also be expressed by a standard normal variable Z:

$$TH_n^*(t) = TH_n(t) + \sigma Z \qquad [3.13]$$

With Equation [3.13] embedded, Equation [3.11] is rewritten into:

$$P_c = P\left(Z \leq \frac{TH_n^{critical}(t) - TH_n(t)}{\sigma}\right) \qquad [3.14]$$

Therefore, driver n's perceived crash probability for the next moment $t + \tau$ is defined as:

$$P_c = \Phi\left(\frac{TH_n^{critical}(t) - TH_n(t)}{\sigma}\right) \qquad [3.15]$$

Equation [3.15] shows that the perceived crash probability has a form of the cumulative distribution function of the standard normal distribution. The value of $\frac{TH_n^{critical}(t)-TH_n(t)}{\sigma}$ determines how driver n perceives the crash probability, as illustrated in Figure 3.4. When the actual time headway is equal to the critical time headway, i.e., $TH_n^{critical}(t) = TH_n(t)$, driver n perceives 50% chance of crashing. As the actual time headway gets greater than the critical time headway, i.e., $TH_n^{critical}(t) < TH_n(t)$, the perceived crash probability becomes smaller and driver n feels less likely to crash into the leading vehicle at the next moment $t + \tau$.

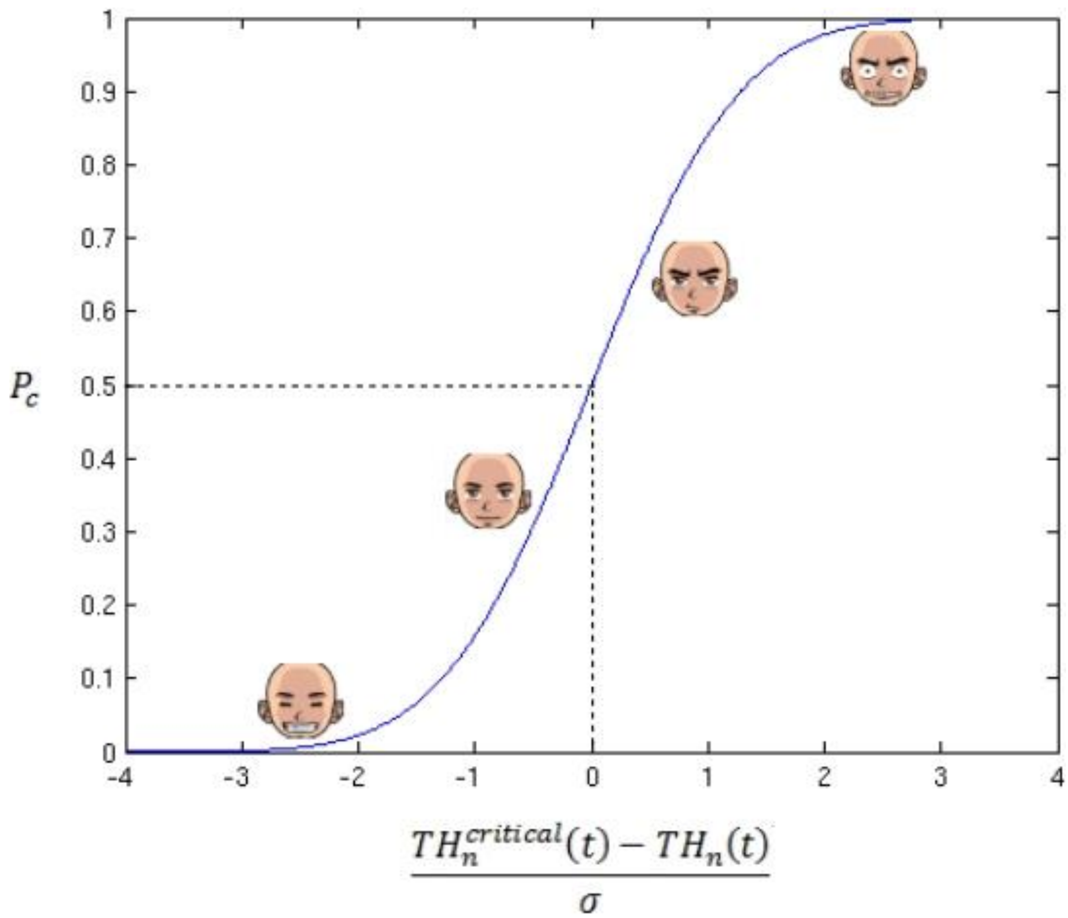

Figure 3.4 Perceived crash probability P_c of driver n

Since crash and safety are mutually exclusive and collectively exhausted events in vehicle following, the perceived probability of safety maintained for the next moment $t + \tau$ is:

$$P_s = 1 - \Phi\left(\frac{TH_n^{critical}(t) - TH_n(t)}{\sigma}\right) \quad [3.16]$$

In addition to the perceived probabilities (i.e., subjective probabilities), state-dependent expected utility theory requires utility functions that are dependent on the likely states. Moreover, state-dependent utility functions are derived from the constant relative risk aversion model to incorporate risk attitudes. If a crash occurred (i.e., in the crash state), driver n's disutility (i.e., negative utility) would be dependent on the square of the current speed $v_n(t)^2$:

$$U_c = -\omega \times \frac{(v_n(t)^2)^{(1-\gamma)}}{1-\gamma} \quad [3.17]$$

where ω is perceived crash severity factor; and

γ refers to risk attitudes.

Specifically, $\gamma > 0$ indicates risk aversion; it reveals risk-prone behaviour when $\gamma < 0$; and $\gamma = 0$ represents risk-neutral behaviour. ω measures drivers' sensitivity to crash losses, and γ shows the impact of crash risks on drivers' behaviour. They are another two parameters to be calibrated.

In the state of safety, driver n would successfully reach the speed $v_n(t+\tau)$ at the next moment $t+\tau$. Therefore, the corresponding utility function depends on the new speed:

$$U_s = \frac{\left(v_n(t+\tau)\right)^{1-\gamma}}{1-\gamma} \tag{3.18}$$

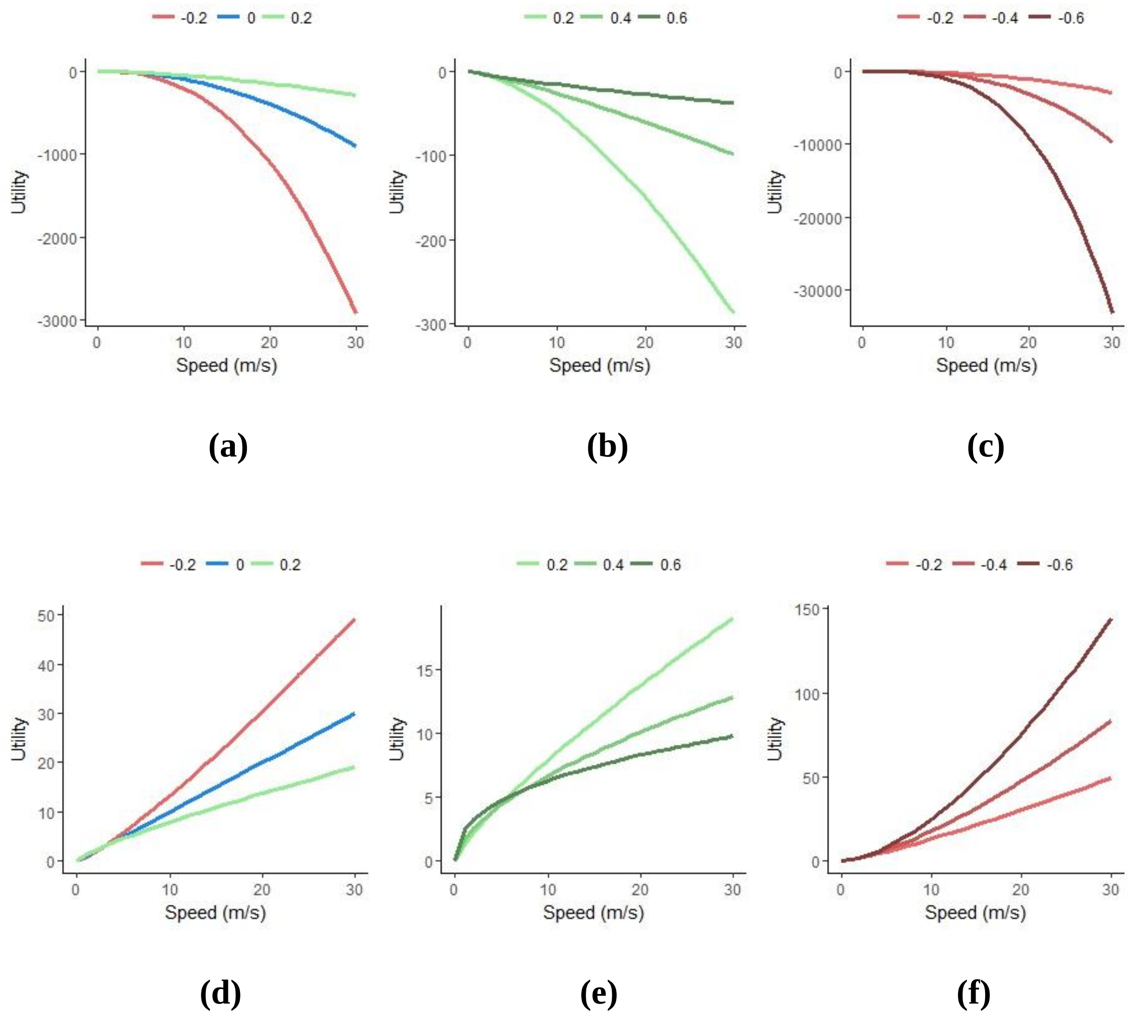

Figure 3.5 Utility functions with different risk attitudes for (a-c) crash state with $\omega = 1$ and (d-f) safety state

The utility functions with different risk attitudes γ are plotted in Figure 3.5. The legend is on the top of each graph, in which each number represents a value of risk attitudes. For example, 0.2 means $\gamma = 0.2$, which refers to risk averse. The utility functions with three types of risk attitudes ($\gamma = -0.2$, $\gamma = 0$ and $\gamma = 0.2$) are compared in the states of crash and safety, as shown in Figure 3.5 (a) and (d). Figure 3.5 (b) and (e) compare the utility functions with risk aversion ($\gamma = 0.2$, $\gamma = 0.4$ and $\gamma = 0.6$), while Figure 3.5 (c) and (f) depict the comparison of the utility functions with different risk-taking attitudes ($\gamma = -0.2$, $\gamma = -0.4$ and $\gamma = -0.6$). It is shown that the disutility in the state of crash in Figure 3.5 (a-c) far outnumbers the utility in the state of safety in Figure 3.5 (d-f). This reflects that driver n is certainly unwilling to be involved in a crash due to a great deal of disutility caused. Hence, driver n takes safety as the priority while driving, which is consistent with the reality. In Figure 3.5 (a-c), the disutility keeps growing as the crashing speed increases, no matter which type of risk attitudes it is. The more risk-taking driver n is, the greater disutility he/she suffers from a crash. Figure 3.5 (d-f) suggest that driver n obtains more utility with the increase in travel speed, and a more risk-taking attitude produces larger utility.

Driver n's state-dependent expected utility associated with the speed $v_n(t+\tau)$ can be described as:

$$SDEU[v_n(t+\tau)] = P_c U_c + P_s U_s \qquad [3.19]$$

Driver n is assumed to choose the speed that brings the maximum state-dependent expected utility. Hence, the first derivative of $SDEU[v_n(t+\tau)]$ should be equal to zero:

$$\frac{dSDEU[v_n(t+\tau)]}{dv_n(t+\tau)} = 0 \qquad [3.20]$$

Based on Equations [3.15]-[3.20], the vehicle following model is proposed as:

$$SH_n(t) = L_{n-1} - v_{n-1}(t) \times \tau + \frac{\tau}{2} \times \left(v_n(t+\tau) + v_n(t)\right) + v_n(t) \times \sigma \times \sqrt{-2 \times ln\left(\frac{2 \times v_n(t) \times \sqrt{2 \times \pi} \times \sigma \times v_n(t+\tau)^{-\gamma} \times (1-\gamma)}{(v_n(t+\tau)^{1-\gamma} + \omega \times (v_n(t)^2)^{(1-\gamma)}) \times \tau}\right)} \qquad [3.21]$$

It should be noted that $v_n(t+\tau) \neq 0$ is assumed in the model derivation. The detailed model formulation is presented in Appendix A.

3.5 Macroscopic formulation

3.5.1 Flow-density relation

The flow-density relation can be derived from the proposed vehicle following model in the steady-state condition. Each vehicle travels at a constant speed $\overline{v}$ in the steady-state condition, as shown in Figure 3.6.

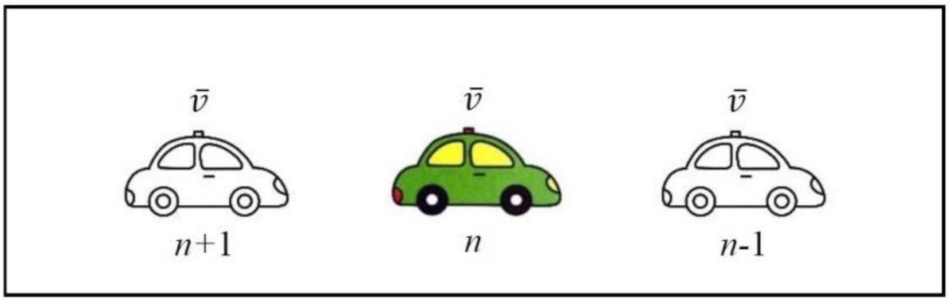

Figure 3.6 Vehicle following in the steady-state condition

Substituting $\bar{v}$ for $v_{n-1}(t)$, $v_n(t)$ and $v_n(t+\tau)$ in Equation [3.21], the average space headway can be obtained as:

$$\overline{SH} = \bar{L} + \bar{v} \times \sigma \times \sqrt{-2 \times ln\left(\frac{2 \times \sqrt{2 \times \pi} \times \sigma \times (1-\gamma)}{(1+\omega \times \bar{v}^{(1-\gamma)}) \times \tau}\right)} \qquad [3.22]$$

where $\bar{L}$ is the average length of all the vehicles in the steady state condition.

Given that density is the inverse of the average space headway, density can be expressed as:

$$k = \frac{1}{\overline{SH}} \qquad [3.23]$$

Density in the unit of vehicles per km per lane is hence written as:

$$K = \frac{1000}{\overline{SH}} \qquad [3.24]$$

Flow in the unit of vehicles per hour per lane is also obtained as:

$$Q = \frac{1000}{\overline{SH}} \times V \qquad [3.25]$$

where V refers to the space mean speed in the unit of km per hour,

and is equal to $3.6 \times \bar{v}$.

With Equations [3.22], [3.24] and [3.25], the resulting flow-density relation is presented in Figure 3.7. The congested branch of the flow-density relation is plotted by the proposed vehicle following model with $\gamma = 0.5$, $\bar{L} = 7\text{m}$, $\omega = 5$, $\delta = 1\text{s}$ and $\tau = 0.5\text{s}$.

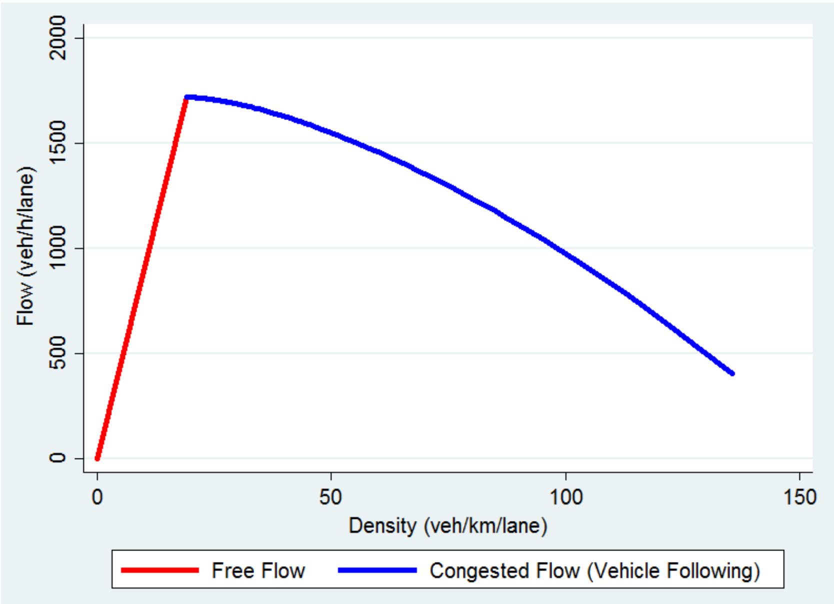

Figure 3.7 Flow-density relation with the congested branch based on the proposed vehicle following model

3.5.2 Sensitivity analysis

This section is to study how varying values of parameters and variables impact on the resulting flow-density relation. There are totally four parameters and one variable in Equation [3.22] that could affect the flow-density relation. The four parameters are risk attitudes (γ), perceived crash severity (ω), time interval (τ) and standard deviation of perceived time headway (σ), while the one variable is average length ($\bar{L}$). When varying one of these parameters and variable, it is necessary to fix others' values. Hence, the default values are listed as follows: $\gamma = 0.7$, $\omega = 3.5$, $\delta = 1\text{s}$, $\tau = 0.6\text{s}$, and $\bar{L} = 5\text{m}$.

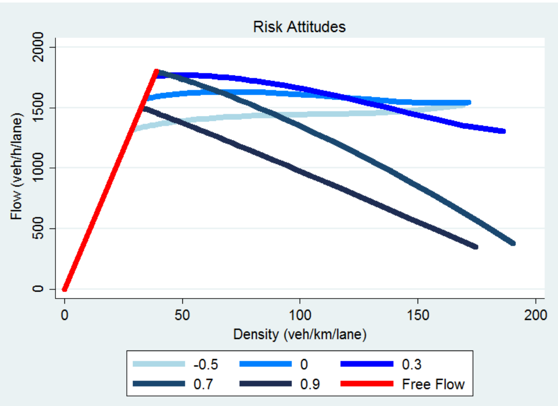

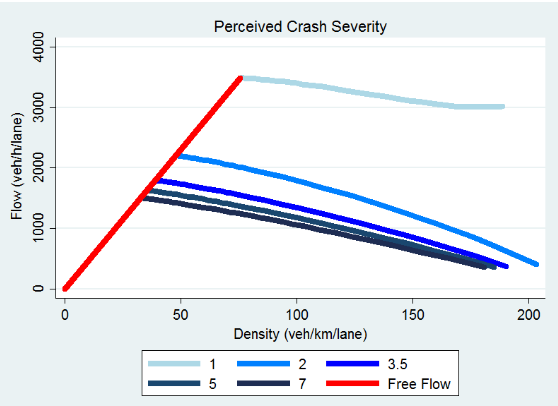

(a) **(b)**

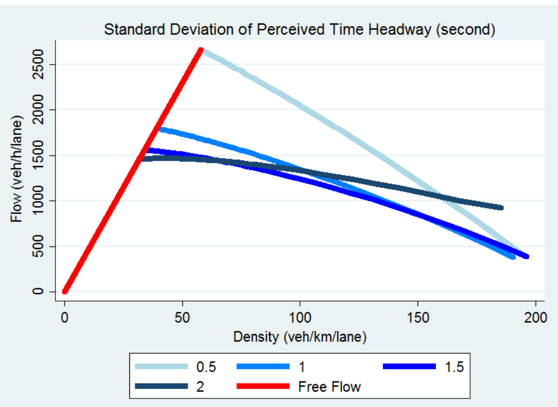

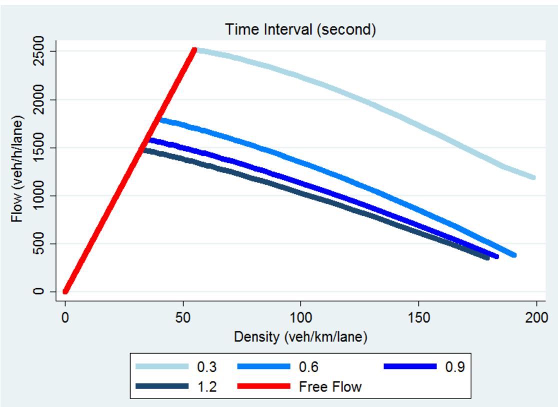

(c) **(d)**

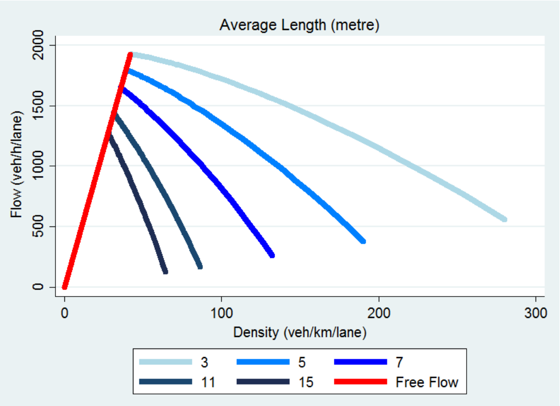

(e)

Figure 3.8 Flow-density relations with varying values of (a) risk attitudes, (b) perceived crash severity, (c) standard deviation of perceived time headway, (d) time interval, and (e) average length

Figure 3.8 displays the flow-density relations with different values of the selected parameters and variable. When individual drivers in vehicle following have a more risk-averse attitude, the perception of a more severe crash, a greater standard deviation of perceived time headway, a longer time interval for calculating the future speed and a longer vehicle, it is found to reduce the capacity of traffic facilities and cause more congestion in macroscopic traffic.

3.6 Conclusions

The modelling of this thesis focuses on perception and decision making in the decision process of vehicle following behaviour given by Rothery (1992). The theoretical framework of modelling perception and decision making in vehicle following is presented, as shown in Figure 1.2. For perception of traffic dynamics, how the perception of time headway differs from the reality is studied by introducing the normal distribution of the perceived time headway. As for risk perception, the perceived crash probability is derived from the normal distribution of the perceived time headway while the perceived crash severity factor is embedded into the crash disutility function. As one of the classical decision theories under risk, state-dependent expected utility theory provides a solid framework for mathematically modelling the decision making in vehicle following. Specifically, the concepts of subjective probability and state-dependent utility are utilised by the modelling of this thesis. Two states associated with vehicle following behaviour are crashing into the leading vehicle and staying safe. The parameter of risk attitudes is incorporated by deriving utility functions from the constant relative risk aversion model.

Furthermore, some underlying assumptions of the modelling of this thesis are elaborated, which is necessary for understanding the scope of the proposed vehicle following model. First of all, single-lane vehicle following behaviour is under the consideration of the modelling of this thesis. Secondly, vehicle following would end if any interruptions happen such as other vehicles merging into the gap, and the occurrence of lane changing. Thirdly, the driver of the following vehicle aims to reach the destination as quickly as possible under the condition of driving safety. The last hypothesis is that the time period of a complete vehicle following consists of a series of equal time intervals. At the beginning of each time interval, the driver of the following vehicle makes a choice of speed that is expected to reach at the end. The following vehicle travels at a constant acceleration/deceleration to reach the selected speed. If a crash happened to the following vehicle during a time interval, the crashing speed is assumed to be the speed at the beginning of this time interval. During each time interval, the leading vehicle is assumed to travel constantly at the initial speed.

Under the above assumptions, the vehicle following model is successfully proposed. In addition, the incorporation of the perceived time headway, risk perception and risk attitudes is mathematically specified. Besides the microscopic modelling, the flow-density relation is derived from the suggested vehicle following model. Through macroscopic sensitivity analysis, a more risk-averse attitude, the perception of a more severe crash, a greater standard deviation of perceived time headway, a longer time interval for calculating the future speed and a longer vehicle length are found to reduce the capacity of traffic facilities and cause more congestion in macroscopic traffic.

CHAPTER 4. MODEL CALIBRATION AND VALIDATION

4.1 Introduction

Model calibration is a technique of using statistical and mathematical methods to find the optimal values of model parameters against the field data. Model validation is to verify the effectiveness of model by comparing the predicted values of variables calculated by the model with the observed counterpart. These two techniques are of vital significance to demonstrate the validity and feasibility of a mathematical model.

This chapter is to introduce the calibration and validation of the proposed vehicle following model against the field observation. The field data used for calibration and validation will be detailed. The techniques used for processing the data are also specified. The calibration results are obtained by using a nonlinear least-squares method written in Stata by Danuso (1992) and Royston (1993). As statistical analysis software, Stata enables users to utilise built-in statistical methods and automate the analysis process by programming. In the study of this thesis, Stata 13.1 MP Edition is used. After that, the results of model calibration and validation are discussed. Some key findings are also presented.

4.2 Data collection

The vehicle-trajectory data collected at a freeway section of I-80 Emeryville are used for the empirical calibration and validation. To make the original data suitable for the use of model calibration and validation, some data processing techniques are applied. The Stata code for data processing is displayed in Appendix B.

4.2.1 Data description

The study of this thesis uses vehicle trajectories of NGSIM I-80 Emeryville data to empirically calibrate and validate the proposed vehicle following model. The vehicle-trajectory dataset includes the information regarding vehicle ID, time, lateral coordinate, longitudinal coordinate, vehicle length, vehicle velocity, lane position, preceding vehicle ID, and space headway. Vehicle trajectories were recorded every 0.1 seconds. Since vehicle following usually occurs in the peak-hour traffic, the vehicle-trajectory dataset collected from 5:15pm to 5:30pm on April 13th, 2005 is used by the study of this thesis. The study area is a straight 503-metre-long section in the northbound direction of Eastshore Freeway in Emeryville, California, U.S., as shown in Figure 4.1. The study area carries the concurrent traffic of I-80 East and I-580 West. There are six lanes on the main roadway (lane 1-6) and one freeway on-ramp. Lane 1 is an HOV lane that is restricted to high-occupancy vehicles.

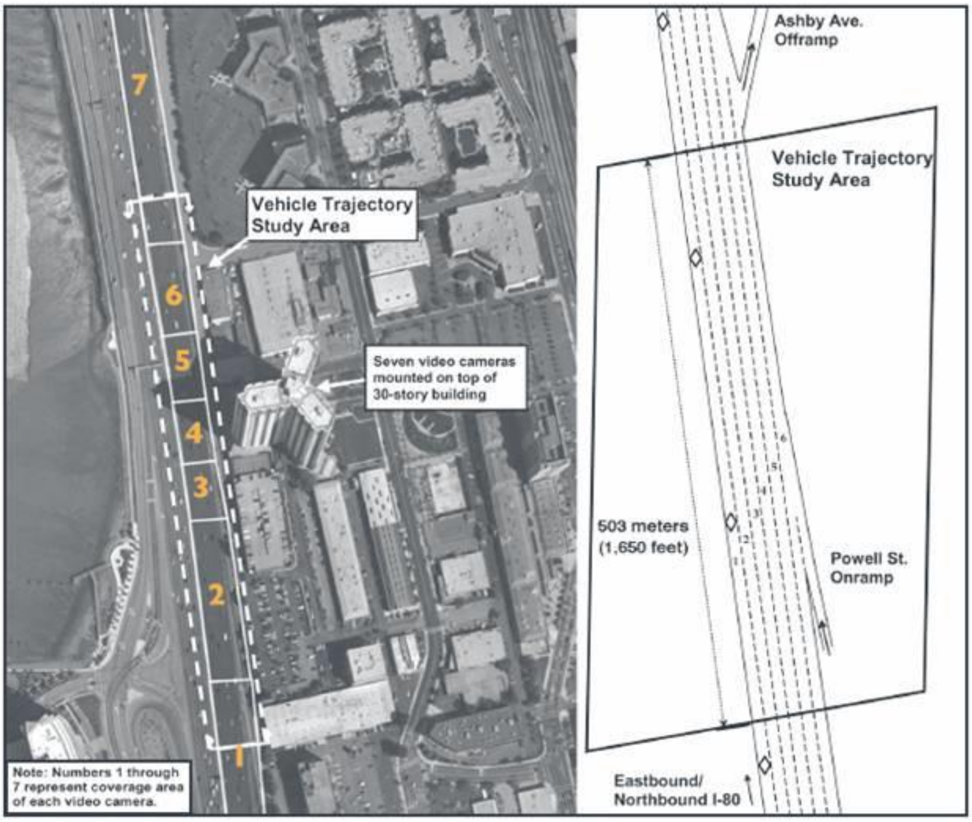

Figure 4.1 Study area at the concurrency of I-80 East and I-580 West (Alexiadis et al., 2004)

4.2.2 Data smoothing

In the vehicle-trajectory data, velocity and space headway are numerically derived from vehicle positions without any processing (Thiemann et al., 2008). Therefore, errors of position measurements would inevitably cause biases in velocity and space headway. For this reason, the smoothing method of symmetric exponential moving average (sEMA) developed by Thiemann et al. (2008) is applied to velocity and space headway. The procedure of getting velocity smoothed is differentiating original position to velocity, then smoothing velocity with the method of sEMA. The first step of getting space headway smoothed is to smooth original position by means of the sEMA method. Hence, smoothed space headway is the difference in smoothed position between a vehicle and its leader.

4.2.3 Data filling

In addition to the following vehicle's velocity and space headway, the preceding vehicle's velocity and length, as well as the following vehicle's future velocity after the time interval, are required for the empirical calibration and validation. These missing data need to be obtained from the existing data. This is done by matching vehicle ID with preceding vehicle ID to obtain velocity and length of the preceding vehicle, and matching vehicle ID and time to get the following vehicle's future velocity after the time interval.

4.2.4 Global filtering

The study of this thesis focuses on modelling a complete vehicle following. Specifically, a vehicle following would end if any interruptions occur such as other vehicles merging into the gap, rear-end crashing and lane changing. These interruptions have therefore been filtered out. As mentioned in Section 3.4, $v_n(t)$ and $v_n(t+\tau)$ cannot be zero. Hence, only the data with the non-zero following vehicle's velocity and the non-zero following vehicle's future velocity after the time interval have been kept.

4.2.5 Data segmentation

The study of this thesis aims to investigate four types of vehicle following: Car follows Car, Car follows Truck, Truck follows Car, and Truck follows Truck. The vehicle-trajectory dataset has been split into four corresponding sub-datasets. Vehicle length is used as a criterion to classify vehicles into two types (i.e., car and truck). According to the length-based vehicle classification scheme introduced by Weinblatt et al. (2013), the length of 6.75 feet (2.0574 metres) is the boundary between motorcycles and cars while the length of 22 feet (6.7056 metres) separates cars and trucks. In other words, the car length ranges from 2.0574 metres to 6.7056 metres while any vehicles with the length more than 6.7056 metres are categorised as a truck.

4.2.6 Additional filtering

Vehicle following is a common phenomenon in traffic congestion. To find the vehicle-trajectory data that describe the vehicle following in heavy traffic, an appropriate range of time headway needs to be determined. On the one hand, too short time headway (less than 1s) is found to be more accident-prone (Evans and Wasielewski, 1982), thus interrupting vehicle following. On the other hand, traffic with overlong time headway (more than 3s) is in a less congested condition and hence outside the scope of vehicle following. Therefore, the time-headway range for Car follows Car and Truck follows Car is set to be 1-3s. Since truck-following vehicles generally keep a relatively long headway due to truck length and safety reasons, the upper bound of time headway for following a truck is set to 5s. The resulting ranges of time headway for four types of vehicle following are listed as follows: 1-3s for Car follows Car and Truck follows Car, 1-5s for Car follows Truck and Truck follows Truck. The vehicle-trajectory data with the unqualified time headway have therefore been filtered out.

4.3 Results and discussion

This section presents the results of the model calibration and validation against the vehicle-trajectory data. In addition, the results under four types of vehicle following are compared. Stata (statistical analysis software) is used for performing the model calibration and validation. The calibration results are obtained by using a nonlinear least-squares method written in Stata by Danuso (1992) and Royston (1993). The Stata code for model calibration is shown in Appendix C. Each sub-dataset of the vehicle-trajectory data is randomly divided into a calibration set (70%) and a validation set (30%). The calibration set is utilised for calibrating the model parameters (i.e., standard deviation of perceived time headway, risk attitudes, perceived crash severity factor and time interval). After that, the parameter estimates obtained by calibration are used to calculate the predicted space headway of the validation set. The model validation is implemented by comparing the predicted space headway with the corresponding observations of the validation set. The Stata code for model validation can be seen in Appendix D.

4.3.1 Model calibration

4.3.1.1 Time interval

Drivers are assumed to anticipate the future speed after a certain time interval. It is necessary to calibrate the time interval of drivers' anticipation. The calibration of the time interval is measured by the root-mean-square error (RMSE). A smaller value of RMSE indicates a better prediction of space headway. The optimal time interval yields the least value of RMSE. 0.5, 0.6, 0.7, …, 2s are taken as time interval candidates.

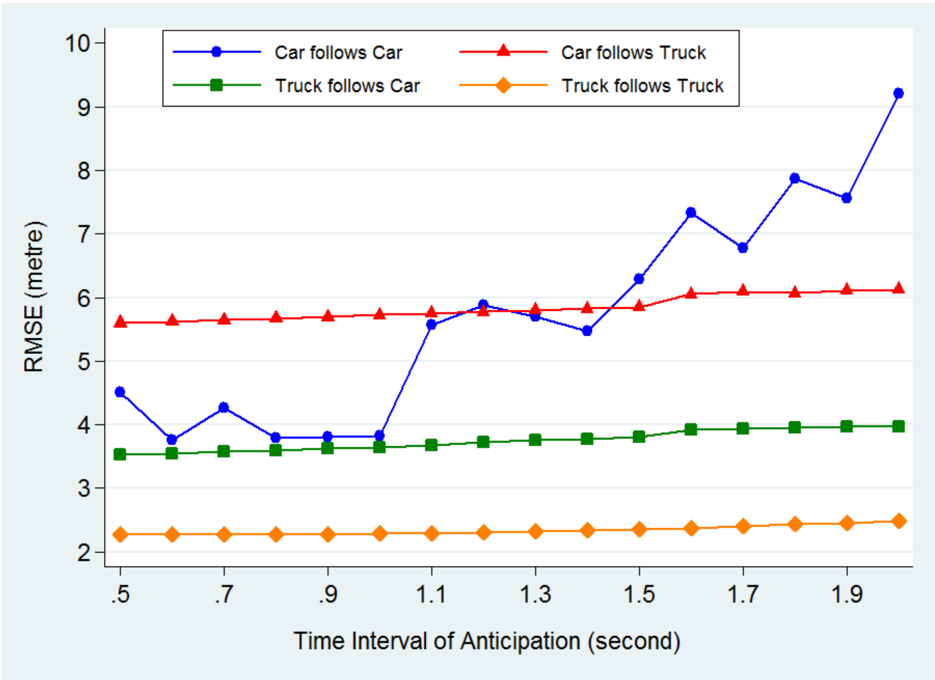

Figure 4.2 Time interval and the corresponding RMSE for four types of vehicle following

Figure 4.2 depicts the RMSE obtained with each time interval candidate for four types of vehicle-following. In general, a smaller time interval has a lower RMSE indicating a better prediction of space headway. In Car follows Truck, Truck follows Car, and Truck follows Truck, the value of RMSE increases slightly with the time interval. In Car follows Car, the value of RMSE starts a fluctuating growth when the time interval is larger than 1 second. The explanation behind this is that the massive number of the Car-follows-Car observations amplify the impact of the time interval on RMSE. For Car follows Car and Truck follows Truck, the time headway of 0.6 seconds has the lowest RMSE. The optimal time interval for Car follows Truck and Truck follows Car is 0.5 seconds.

4.3.1.2 Risk attitudes, perceived crash severity and perceived time headway

Besides the optimal time intervals, the estimates of risk attitudes, perceived crash severity and standard deviation of perceived time headway are obtained by using a nonlinear least-squares method written in Stata by Danuso (1992) and Royston (1993). The detailed calibration results are listed in Table 4.1.

Table 4.1 Model calibration results for four types of vehicle following

Type	Time Interval (second)	Obs.	RMSE	Parameter	Coefficient	Standard Error	t	p>|t|
Car follows Car	0.6	443202	3.763	σ (second)	1.047	0.002	429.026	0
				γ	0.725	0.003	268.221	0
				ω	3.476	0.024	144.550	0
Car follows Truck	0.5	11506	5.598	σ (second)	1.538	0.034	44.940	0
				γ	0.656	0.025	26.502	0
				ω	4.559	0.156	29.263	0
Truck follows Car	0.5	5778	3.530	σ (second)	1.217	0.029	42.326	0
				γ	0.512	0.037	13.827	0
				ω	4.929	0.107	46.053	0
Truck follows Truck	0.6	880	2.266	σ (second)	1.413	0.043	32.958	0
				γ	0.670	0.035	19.219	0
				ω	2.665	0.156	17.056	0

It should be noted that the proposed vehicle following model is developed based on an individual driver, and the vehicle-trajectory data used in the study of this thesis include multiple drivers. The calibration results presented in Table 4.1 therefore indicate the collective risk attitudes and perceived crash severity which represent the average behaviour of multiple drivers.

Before drawing the findings, it is necessary to reiterate what the parameters stand for. σ refers to the standard deviation of perceived time headway, which measures how drivers' perception of time headway deviates from the reality. As for risk attitudes (γ), it reflects people's behavioural pattern under risk. $\gamma>0$ suggests risk-averse behaviour; $\gamma=0$ indicates risk-neutral behaviour; and $\gamma<0$ represents risk-loving behaviour. In the context of vehicle following, risk is related to read-the end crash. The perceived crash severity factor (ω) suggests drivers' sensitivity to crash losses. The greater crash losses (i.e., the more serious crash) a driver perceives, the larger ω it is in his/her disutility function.

In Table 4.1, car drivers following a truck are found to have the highest standard deviation (σ=1.538s) across four types of vehicle following, which indicates the strongest fluctuation in drivers' time-headway perception under this situation. Conversely, car drivers following a car have the perception closer to the reality (σ=1.047s). The reason for this is that trucks usually have a larger variability of length than cars, and it is also difficult to know the exact length of a truck from the behind, let alone under the pressure of following a truck. Therefore, compared with following a truck, car drivers following a car have the more accurate time-headway perception. A similar finding is also revealed for truck drivers following a car (σ=1.217s) and truck (σ=1.413s). Hence, following a car facilitates a more accurate time-headway perception, which is consistent with the reality.

Table 4.1 also reveals that car drivers have a larger difference in the standard deviation (σ) than truck drivers when the leading vehicle switches from a car to a truck. This suggests that car drivers' time-headway perception shows a stronger sensitivity to the leading vehicle. This is because truck drivers are generally more well-trained than car drivers in terms of perception and driving skills, and professional truck drivers can maintain a relatively stable time-headway perception in any vehicle following.

Table 4.1 shows positive coefficients of risk attitudes (γ) across four types of vehicle following, which suggests that drivers' behavioural pattern is risk aversion. Specifically, truck drivers following a car have the least risk aversion (γ=0.512), which means that they are not as worried about crash risk as drivers in the other three situations. The reason is that the height advantage of trucks provides a broad field of driving vision and facilitates a thorough observation of the surroundings, which gives truck drivers more confidence of safety and makes them less risk averse. Car drivers following a car (γ=0.725) are aware of more crash risks than following a truck (γ=0.656). This result seems to clash with intuition. However, according to a survey of rear-end crashes from 2006 to 2010 in the metropolitan area of Australia (Beck, 2015), the struck vehicles in 77.7% of rear-end casualty crashes and the striking vehicles in 82.9% were private cars and 4WDs, while the struck vehicles in 5.1% of rear-end casualty crashes and the striking vehicles in 7.9% were trucks and buses. This suggests that rear-end crashes between cars are much more common than those between a car and a truck. With the greater risk of crashing into a car, car drivers following a car are more risk averse than following a truck.

As for perceived crash severity factor (ω) for four types of vehicle following, Truck follows Car (ω=4.929) and Car follows Truck (ω=4.559) are higher than the other two situations, which indicates that both car and truck drivers are more concerned about crash losses when following a different type of vehicle. In other words, they perceive a greater seriousness of crashing into a different type of vehicle. This is attributed to the huge difference between a car and a truck in terms of height, weight and general safety. By contrast, car (ω=3.476) and truck (ω=2.665) drivers following the same type of vehicle tend to perceive a less severe crash.

Table 4.2 displays the results of z-test for comparing the coefficients between four types of vehicle following to identify the statistical difference. In Table 4.2, CfC, CfT, TfC and TfT represent Car follows Car, Car follows Truck, Truck follows Car and Truck follows Truck, respectively. This statistical test is based on the work by Clogg et al. (1995).

Table 4.2 Z-test results for comparing coefficients between four types of vehicle following

Coefficient Comparison	σ (second)		γ		ω	
	z	p>|z|	z	p>|z|	z	p>|z|
CfC - CfT	-14.416	0.000	2.740	0.006	-6.862	0.000
CfC - TfC	-5.848	0.000	5.738	0.000	-13.250	0.000
CfC - TfT	-8.502	0.000	1.566	0.117	5.138	0.000
CfT - TfC	7.183	0.000	3.225	0.001	-1.956	0.050
CfT - TfT	2.280	0.023	-0.325	0.745	8.585	0.000
TfC - TfT	-3.779	0.000	-3.102	0.002	11.968	0.000

Table 4.2 reports that all the calibrated standard deviations of perceived time headway (σ) are mutually different at a 95% confidence level, which statistically differentiate one vehicle-following situation from another. In addition, drivers in Car follows Car and Truck follows Truck (p>0.1) do not have a statistically significant difference in risk attitudes (γ), nor do drivers in Car follows Truck

and Truck follows Truck ($p>0.1$). The perceived crash severity factor (ω) is found to be significantly different between each pair of the vehicle-following situations ($p<0.05$), with the exception of Car follows Truck and Truck follows Car ($p>0.05$). However, the perceived crash severity factors of Car follows Truck and Truck follows Car are statistically different at a 90% confidence level ($p<0.1$).

4.3.2 Model validation

Besides the optimal time intervals and the parameter estimates obtained by calibration as shown in Table 4.1, vehicle speed and length of the validation sets are used to generate the predicted space headway for model validation. For each type of vehicle following, 30% of the sub-dataset is randomly selected to form the validation set. The comparison of predicted and observed space headway for four types of vehicle following is presented subsequently.

4.3.2.1 R-squared and root-mean-squared error

Figure 4.3 shows that the predicted space headway closely approximates the observed counterpart with the fitting line of y=x for four types of vehicle following.

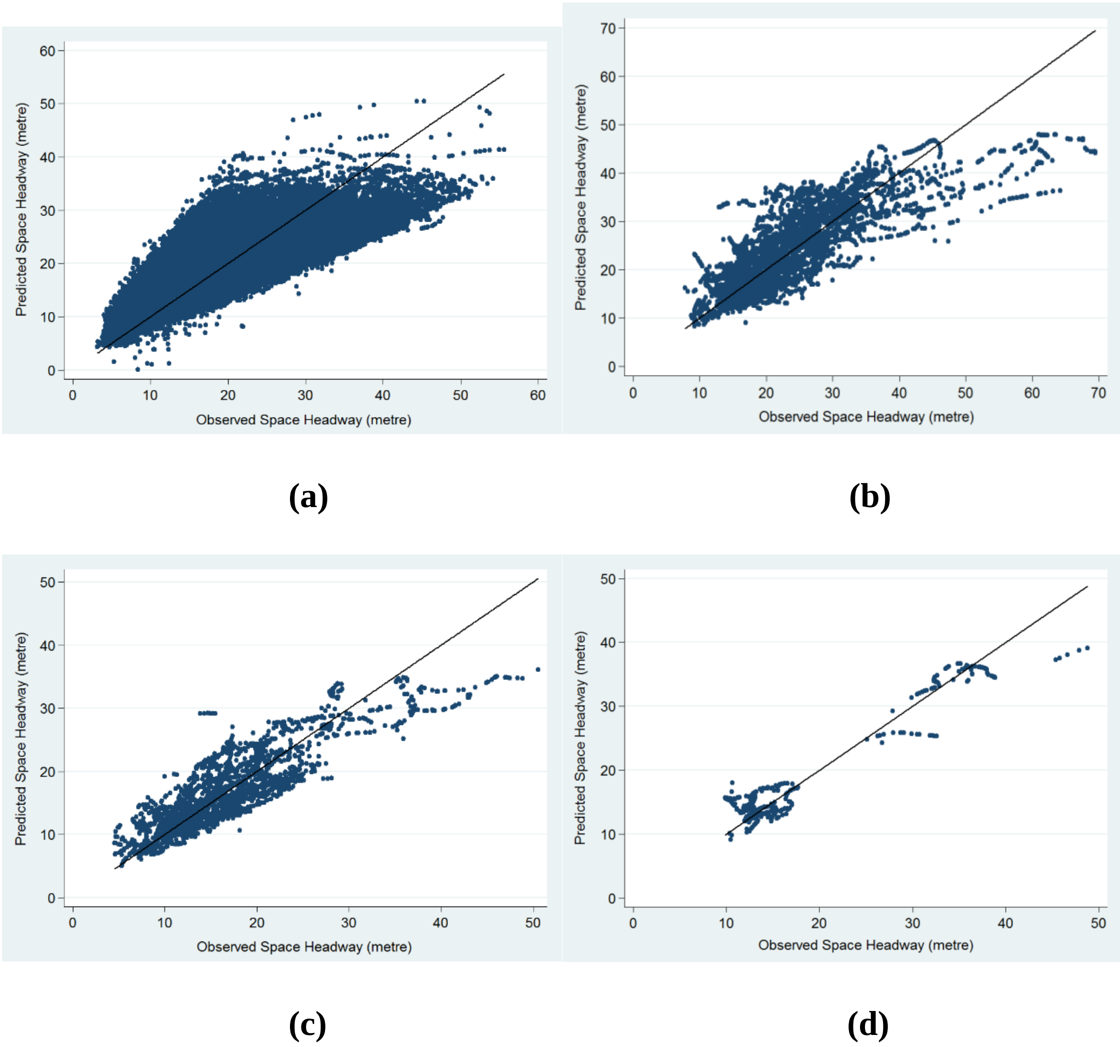

Figure 4.3 Comparison of observed and predicted space headway with the fit of y=x for (a) Car follows Car, (b) Car follows Truck, (c) Truck follows Car, and (d) Truck follows Truck

In addition, the R-squared for the fit of y=x and root-mean-square error (RMSE) are calculated to measure the accuracy of the space-headway prediction, as shown in Table 4.3. The results of R-squared and RMSE quantitatively validate the prediction of the proposed model for four types of vehicle following.

Table 4.3 R-squared for the fit of y=x and RMSE of space-headway prediction for four types of vehicle following

Type	R-Squared	RMSE (metre)
Car follows Car	0.688	3.763
Car follows Truck	0.791	5.545
Truck follows Car	0.781	3.514
Truck follows Truck	0.814	2.439

4.3.2.2 Kernel density

The kernel densities of predicted and observed space headway for four types of vehicle following are compared in Figure 4.4. It is evident that the kernel densities of predicted space headway show a similar curve with those of observed counterpart across four types of vehicle following despite a few imperfect matches.

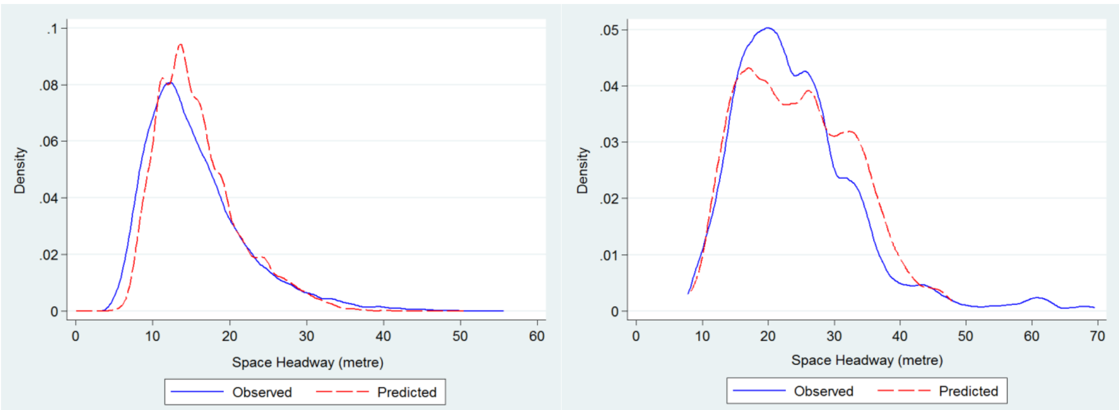

(a) (b)

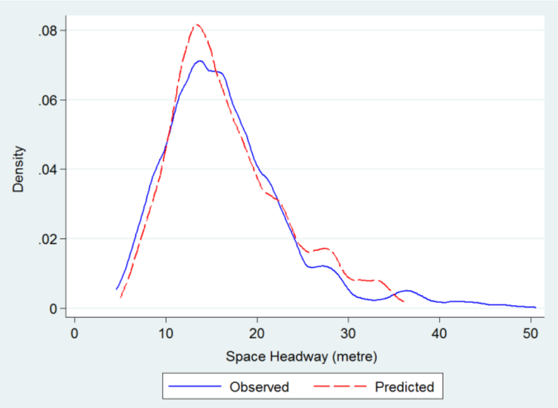

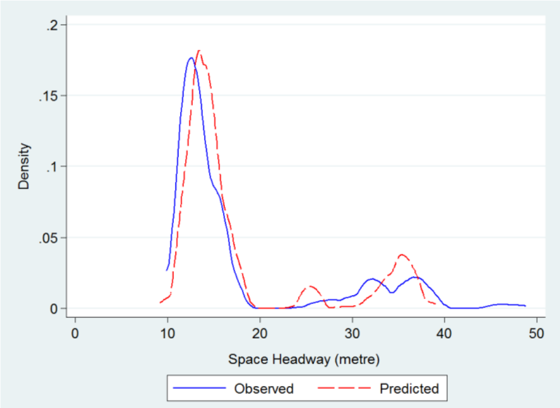

(c) **(d)**

Figure 4.4 Comparison of kernel densities of observed and predicted space headway for (a) Car follows Car, (b) Car follows Truck, (c) Truck follows Car, and (d) Truck follows Truck

4.3.2.3 Histogram of deviation

The histograms of the deviations between predicted and observed space headway for four types of vehicle following are plotted in Figure 4.5. The majority of the deviations for Car follows Car and Car follows Truck lie between -10 and 10 metres, and Truck follows Car has most of the deviations between -5 and 5 metres with most of the deviations of Truck follows Truck within -3 and 3 metres. The majority of the deviations in each histogram of Figure 4.5 are around 0, which further demonstrates the proposed model's ability to reproduce the observed space headway in four vehicle-following situations.

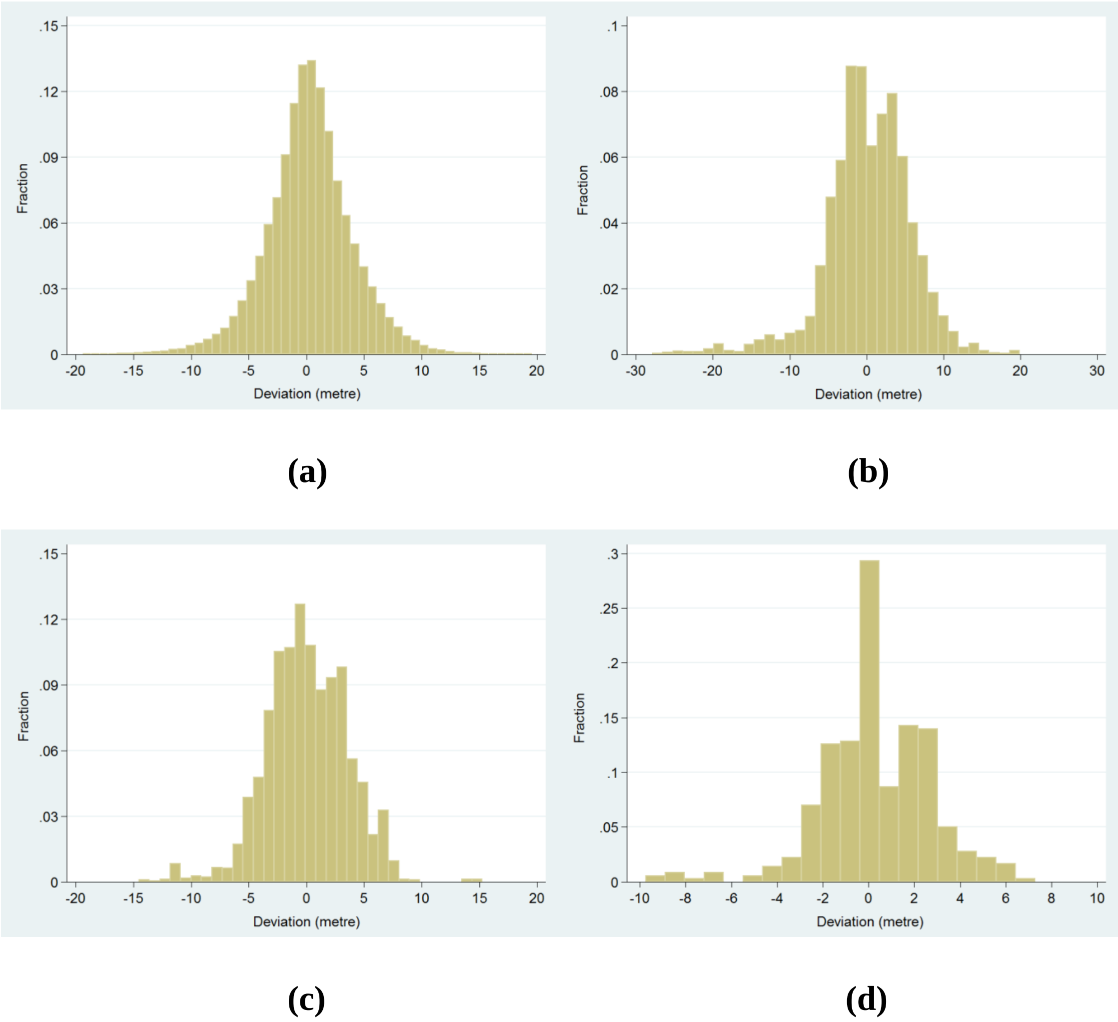

Figure 4.5 Histograms of deviations between observed and predicted space headway for (a) Car follows Car, (b) Car follows Truck, (c) Truck follows Car, and (d) Truck follows Truck

4.4 Conclusions

The vehicle-trajectory data collected at a freeway section of I-80 Emeryville are used for the empirical calibration and validation. To make the original data suitable for model calibration and validation, some data processing techniques, such as smoothing, filtering, filling and segmentation, are applied. To investigate the proposed model in four types of vehicle following, the vehicle-trajectory data are segmented into four corresponding sub-datasets: Car follows Car, Car follows Truck, Truck follows Car, and Truck follows Truck. Each sub-dataset is randomly separated into a calibration set (70%) and a validation set (30%).

The calibration results are obtained by using a nonlinear least-squares method written in Stata by Danuso (1992) and Royston (1993). It is found that drivers when following a car show a more accurate and stable time-headway perception than following a truck. Truck drivers tend to have a more stable time-headway perception and less risk aversion than car drivers. When following a different type of vehicle, drivers are shown to perceive greater crash losses.

Subsequently, the proposed model is utilised to predict space headway by using the optimal time intervals, parameter estimates, vehicle speed and length data. The predicted space headway is compared with the observed values of the validation sets in terms of RMSE, R-squared of y=x fit, kernel density, and deviation histogram. The comparison results further validate the effectiveness of the proposed model and the relevant findings.

CHAPTER 5. MODEL SIMULATION

5.1 Introduction

Traffic simulation is commonly used in transport research for studying driving behaviour. Traffic simulation can provide visual demonstrations of traffic states or scenarios and even reproduce continuous traffic dynamics of the field observation. Simulation results can be used for detailed data analysis and validating driving behavioural models.

The objective of traffic simulation in this chapter is to transform the theoretical vehicle following model proposed by this thesis into an effective simulation tool that can be used to reproduce the real-life traffic dynamics of the study area. The effectiveness of the simulation tool is measured by empirical comparison of traffic quantities such as flow, space mean speed, time mean speed, inflow and outflow. Furthermore, simulated traffic states of the before- and after-on-ramp sections of the study area are studied through fundamental diagrams. The heterogeneity (i.e., scattered patterns) of the fundamental diagrams are also analysed.

The simulation is implemented with a microscopic traffic simulator (Aimsun). Aimsun provides the abilities to accurately create any road geometry, externally load user-defined microscopic models written in C++, numerically present the simulation results, and animatedly output the simulation runs in 2D and 3D. In the study of this thesis, Aimsun 8.2.1 Advanced Edition is used in the operating system Windows 7 Enterprise Edition.

The incorporation of the proposed vehicle following model into Aimsun is achieved by writing the corresponding C++ code and running the code via Aimsun microSDK (Software Development Kit). To activate the function of microSDK, a licence of Aimsun Microscopic Simulator Behavioural Models SDK is needed. All the licence information is stored in an Aimsun dongle. The C++ code is written by using Microsoft Visual Studio 2017 Enterprise Edition.

5.2 Construction of Simulation Model

The first step of running traffic simulation in Aimsun is to build a simulation model (i.e., a simulated traffic network or a road section). In the study of this thesis, the main purpose of the simulation is to reproduce traffic dynamics on the freeway section of NGSIM I-80 in Emeryville of California, U.S., where the data used for calibration and validation were collected. Therefore, the creation of the simulation model is based on the geometric characteristics of the freeway section.

The summary report prepared by CambridgeSystematics (2005b) includes an illustration for the geometric design of the study area, as shown in Figure 5.1.

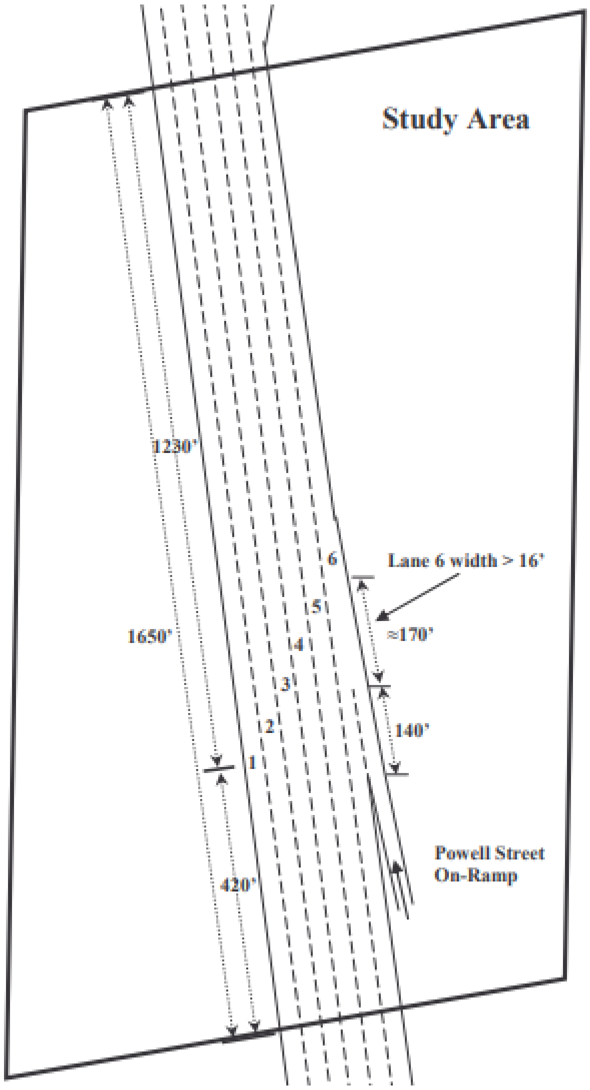

Figure 5.1 Geometric design of the study area on NGSIM I-80 (CambridgeSystematics, 2005b)

Figure 5.1 shows that the study area is a 1650-feet-in-length (503 metres) straight freeway section with six lanes on the main roadway and one on-ramp. Lane 1 is restricted to high-occupancy vehicles (i.e., HOV Lane). The merging of the on-ramp traffic and the mainstream traffic starts at the location 420 feet (128 metres) away from the freeway entrance. The merging section has the length of 310 feet (95 metres). The speed limit along the study area is at 65mph (105kph). The width of each freeway lane is 12 feet (3.66 metres). With the detailed geometric information of the study area, the simulation model is created in Aimsun, as shown in Figure 5.2. The left-most lane is set to be an HOV lane.

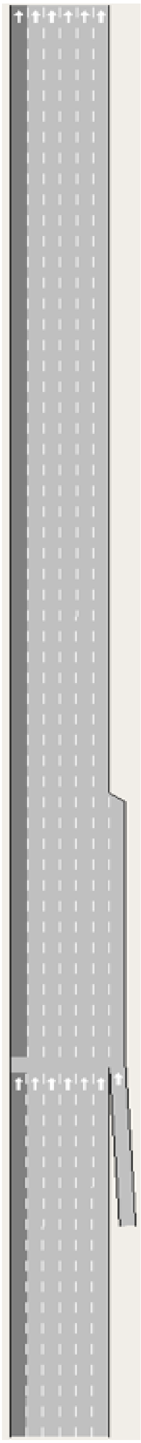

Figure 5.2 Simulation model of the study area in Aimsun

5.3 Setting of Traffic Demand

After the creation of the simulation model, traffic demand needs to be determined. In the study area, there are two origins (freeway entrance and on-ramp) and one destination (freeway exit). The summary report by CambridgeSystematics (2005b) gives the flow from the origins for every five minutes from 05:15 p.m. to 05:30 p.m. This flow is used as the input flow for the simulation model.

A warming-up simulation is also undertaken to create traffic flow at the beginning of the simulation exercise. To reproduce the real traffic dynamics of the study area, the flow from the origins from 05:00 p.m. to 05:15 p.m. presented by CambridgeSystematics (2005a) is inputted into the simulation model.

5.4 Integration of Vehicle Following Model

Aimsun allows users to overwrite the default driving behavioural models, including vehicle following and lane changing models, via microSDK (i.e., Software Development Kit), which offers the potential of running traffic simulation based on user-defined models.

To facilitate the simulation, the proposed vehicle following model needs to output future speed, which is therefore transformed into:

$$v_n(t+\tau) = 2 \times v_{n-1}(t) - v_n(t) + \frac{2}{\tau} \times$$

$$\left(SH_n(t) - v_n(t) \times \sigma \times \sqrt{-2 \times ln\left(\frac{2 \times \sqrt{2 \times \pi} \times \sigma \times (1-\gamma)}{(1 + \omega \times v_n(t)^{(1-\gamma)}) \times \tau}\right)} - L_{n-1} \right) \quad [5.1]$$

where $v_n(t+\tau)$ refers to the future speed of driver n after time interval τ from time t.

In addition, the proposed vehicle following model is combined with the lane changing model proposed by Gipps (1986a, 1986b) offered by default in Aimsun for the implementation of the simulation exercise.

Since the driving behavioural models of Aimsun are written in C++ language, the default vehicle following model is rewritten into the proposed vehicle following model as shown in Equation [5.1] by using Microsoft Visual Studio 2017. The complete C++ code is presented in Appendix E. It should be noted that the values of the model parameters used for simulation are obtained by the calibration and validation against the empirical data. The calibration and validation of the proposed vehicle following model are articulated in Chapter 4.

5.5 Simulation Results

Figure 5.3 gives a glance at the simulated traffic scenarios at four different locations of the study area, i.e., freeway entrance, freeway exit, on-ramp and merging section.

(a)

(b)

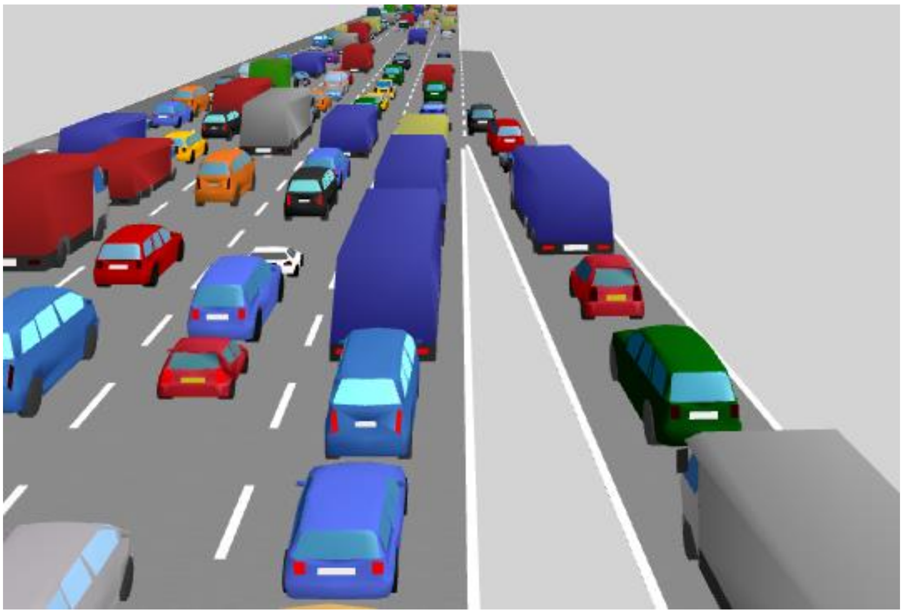

(c)

(d)

Figure 5.3 Simulated traffic scenarios at (a) freeway entrance, (b) freeway exit, (c) on-ramp and (d) merging section

5.5.1 Error Measurement

To measure the difference between the observed traffic dynamics and the traffic dynamics simulated by the proposed model, error measurement is needed. There are three error measures that have been commonly used: absolute error measure, relative error measure and mixed error measure. These error measures are defined as:

$$absolute\ error = \sqrt{\sum_{i}^{n}\left(d_i^{sim} - d_i^{obs}\right)^2 \times \frac{1}{(\sum_i^n d_i^{obs})^2}} \qquad [5.2]$$

$$relative\ error = \sqrt{\sum_{i}^{n}\left(\frac{d_i^{sim} - d_i^{obs}}{d_i^{obs}}\right)^2} \qquad [5.3]$$

$$mixed\ error = \sqrt{\sum_{i}^{n}\frac{\left(d_i^{sim} - d_i^{obs}\right)^2}{d_i^{obs}} \times \frac{1}{\sum_i^n d_i^{obs}}} \qquad [5.4]$$

where d_i^{sim} refers to the simulated value of data point i;

d_i^{obs} is the observed value of data point i; and

n represents the total number of data points.

To compare the effectiveness of these error measures, six test data sets, including simulated and observed values, are randomly created. In each test data set, there are three pairs of simulated and observed values. For simplicity, observed values are constant, and each test data set contains the same error in average value between simulated and observed values. In particular, test data sets 1, 2 and 3 have exactly the same average simulated values with different degrees of data dispersion. So do test data sets 4, 5 and 6. Test data sets 1, 2 and 3 have the larger values than test data sets 4, 5 and 6. Test data sets 1 and 4 show the same pattern of data dispersion. So do test data sets 2 and 5. Likewise, test data sets 3 and 6. Table 5.1 illustrates that the absolute error measure underestimates errors while the relative error measure overestimates errors across the six test data sets in comparison with the mixed error measure. The vehicle following studies by Kesting and Treiber (2008) and Hamdar et al. (2015) use the mixed error measure as the main measurement for validation and cross-comparison, and consider 0.3 as a reasonable mixed error threshold. The mixed error measure is therefore utilised by the study of this thesis.

Table 5.1 Comparison of three error measures using test data sets

	Test Data Set 1		Test Data Set 4	
	Simulated	**Observed**	**Simulated**	**Observed**
	100	95	10	5
	100	95	10	5
	100	95	10	5
Average	100	95	10	5
Absolute Error	0.030386856		0.577350269	
Relative Error	0.091160569		1.732050808	
Mixed Error	0.052631579		1	
	Test Data Set 2		**Test Data Set 5**	
	Simulated	**Observed**	**Simulated**	**Observed**
	150	95	15	5
	150	95	15	5
	0	95	0	5
Average	100	95	10	5
Absolute Error	0.430808041		1	
Relative Error	1.292424122		3	
Mixed Error	0.746181415		1.732050808	
	Test Data Set 3		**Test Data Set 6**	
	Simulated	**Observed**	**Simulated**	**Observed**
	300	95	30	5
	0	95	0	5
	0	95	0	5
Average	100	95	10	5
Absolute Error	0.860007086		1.732050808	
Relative Error	2.580021259		5.196152423	
Mixed Error	1.489575968		3	

5.5.2 Flow, Time Mean Speed and Space Mean Speed

Flow, time mean speed and space mean speed are three main traffic measurements that describe traffic dynamics of a road section or network. The simulation results are therefore compared with the observations in terms of flow, time mean speed and space mean speed. Flow is the average number of vehicles per hour that have passed through a road section or network during the simulation period. The vehicles are counted when leaving the road section or network via an exit. Time mean speed is the average of the spot speeds of all the vehicles that have passed the midpoint of a study section during the simulation period, which is calculated using the following equation:

$$v_{time}(t,s) = \frac{\sum_{i}^{n(t,s)} v_{spot}^{i}(t,s)}{n(t,s)} \qquad [5.5]$$

where $v_{time}(t,s)$ refers to the time mean speed measured at the centre of section s during time period t;

$v_{spot}^{i}(t,s)$ is the spot speed of vehicle i measured at the centre of section s during time period t; and

$n(t,s)$ represents the total number of the vehicles measured at the centre of section s during time period t.

The calculation of space mean speed is dividing the total distance travelled by all the vehicles in a road section or network by the total travel time of these vehicles during the simulation period, as shown in Equation [5.6]:

$$v_{space}(t,s) = \frac{\sum_{i}^{m(t,s)} dis^{i}(t,s)}{\sum_{i}^{m(t,s)} tt^{i}(t,s)} \quad [5.6]$$

where $v_{space}(t,s)$ refers to the space mean speed in section s during time period t;

$dis^{i}(t,s)$ is the distance travelled by vehicle i in section s during time period t;

$tt^{i}(t,s)$ represents the travel time taken by vehicle i in section s during time period t; and

$m(t,s)$ refers to the total number of the vehicles in section s during time period t.

The comparisons of flow, space mean speed and time mean speed obtained by the simulation and the field observation are shown in Tables 5.2 and 5.3. As discussed in the last section, mixed error method gives a more accurate error measurement compared to absolute and relative error methods. Thus, mixed error method is solely used for measuring the difference between the simulated and observed values. Since the field observations were collected from 5:15 p.m. to 5:30 p.m., the 15-min simulation is implemented for consistency. Table 5.2 compares the simulated and empirical flow, space mean speed and time mean speed by three consecutive 5-minute periods from 5:15 p.m. to 5:30 p.m. The simulated flow and space mean speed are considered reasonable with the mixed error less than 0.3. Time mean speed has a larger mixed error, which can be explained as follows. Given space mean speed and time mean speed in Table 5.2, the standard deviation of spot speeds can be obtained based on the relationship between space mean speed and time mean speed, as shown in Equation [5.7] (Mathew and Rao, 2017). It is found that the standard deviation of spot speeds in the field observation is much greater than the one in the simulation. In other words, the observed spot speeds are much more dispersed than the simulated values. Based on the relationship between time mean speed and spot speed, as shown in Equation [5.5], dispersed spot speeds in the field observation would generate a dispersed time mean speed in the field obseravtion which is difficult to be simulated. As a result, a relatively large deviation of the simulated time mean speed from the observed value occurs.

$$v_{time}(t,s) = v_{space}(t,s) + \frac{\sigma^2_{spot\ speed}(t,s)}{v_{space}(t,s)} \qquad [5.7]$$

where $\sigma_{spot\ speed}(t,s)$ refers to the standard deviation of all the spot speeds measured at the centre of section s during time period t.

Table 5.2 Comparison of simulated and observed flow, space mean speed and time mean speed by time period

	Flow (vph)	
Time Period	**Simulated**	**Observed**
5:15 p.m. - 5:20 p.m.	6072	4860
5:20 p.m. - 5:25 p.m.	6672	8136
5:25 p.m. - 5:30 p.m.	5892	5760
Average	6212	6252
Mixed Error	0.1741	
	Space Mean Speed (kph)	
Time Period	**Simulated**	**Observed**
5:15 p.m. - 5:20 p.m.	14.93	21.92
5:20 p.m. - 5:25 p.m.	15.00	21.19
5:25 p.m. - 5:30 p.m.	14.86	15.91
Average	14.93	19.67
Mixed Error	0.2638	
	Time Mean Speed (kph)	
Time Period	**Simulated**	**Observed**
5:15 p.m. - 5:20 p.m.	18.99	29.05
5:20 p.m. - 5:25 p.m.	18.58	29.18
5:25 p.m. - 5:30 p.m.	17.86	25.19
Average	18.48	27.81
Mixed Error	0.3369	

Table 5.3 depicts the comparison of the simulated and observed flow, space mean speed and time mean speed by lane from 5:15 p.m. to 5:30 p.m. The simulated flow for each lane is shown to be highly consistent with the field observation with the mixed error less than 0.06. The simulation based on the proposed vehicle following model also reproduces the real-life space and time mean speed for each lane with the mixed errors around 0.16 and 0.23, respectively. In addition to the numerical comparison, Figure 5.4 displays the

graphical comparison of the simulated and observed flow, space mean speed and time mean speed by lane from 5:15 p.m. to 5:30 p.m. The reproduction of flow, space mean speed and time mean speed for each lane in the 15-minute period is clearly presented in Figure 5.4.

Table 5.3 Comparison of simulated and observed flow, space mean speed and time mean speed by lane

	Flow (vph)	
Lane	**Simulated**	**Observed**
1	1308	1369
2	932	925
3	756	799
4	1036	918
5	932	971
6	1248	1268
Average	1035	1042
Mixed Error	0.0595	
	Space Mean Speed (kph)	
Lane	**Simulated**	**Observed**
1	34.21	36.40
2	20.55	16.61
3	15.51	13.60
4	14.92	14.68
5	15.56	11.64
6	15.52	15.11
Average	19.38	18.01
Mixed Error	0.1572	
	Time Mean Speed (kph)	
Lane	**Simulated**	**Observed**
1	36.14	45.59
2	21.28	24.28
3	16.20	20.31
4	15.68	22.00
5	16.92	24.16
6	17.20	22.85
Average	20.57	26.53
Mixed Error	0.2317	

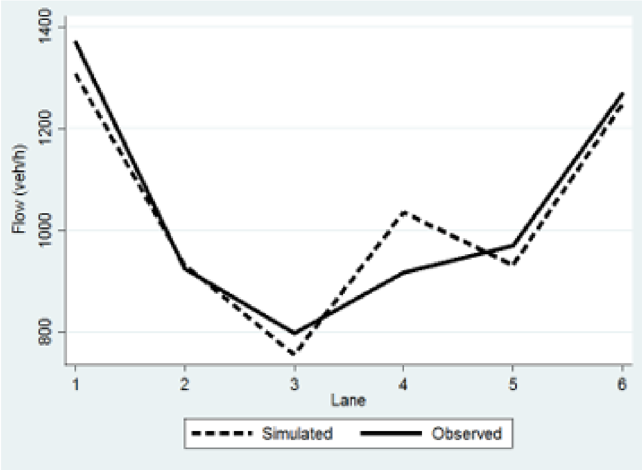

(a)

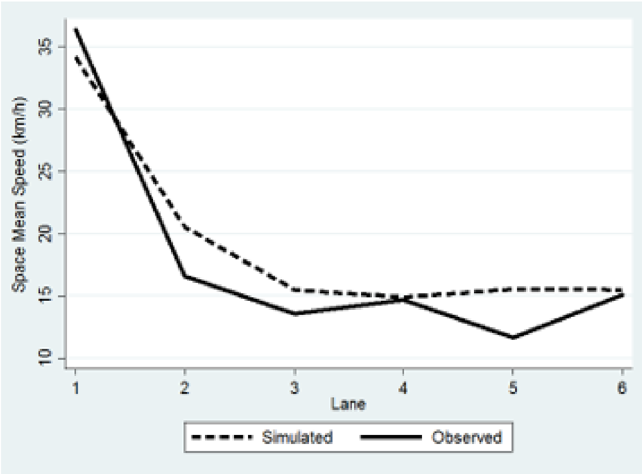

(b)

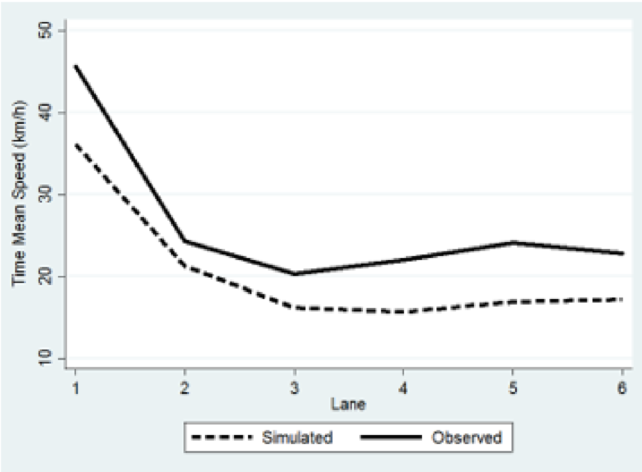

(c)

Figure 5.4 Comparison of simulated and observed flow, space mean speed and time mean speed by lane

5.5.3 On-Ramp Inflow, Freeway Inflow and Freeway Outflow

The input-output comparison of the simulation and the empirical data for the study area is conducted in this section. It should be noted that inflow and outflow are calculated by counting entering and exiting vehicles within a certain time period (not necessarily within an-hour period), respectively. In the study area, as shown in Figure 5.1, there are two entrances via the on-ramp and carriageway of the freeway as well as one exit via the carriageway of the freeway. Therefore, on-ramp inflow and freeway inflow refer to the number of the vehicles entering via the on-ramp and carriageway of the freeway, while freeway outflow is the number of the vehicles exiting via the carriageway of the freeway.

The comparison of the simulated and observed on-ramp inflow, freeway inflow and freeway outflow is conducted for three consecutive 5-minute periods from 5:15 p.m. to 5:30 p.m. as shown in Table 5.4. The simulated on-ramp inflow, freeway inflow and freeway inflow are shown to be close to the observed data for the three consecutive 5-minute periods and the entire 15-minute period with all the mixed errors less than 0.17.

Table 5.4 Comparison of simulated and observed on-ramp inflow, freeway inflow and freeway outflow by time period

	Time Period 5:15 p.m. - 5:20 p.m. Simulated	Observed
On-Ramp Inflow (veh)	63	81
Freeway Inflow (veh)	472	555
Freeway Outflow (veh)	506	613
Mixed Error	0.1676	
	Time Period 5:20 p.m. - 5:25 p.m. Simulated	**Observed**
On-Ramp Inflow (veh)	69	71
Freeway Inflow (veh)	465	558
Freeway Outflow (veh)	556	584
Mixed Error	0.1180	
	Time Period 5:25 p.m. - 5:30 p.m. Simulated	**Observed**
On-Ramp Inflow (veh)	68	48
Freeway Inflow (veh)	427	381
Freeway Outflow (veh)	491	518
Mixed Error	0.1271	
	Sum 5:15 p.m. - 5:30 p.m. Simulated	**Observed**
On-Ramp Inflow (veh)	200	200
Freeway Inflow (veh)	1364	1494
Freeway Outflow (veh)	1553	1715
Mixed Error	0.0884	

Table 5.5 presents the comparison of the simulated and observed freeway inflow by time period and lane from 5:15 p.m. to 5:30 p.m. Table 5.6 compares the freeway outflow obtained by the simulation and the field observation for each time period and lane. Based on the mixed error measure, the simulated freeway outflow for each time period and lane shows a better fit for the empirical data than the simulated freeway inflow. This is because Aimsun only allows users to set the overall input flow for each entrance rather than the specific input flow for each lane. In contrast, the output flow could be well controlled by the proposed vehicle following model along with other default driving behavioural models.

Table 5.5 Comparison of simulated and observed freeway inflow by time period and lane

	Time Period 5:15 p.m. - 5:20 p.m.	
Lane	**Simulated**	**Observed**
1	112	127
2	105	84
3	76	78
4	78	94
5	64	96
6	29	76
Average	77	93
Mixed Error	0.2987	
	Time Period 5:20 p.m. - 5:25 p.m.	
Lane	**Simulated**	**Observed**
1	107	128
2	105	91
3	78	89
4	74	89
5	61	83
6	33	78
Average	76	93
Mixed Error	0.2720	
	Time Period 5:25 p.m. - 5:30 p.m.	
Lane	**Simulated**	**Observed**
1	90	126
2	82	57
3	72	38
4	65	52
5	75	60
6	39	48
Average	71	64
Mixed Error	0.3980	
	Sum 5:15 p.m. - 5:30 p.m.	
Lane	**Simulated**	**Observed**
1	309	381
2	292	232
3	226	205
4	217	235
5	200	239
6	101	202
Average	224	249
Mixed Error	0.2448	

Table 5.6 Comparison of simulated and observed freeway outflow by time period and lane

	Time Period 5:15 p.m. - 5:20 p.m.	
Lane	**Simulated**	**Observed**
1	109	123
2	83	99
3	88	86
4	64	94
5	72	94
6	90	117
Average	84	102
Mixed Error	0.2027	
	Time Period 5:20 p.m. - 5:25 p.m.	
Lane	**Simulated**	**Observed**
1	123	136
2	86	94
3	62	83
4	93	85
5	79	77
6	113	109
Average	93	97
Mixed Error	0.1184	
	Time Period 5:25 p.m. - 5:30 p.m.	
Lane	**Simulated**	**Observed**
1	95	131
2	64	81
3	39	57
4	102	64
5	82	71
6	109	114
Average	82	86
Mixed Error	0.2902	
	Sum 5:15 p.m. - 5:30 p.m.	
Lane	**Simulated**	**Observed**
1	327	390
2	233	274
3	189	226
4	259	243
5	233	242
6	312	340
Average	259	286
Mixed Error	0.1233	

5.5.4 Simulated Traffic States of Before- and After-On-Ramp Sections

The simulated traffic states of the before- and after-on-ramp sections in the study area are studied in terms of flow, space mean speed and density. The availability of these quantities in Aimsun facilitates the comparison of macroscopic traffic. Flow, space mean speed and density are calculated for every one minute during the 15-minute simulation period (i.e., 5:15 p.m. to 5:30 p.m.). The before-on-ramp section is 128 metres long and comprised of six lanes on the carriageway and one on-ramp as shown in Figure 5.5. The after-on-ramp section includes six lanes on the main roadway (seven lanes in the merging section) and has the length of 375 metres as shown in Figure 5.6.

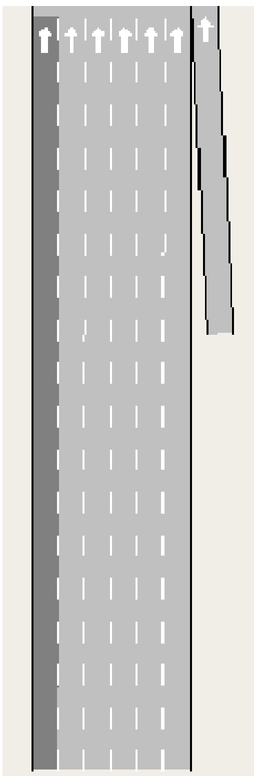

Figure 5.5 Before-on-ramp section of the study area in Aimsun

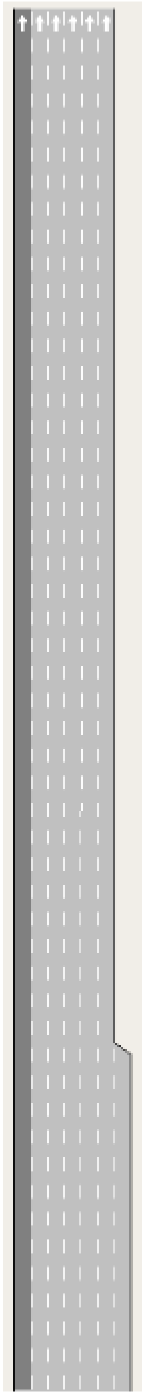

Figure 5.6 After-on-ramp section of the study area in Aimsun

Figure 5.7 displays the flow-density relation of the simulated traffic of the before- and after-on-ramp sections by lane. The green arrow in Figure 5.7 (a) shows an increasing flow with density, which suggests free-flow traffic state for lane 1 (HOV lane). The red arrows in Figure 5.7 (b) – (f) indicate a decline in flow as density grows, which represents congested traffic state for lane 2 to 6. Figures 5.8 and 5.9 describe the flow-speed and speed-density relations of the simulated traffic of the before- and after-on-ramp sections by lane. The free-flow state of lane 1 (green arrow) is also illustrated in Figures 5.8 (a) and 5.9 (a), while the congested state of lane 2 to 6 (red arrow) emerge in the rest of Figures 5.8 and 5.9.

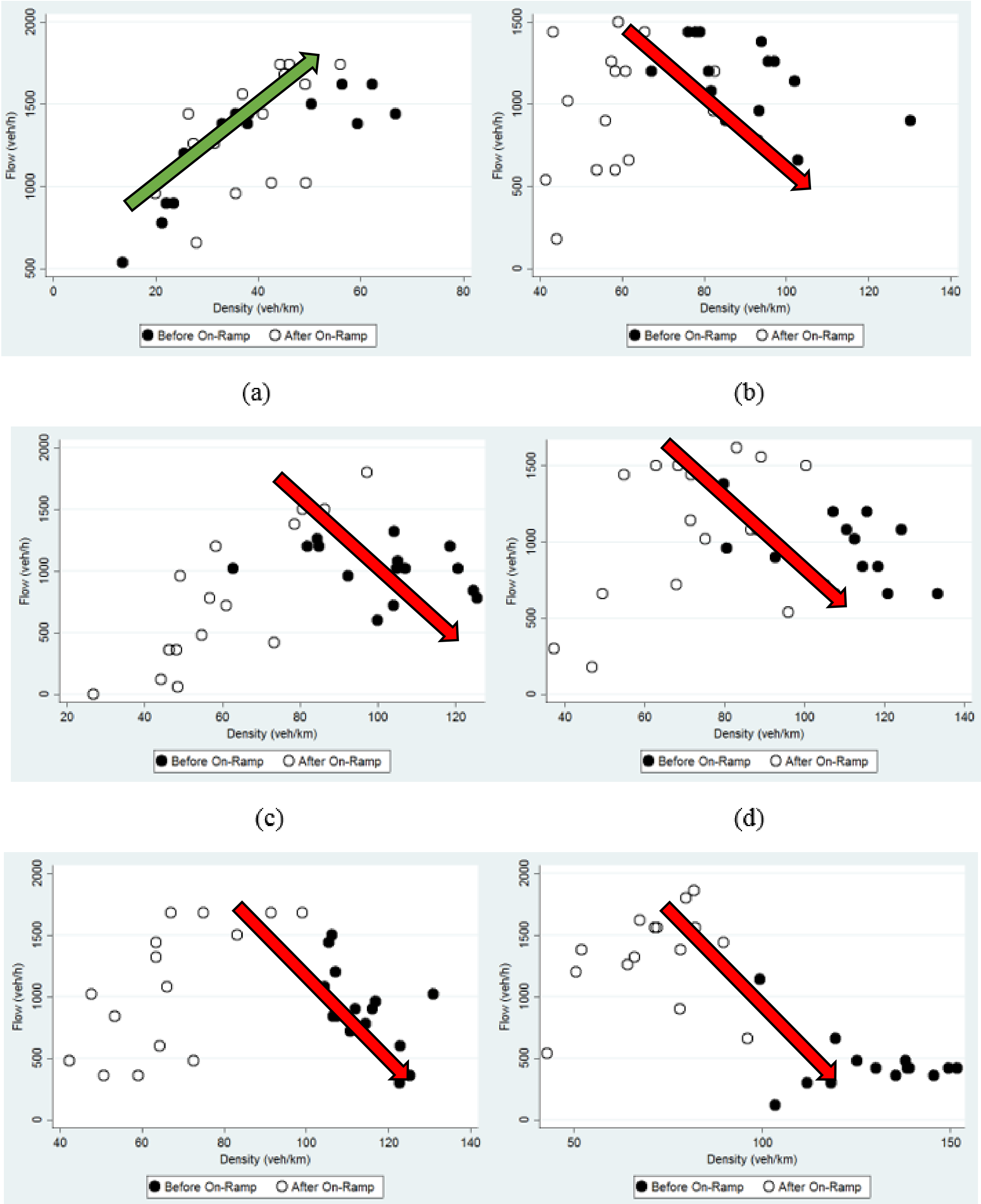

(a) (b)

(c) (d)

(e) (f)

Figure 5.7 Flow-density relation of simulated traffic of before- and after-on-ramp sections for (a) lane 1 to (f) lane 6

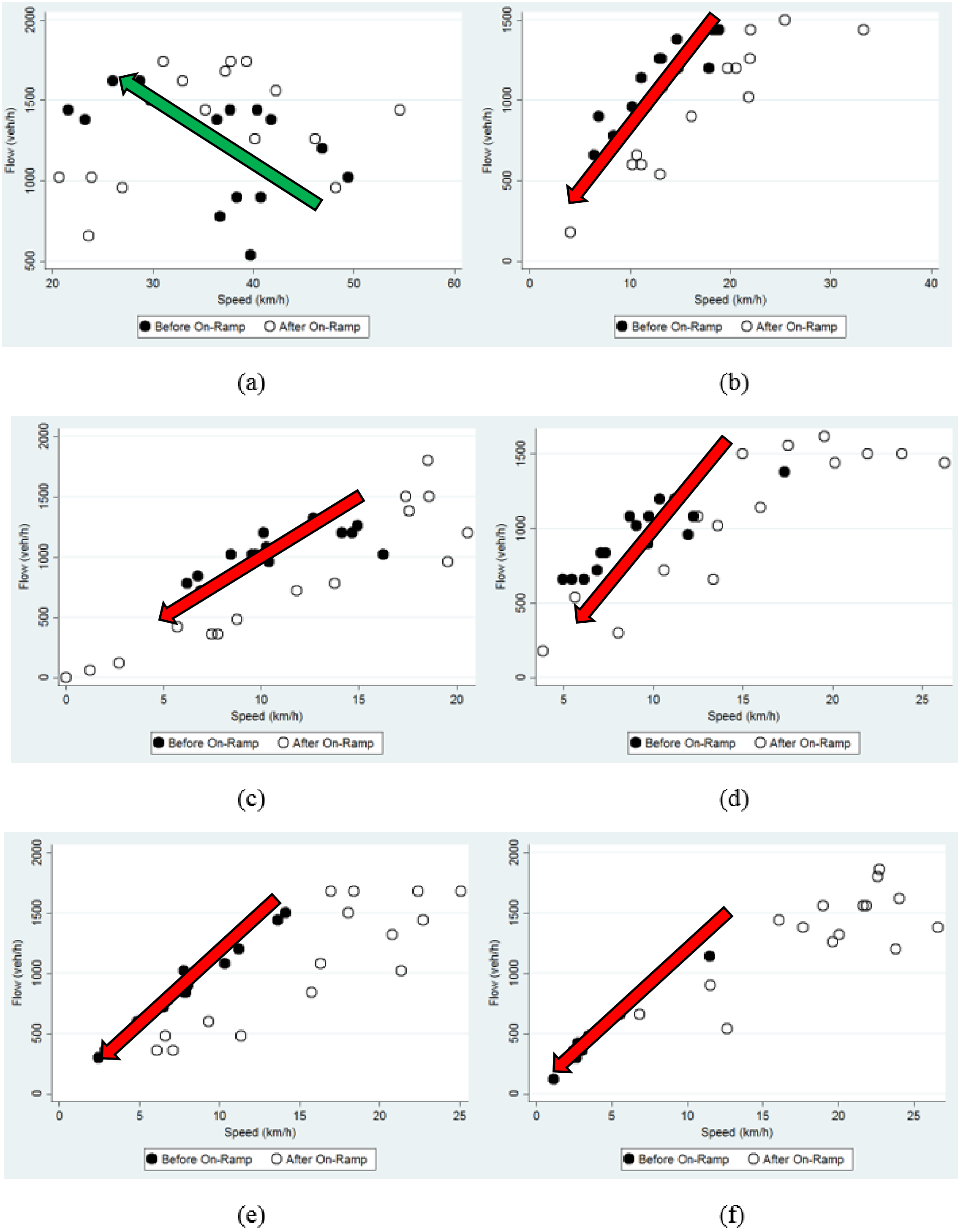

Figure 5.8 Flow-speed relation of simulated traffic of before- and after-on-ramp sections for (a) lane 1 to (f) lane 6

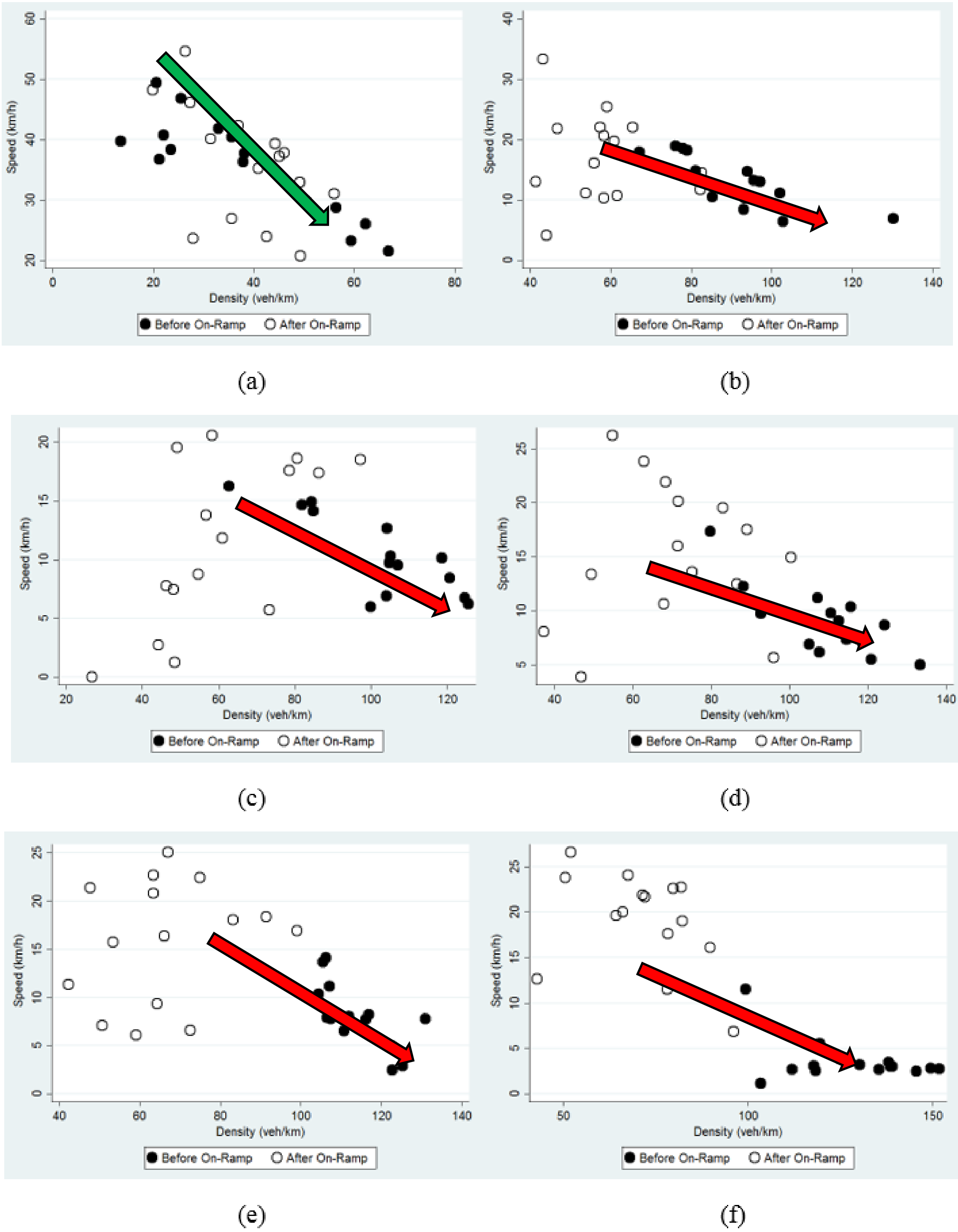

Figure 5.9 Speed-density relation of simulated traffic of before- and after-on-ramp sections for (a) lane 1 to (f) lane 6

Figure 5.10 displays three fundamental diagrams of the simulated macroscopic traffic of the before- and after-on-ramp sections. In all of the three fundamental diagrams (flow-density, flow-speed and speed-density relations), the before-on-ramp section shows a smoother transition from the free-flow state (green arrow) to the congested state (red arrow) than the after-on-ramp section. It is also found that some scattered points (in the blue circle) appear in the fundamental diagrams of the after-on-ramp section. The occurrence of these scattered points is attributed to traffic disturbance caused by the merging vehicles originating from the on-ramp.

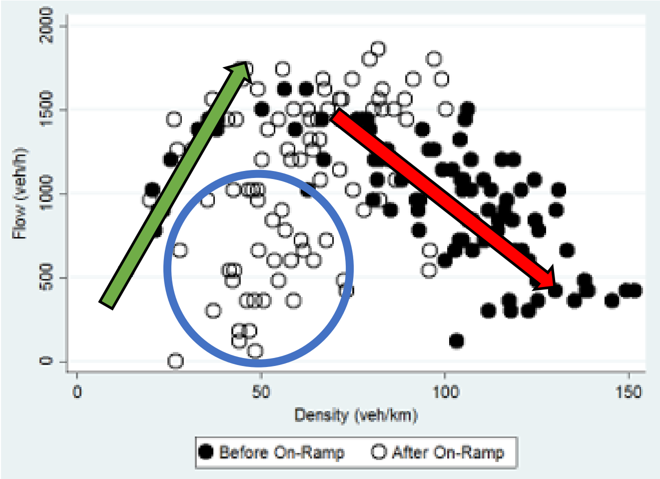

(a)

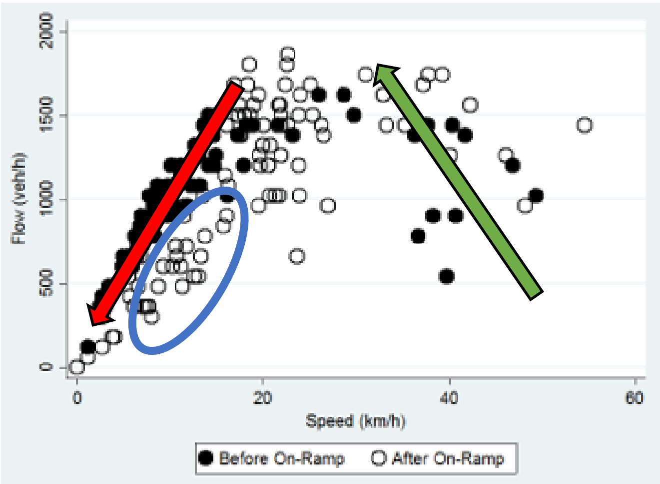

(b)

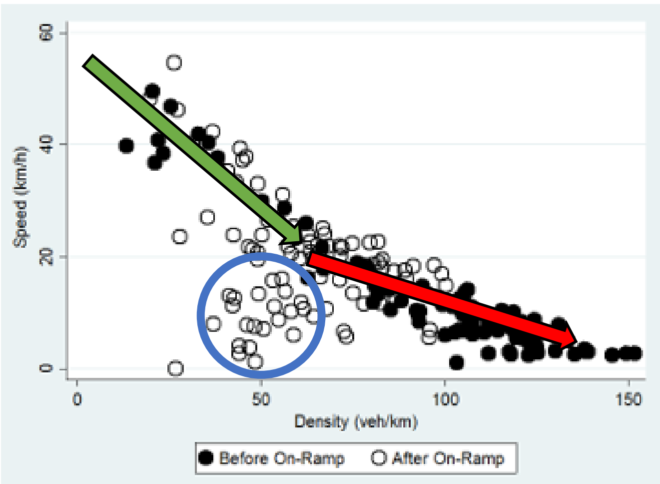

(c)

Figure 5.10 Comparison of simulated traffic of before- and after-on-ramp sections by (a) flow-density, (b) flow-speed and (c) speed-density relations

5.6 Conclusions

A simulation model in Aimsun is built in this chapter, which imitates the geometric design of the study area. The observed input flow of the study area is set to be traffic demand for the simulation. The proposed vehicle following model is incorporated into Aimsun through microSDK (Software Development Kit).

The comparison of the simulated and observed traffic dynamics of the study area is conducted in terms of flow, space mean speed and time mean speed. The input-output flow of the simulation and the field observation is also compared. The mixed error measure is used for effectively measuring the errors of the simulation. Based on the mixed error measurements, the simulation presents a reasonably accurate reproduction of the observed traffic dynamics of the study area.

The simulated traffic states of the before- and after-on-ramp section of the study area are analysed through fundamental diagrams. It is found that lane 1 (HOV lane) for both sections is in the free-flow traffic state while lanes 2-6 are in the distinct congested state from 5:15 p.m. to 5:30 p.m. In addition, the before-on-ramp section displays a smooth transition from the free-flow state to the congested state in the fundamental diagrams. As for the after-on-ramp section, some scattered points emerge in the fundamental diagrams. The occurrence of these scattered points is due to the traffic disruption caused by the merging vehicles originating from the on-ramp.

CHAPTER 6. THESIS CONCLUSIONS AND FUTURE RESEARCH

The study of this thesis proposes a vehicle following model that mathematically characterises perception and decision making. The corresponding flow-density relation is also derived. Perception of traffic dynamics and risk perception are introduced as the representation of perception while decision theory under risk and risk attitudes are incorporated for modelling decision making. Subsequently, the proposed model is empirically calibrated against the vehicle-trajectory data that were collected at a freeway section of I-80 Emeryville, California, U.S. Drivers' heterogeneity in perception and decision making under different types of vehicle following situations are therefore explored. The results of model prediction and simulation are further compared with the field observation, which demonstrates the ability of the proposed vehicle following model to reproduce the real-life traffic dynamics.

The key findings and conclusions drawn from each main chapter of this thesis are detailed below.

In Chapter 2, there are two gaps in the existing research of vehicle following. The first one is the insufficient mathematical specification and empirical calibration of drivers' perception (especially perception of traffic dynamics). Another lacuna lies in the lack of theoretic variation in modelling decision making in vehicle following. Due to the vital significance of perception and decision making in the decision process of vehicle following (Rothery, 1992), exploring research enhancements to these two components would provide novel insights into human decision associated with vehicle following. As an important attribute of driving, risk is indispensable in characterising the decision process of vehicle following. The consideration of risk in perception and decision making brings about the inclusion of risk perception and risk attitudes, respectively. These two risk attributes are the subjective appraisal of the probabilities and consequences of risks. They advance decision theoretic modelling by taking into account the presence of risk and quantifying the impact of risk on human perception and decision making. The literature on risk perception and risk attitudes has also been reviewed, demonstrating their significance within various areas of decisions under risk and their absence in the vehicle-following context. The author of this thesis thus expects they are of the similar significance in modelling perception and decision making of vehicle following.

In Chapter 3, the theoretical framework of modelling the decision process of vehicle following is elaborated. For perception of traffic dynamics, how the perception of time headway differs from the reality is studied by introducing the normal distribution of the perceived time headway. As for risk perception, the perceived crash probability is derived from the normal distribution of the perceived time headway while the perceived crash severity factor is embedded into the crash disutility function. As one of the classical decision theories under risk, state-dependent expected utility theory is used as a mathematical framework for modelling the decision making in vehicle following. Specifically, the concepts of subjective probability and state-dependent utility are utilised by the modelling of this thesis. Two states associated with vehicle following behaviour are crashing into the leading vehicle and staying safe. The parameter of risk attitudes is incorporated by deriving utility functions from the constant relative risk aversion model. Furthermore, some basic assumptions of the modelling of this thesis are presented. Under these assumptions, the vehicle following model is successfully proposed. In addition, the incorporation of the perceived time headway, risk perception and risk attitudes is mathematically specified. Besides the microscopic modelling, the flow-density relation is derived from the proposed vehicle following model. Through macroscopic sensitivity analysis, a more risk-averse attitude, the perception of a more severe crash, a greater standard deviation of perceived time headway, a longer time interval for calculating the future speed and a longer vehicle are found to reduce the capacity of traffic facilities and cause more congestion in macroscopic traffic.

In Chapter 4, the vehicle-trajectory data collected at a freeway section of I-80 Emeryville are used for the empirical calibration and validation. To make the original data suitable for model calibration and validation, some data processing techniques, such as smoothing, filtering, filling and segmentation, are applied. To investigate the proposed model in four types of vehicle following, the vehicle-trajectory data are segmented into four corresponding sub-datasets: Car follows

Car, Car follows Truck, Truck follows Car, and Truck follows Truck. Each sub-dataset is randomly separated into a calibration set (70%) and a validation set (30%). The calibration results are obtained by using a nonlinear least-squares method written in Stata by Danuso (1992) and Royston (1993). It is found that drivers when following a car show a more accurate and stable time-headway perception than following a truck. Truck drivers tend to have a more stable time-headway perception and less risk aversion than car drivers. When following a different type of vehicle, drivers are shown to perceive greater crash losses. Subsequently, the predicted space headway is compared with the observed value of the validation sets in terms of RMSE, R-squared of y=x fit, kernel density, and deviation histogram. The comparison results further validate the effectiveness of the proposed model and the relevant findings.

In Chapter 5, the simulation based on the proposed vehicle following model is successfully implemented in Aimsun. The comparison of the simulated and observed traffic dynamics of the study area is conducted in terms of flow, space mean speed and time mean speed. The input-output flow of the simulation and the field observation is also compared. Based on the mixed error measurements, the simulation presents a reasonably accurate reproduction of the observed traffic dynamics of the study area. The simulated traffic states of the before- and after-on-ramp section of the study area are analysed through fundamental diagrams. It is found that lane 1 (HOV lane) for both sections is in the free-flow traffic state while lane 2-6 are in the distinct congested state during 5:15 p.m. to 5:30 p.m. In addition, the before-on-ramp section displays a smooth transition from the free-flow state to the congested state in the fundamental diagrams. As for the after-on-ramp section, some scattered points emerge in the fundamental diagrams. The occurrence of these scattered points results from traffic disruption caused by the merging vehicles originating from the on-ramp.

Within the scope of vehicle following research, the study of this thesis bridges the gap in the existing literature that shows a lack of attention to perception and making in the decision process of vehicle following. Within the scope of transport research, the study of this thesis develops a fundamental modelling framework for unifying traffic operations and safety analysis both microscopically and macroscopically. Besides the accurate reproduction of traffic dynamics, the proposed model has the potential of interpreting risky driving behaviour and identifying dangerous driving spots when utilised for safety analysis. In addition, the proposed model provides an opportunity to evaluate the impacts of traffic management and road environment on drivers' perception and decision making.

Apart from transport, the study of this thesis has a promising application to insurance field. Real-time insurance which changes the insurance premiums based on driver performance does affect driving behaviour. The modelling framework proposed in the study of this thesis therefore facilitates the evaluation of such real-time insurance policies.

Future research directions are discussed to demonstrate the potential of the study of this thesis. There are three promising directions for future study. The first one is to evaluate the safety of the simulated traffic of the study area by using the Surrogate Safety Assessment Model (SSAM). The SSAM is an effective tool for assessing the safety of traffic facilities before accidents actually occur. Moreover, crash patterns of the simulation based on the proposed vehicle following model can be investigated by relaxing the safety constraints and compared with the realistic crash data.

The second direction is to collect the demographical data of drivers as well as their driving data. Through the empirical calibration of the proposed vehicle following model, the impact of drivers' demographical characteristics on risk attitudes and risk perception could be investigated.

The last one is to apply the proposed modelling framework to other driving behaviours such as lane changing and gap acceptance. A fundamentally new modelling framework incorporating risk perception and risk attitudes will be developed to study microscopic and macroscopic driving behaviour in a holistic manner.

REFERENCES

ALEXIADIS, V., COLYAR, J., HALKIAS, J., HRANAC, R. & MCHALE, G. 2004. The next generation simulation program. *Institute of Transportation Engineers. ITE Journal,* 74**,** 22.

ANDERSEN, G. J. & SAUER, C. W. 2007. Optical information for car following: The driving by visual angle (DVA) model. *Human factors,* 49**,** 878-896.

ANDERSEN, S., HARRISON, G. W., HOLE, A. R. & RUTSTRÖM, E. E. 2009. Non-linear mixed logit and the characterization of individual heterogeneity.

ANSCOMBE, F. J. & AUMANN, R. J. 1963. A definition of subjective probability. *The annals of mathematical statistics,* 34**,** 199-205.

ARBIS, D., DIXIT, V. V. & RASHIDI, T. H. 2016. Impact of risk attitudes and perception on game theoretic driving interactions and safety. *Accident Analysis & Prevention,* 94**,** 135-142.

ARDEKANI, S. A. 1984. The two-fluid characterization of urban traffic: Theory, observation, and experiment.

ARDEKANI, S. A., WILLIAMS, J. C. & BHAT, S. 1992. Influence of urban network features on quality of traffic service. *Transportation Research Record*.

ARROW, K. T. J. 1965. The theory of risk aversion. *Arrow KJ, Aspects of the theory of risk-bearing*.

AVINERI, E. 2006. The effect of reference point on stochastic network equilibrium. *Transportation Science,* 40**,** 409-420.

AVINERI, E. & PRASHKER, J. N. 2005. Sensitivity to travel time variability: travelers' learning perspective. *Transportation Research Part C: Emerging Technologies,* 13**,** 157-183.

AUSTRALIAN GOVERNMENT 2017. Road safety. [ONLINE] Available at: https://infrastructure.gov.au/roads/safety/. [Accessed 6 March 2018].

BARBERIS, N. C. 2013. Thirty years of prospect theory in economics: A review and assessment. *The Journal of Economic Perspectives,* 27**,** 173-195.

BECK, D. 2015. Investigation of key crash types: rear-end crashes in urban and rural environments.

BERNOULLI, D. 1738. Exposition of a New Theory on the Measurement of Risk. *Econometrica,* 22**,** 23-36.

BIJKERK, T. 2007. *Appraisal or Selection: Comparative analysis of traffic risk perception of French and Dutch drivers.* University of Twente.

BLANCHARD, O. J. & FISCHER, S. 1989. *Lectures on macroeconomics,* MIT press.

BLEICHRODT, H., VAN RIJN, J. & JOHANNESSON, M. 1999. Probability weighting and utility curvature in QALY-based decision making. *Journal of mathematical psychology,* 43**,** 238-260.

BROWN, I. & GROEGER, J. 1988. Risk perception and decision taking during the transition between novice and experienced driver status. *Ergonomics,* 31**,** 585-597.

BROWN, I. D. 1990. Drivers' margins of safety considered as a focus for research on error. *Ergonomics*, 33**,** 1307-1314.

CAMBRIDGESYSTEMATICS 2005a. NGSIM I-80 data analysis (05:00 p.m. to 05:15 p.m.) summary report, Federal Highway Administration.

CAMBRIDGESYSTEMATICS 2005b. NGSIM I-80 data analysis (05:15 p.m. to 05:30 p.m.) summary report, Federal Highway Administration.

CAMERER, C. F. & HO, T.-H. 1994. Violations of the betweenness axiom and nonlinearity in probability. *Journal of risk and uncertainty,* 8**,** 167-196.

CHANDLER, R. E., HERMAN, R. & MONTROLL, E. W. 1958. Traffic dynamics: studies in car following. *Operations research,* 6**,** 165-184.

CHARLTON, S. G. & LEWIS-EVANS, B. Explicit and implicit processes in behavioural adaptation to road width. AUSTRALASIAN ROAD SAFETY RESEARCH POLICING EDUCATION CONFERENCE, 2006, SURFERS PARADISE, QUEENSLAND, AUSTRALIA, 2006.

CHRISTENSEN, P. & AMUNDSEN, A. H. 2005. Speed and road accidents: an evaluation of the power model. *Nordic Road and Transport Research,* 17.

CLOGG, C. C., PETKOVA, E. & HARITOU, A. 1995. Statistical methods for comparing regression coefficients between models. *American Journal of Sociology,* 100**,** 1261-1293.

CONNORS, R. D. & SUMALEE, A. 2009. A network equilibrium model with travellers' perception of stochastic travel times. *Transportation Research Part B: Methodological,* 43**,** 614-624.

CRAMER, G. 1728. 1728.«Letters to Nicolas Bernoulli.». *J. Bernoulli*.

DANUSO, F. 1992. Nonlinear regression command. *Stata Technical Bulletin,* 1.

DAVIDSON, D. & SUPPES, P. 1956. A finitistic axiomatization of subjective probability and utility. *Econometrica: Journal of the Econometric Society***,** 264-275.

DE FINETTI, B. La prévision: ses lois logiques, ses sources subjectives. Annales de l'institut Henri Poincaré, 1937. 1-68.

DE FINETTI, B. 1974. *Theory of Probability: A Critical Introductory Treatment. Transl. by Antonio Machi and Adrian Smith,* J. Wiley.

DEJOY, D. M. 1992. An examination of gender differences in traffic accident risk perception. *Accident Analysis & Prevention,* 24**,** 237-246.

DIONNE, G. & HARRINGTON, S. E. 1992. An introduction to insurance economics. *Foundations of Insurance Economics.* Springer.

DIXIT, V., HARRISON, G. & RUTSTROM, E. Estimation of Subjective Beliefs of Crash among Drivers. Kuhmo Nectar Conference for Summer School of Transportation Economics Annual Conference of the ITEA, Stockholm, Sweden, 2011.

DIXIT, V., HARRISON, G. W. & RUTSTRÖM, E. E. 2014. Estimating the subjective risks of driving simulator accidents. *Accident Analysis & Prevention,* 62**,** 63-78.

DIXIT, V., WILMOT, C. & WOLSHON, B. 2012. Modeling risk attitudes in evacuation departure choices. *Transportation Research Record: Journal of the Transportation Research Board***,** 159-163.

DIXIT, V. V. 2013. Behavioural foundations of two-fluid model for urban traffic. *Transportation Research Part C: Emerging Technologies,* 35**,** 115-126.

DIXIT, V. V., HARB, R., MARTÍNEZ, J. & RUTSTRÖM, E. Eliciting risk attitudes from route choices over simulated driving choices. Transportation Research Board 92nd Annual Meeting, 2013.

DIXIT, V. V., HARB, R. C., MARTÍNEZ-CORREA, J. & RUTSTRÖM, E. E. 2015. Measuring risk aversion to guide transportation policy: Contexts, incentives, and respondents. *Transportation Research Part A: Policy and Practice,* 80**,** 15-34.

DULISSE, B. 1997. Methodological issues in testing the hypothesis of risk compensation. *Accident Analysis & Prevention,* 29**,** 285-292.

ELVIK, R., CHRISTENSEN, P. & AMUNDSEN, A. 2004. Speed and road accidents. *An evaluation of the Power Model. TØI report,* 740**,** 2004.

EVANS, L. & WASIELEWSKI, P. 1982. Do accident-involved drivers exhibit riskier everyday driving behavior? *Accident Analysis & Prevention,* 14**,** 57-64.

FARROW, J. A. & BRISSING, P. 1990. Risk for DWI: A new look at gender differences in drinking and driving influences, experiences, and attitudes among new adolescent drivers. *Health Education Quarterly,* 17**,** 213-221.

FINN, P. & BRAGG, B. W. 1986. Perception of the risk of an accident by young and older drivers. *Accident Analysis & Prevention,* 18**,** 289-298.

FRIEDMAN, M. & SAVAGE, L. J. 1948. The Utility Analysis of Choices Involving Risk. *Journal of Political Economy,* 56**,** 279-304.

GAZIS, D. C., HERMAN, R. & POTTS, R. B. 1959. Car-following theory of steady-state traffic flow. *Operations research,* 7**,** 499-505.

GAZIS, D. C., HERMAN, R. & ROTHERY, R. W. 1961. Nonlinear follow-the-leader models of traffic flow. *Operations research,* 9**,** 545-567.

GIPPS, P. 1986a. Multsim: a model for simulating vehicular traffic on multi-lane arterial roads. *Mathematics and Computers in Simulation,* 28**,** 291-295.

GIPPS, P. G. 1986b. A model for the structure of lane-changing decisions. *Transportation Research Part B: Methodological,* 20**,** 403-414.

GOOD, I. J. 1950. Probability and the Weighing of Evidence.

GRAYSON, G. & GROEGER, J. Risk, hazard perception, and perceived control. PROCEEDINGS OF THE NOVICE DRIVERS CONFERENCE HELD BRISTOL, UK, 1-2 JUNE 2000, 2000.

GRAYSON, G., MAYCOCK, G., GROEGER, J., HAMMOND, S. & FIELD, D. 2003. Risk, hazard perception and perceived control.

HACKING, I. 1984. *The emergence of probability: A philosophical study of early ideas about probability, induction and statistical inference,* Cambridge University Press.

HAMDAR, S., TREIBER, M., MAHMASSANI, H. & KESTING, A. 2008. Modeling driver behavior as sequential risk-taking task. *Transportation Research Record: Journal of the Transportation Research Board***,** 208-217.

HAMDAR, S. H., MAHMASSANI, H. S. & TREIBER, M. 2015. From behavioral psychology to acceleration modeling: Calibration, validation, and exploration of drivers' cognitive and safety parameters in a risk-taking environment. *Transportation Research Part B: Methodological,* 78**,** 32-53.

HAMDAR, S. H., TREIBER, M. & MAHMASSANI, H. S. Calibration of a stochastic car-following model using trajectory data: exploration and model properties. Transportation Research Board 88th Annual Meeting, 2009.

HARRISON, G. W., LAU, M. I. & RUTSTRÖM, E. E. 2007. Estimating risk attitudes in denmark: A field experiment*. *The Scandinavian Journal of Economics,* 109**,** 341-368.

HARRISON, G. W. & RUTSTRÖM, E. E. 2009. Expected utility theory and prospect theory: One wedding and a decent funeral. *Experimental Economics*, 12**,** 133-158.

HELLY, W. 1959. SIMULATION OF BOTTLENECKS IN SINGLE-LANE TRAFFIC FLOW. *Symp Theory Traffic Flow Research Laboratories General Motors***,** 207-238.

HENDERSON, V. & HOBSON, D. G. 2002. Real options with constant relative risk aversion. *Journal of Economic Dynamics and Control,* 27**,** 329-355.

HENSHER, D. A., GREENE, W. H. & LI, Z. 2011. Embedding risk attitude and decision weights in non-linear logit to accommodate time variability in the value of expected travel time savings. *Transportation research part B: methodological,* 45**,** 954-972.

HERMAN, R., MONTROLL, E. W., POTTS, R. B. & ROTHERY, R. W. 1959. Traffic dynamics: analysis of stability in car following. *Operations research,* 7**,** 86-106.

HERMAN, R. & ROTHERY, R. W. Car following and steady-state flow. Proceedings of the 2nd International Symposium on the Theory of Traffic Flow. Ed J. Almond, OECD, Paris, 1965.

HOEDEMAEKER, M. & BROOKHUIS, K. A. 1998. Behavioural adaptation to driving with an adaptive cruise control (ACC). *Transportation Research Part F: Traffic Psychology and Behaviour,* 1**,** 95-106.

HOLT, C. A. & LAURY, S. 2002. Risk aversion and incentive effects.

HUMPHREY, N. 1998. Managing speed: Review of current practice for setting and enforcing speed limits.

JIANG, R., WU, Q. & ZHU, Z. 2001. Full velocity difference model for a car-following theory. *Physical Review E,* 64**,** 017101.

JIN, S., WANG, D.-H., HUANG, Z.-Y. & TAO, P.-F. 2011. Visual angle model for car-following theory. *Physica A: Statistical Mechanics and its Applications,* 390**,** 1931-1940.

JONAH, B. A. 1986. Accident risk and risk-taking behaviour among young drivers. *Accident Analysis & Prevention,* 18**,** 255-271.

JONAH, B. A., THIESSEN, R. & AU-YEUNG, E. 2001. Sensation seeking, risky driving and behavioral adaptation. *Accident Analysis & Prevention,* 33**,** 679-684.

KAHNEMAN, D. & TVERSKY, A. 1979. Prospect theory: An analysis of decision under risk. *Econometrica: Journal of the Econometric Society***,** 263-291.

KARNI, E. 1985. *Decision making under uncertainty: The case of state-dependent preferences*.

KARNI, E. 1987. Generalized expected utility analysis of risk aversion with state-dependent preferences. *International Economic Review***,** 229-240.

KARNI, E. 1990. State-dependent preferences. *Utility and Probability.* Springer.

KARNI, E. 1993a. A definition of subjective probabilities with state-dependent preferences. *Econometrica,* 61**,** 187-198.

KARNI, E. 1993b. Subjective expected utility theory with state-dependent preferences. *Journal of Economic Theory,* 60**,** 428-438.

KARNI, E., SCHMEIDLER, D. & VIND, K. 1983. On state dependent preferences and subjective probabilities. *Econometrica: Journal of the Econometric Society***,** 1021-1031.

KELSEY, D. 1992. Risk and risk aversion for state-dependent utility. *Theory and decision,* 33**,** 71-82.

KESTING, A. & TREIBER, M. 2008. Calibrating car-following models by using trajectory data: Methodological study. *Transportation Research Record: Journal of the Transportation Research Board***,** 148-156.

KOMETANI, E. & SASAKI, T. 1959. DYNAMIC BEHAVIOUR OF TRAFFIC WITH A NON-LINEAR SPACING- SPEED RELATIONSHIP. *Symp Theory Traffic Flow Research Laboratories General Motors*.

KONDOH, T., YAMAMURA, T., KITAZAKI, S., KUGE, N. & BOER, E. R. 2008. Identification of visual cues and quantification of drivers' perception of proximity risk to the lead vehicle in car-following situations. *Journal of Mechanical Systems for Transportation and Logistics,* 1**,** 170-180.

KOOPMAN, B. O. 1940. The axioms and algebra of intuitive probability. *Annals of mathematics***,** 269-292.

KOORNSTRA, M. J. 2009. Risk-adaptation theory. *Transportation research part F: traffic psychology and behaviour,* 12**,** 77-90.

KŐSZEGI, B. & RABIN, M. 2006. A model of reference-dependent preferences. *The Quarterly Journal of Economics,* 121**,** 1133-1165.

KŐSZEGI, B. & RABIN, M. 2007. Reference-dependent risk attitudes. *American Economic Review,* 97**,** 1047-1073.

KŐSZEGI, B. & RABIN, M. 2009. Reference-dependent consumption plans. *The American Economic Review,* 99**,** 909-936.

KRAFT, C. H., PRATT, J. W. & SEIDENBERG, A. 1959. Intuitive probability on finite sets. *The Annals of Mathematical Statistics,* 30**,** 408-419.

KREMSLEHNER, R. & MUERMANN, A. 2009. State-Dependent Preferences and Insurance Demand.

LEWIS-EVANS, B. & CHARLTON, S. G. 2006. Explicit and implicit processes in behavioural adaptation to road width. *Accident Analysis & Prevention,* 38**,** 610-617.

LI, Z. & HENSHER, D. 2011. Prospect theoretic contributions in understanding traveller behaviour: a review and some comments. *Transport reviews,* 31**,** 97-115.

LI, Z., TIRACHINI, A. & HENSHER, D. A. 2012. Embedding risk attitudes in a scheduling model: application to the study of commuting departure time. *Transportation science,* 46**,** 170-188.

LU, G., CHENG, B., LIN, Q. & WANG, Y. 2012. Quantitative indicator of homeostatic risk perception in car following. *Safety science,* 50**,** 1898-1905.

LU, G., CHENG, B., WANG, Y. & LIN, Q. 2013. A car-following model based on quantified homeostatic risk perception. *Mathematical Problems in Engineering,* 2013.

LUCE, R. D. & KRUMHANSL, C. L. 1988. Measurement, scaling, and psychophysics. *Stevens' handbook of experimental psychology,* 1**,** 3-74.

LUCE, R. D. & RAIFFA, H. 2012. *Games and decisions: Introduction and critical survey*, Courier Corporation.

MALNACA, K. Risk homeostasis theory in traffic safety. Proceedings of the 21th ICTCT Workshop, 2008.

MATHEW, T. V. & RAO, K. K. 2017. Fundamental relations of traffic flow. *Lecture Notes in Transportation Systems Engineering. Department of Civil Engineering, Indian Institute of Technology Bomday, India.*

MATTHEWS, M. L. & MORAN, A. R. 1986. Age differences in male drivers' perception of accident risk: The role of perceived driving ability. *Accident Analysis & Prevention,* 18**,** 299-313.

MICHAELS, R. Perceptual factors in car following. Proceedings of the 2nd International Symposium on the Theory of Road Traffic Flow (London, England), OECD, 1963.

NEWELL, G. F. 1961. Nonlinear effects in the dynamics of car following. *Operations research,* 9**,** 209-229.

PALACIOS-HUERTA, I. & SERRANO, R. 2006. Rejecting small gambles under expected utility. *Economics Letters,* 91**,** 250-259.

PIPES, L. A. 1953. An operational analysis of traffic dynamics. *Journal of applied physics,* 24**,** 274-281.

PRATT, J. W. 1964. Risk aversion in the small and in the large. *Econometrica: Journal of the Econometric Society***,** 122-136.

PRATT, J. W., RAIFFA, H. & SCHLAIFER, R. 1964. The foundations of decision under uncertainty: An elementary exposition. *Journal of the American Statistical Association,* 59**,** 353-375.

PRIGOGINE, I. & HERMAN, R. 1971. Kinetic theory of vehicular traffic.

RAMSEY, F. P. 1926. The foundations of mathematics. *Proceedings of the London Mathematical Society,* 2**,** 338-384.

REINHARDT-RUTLAND, A. 2001. Seat-belts and behavioural adaptation: the loss of looming as a negative reinforcer. *Safety science,* 39**,** 145-155.

REY, D., DIXIT, V. V., YGNACE, J.-L. & WALLER, S. T. 2016. An endogenous lottery-based incentive mechanism to promote off-peak usage in congested transit systems. *Transport Policy,* 46**,** 46-55.

ROTHERY, R. W. 1992. Car following models. *Trac Flow Theory*.

ROYSTON, P. 1993. Standard nonlinear curve fits update. *Stata Technical Bulletin,* 2.

RUNDMO, T. & IVERSEN, H. 2004. Risk perception and driving behaviour among adolescents in two Norwegian counties before and after a traffic safety campaign. *Safety science,* 42**,** 1-21.

SAIFUZZAMAN, M. & ZHENG, Z. 2014. Incorporating human-factors in car-following models: a review of recent developments and research needs. *Transportation research part C: emerging technologies,* 48**,** 379-403.

SAVAGE, L. J. 1954. *The foundations of statistics,* Courier Corporation.

SCHOEMAKER, P. J. 1982. The expected utility model: Its variants, purposes, evidence and limitations. *Journal of economic literature***,** 529-563.

SENBIL, M. & KITAMURA, R. 2005. Heterogeneity in commuter departure time decision: A prospect theoretic approach. *Applied Research in Uncertainty Modeling and Analysis***,** 369-398.

SIREN, A. & KJÆR, M. R. 2011. How is the older road users' perception of risk constructed? *Transportation research part F: traffic psychology and behaviour,* 14**,** 222-228.

SLOVIC, P. & WEBER, E. U. 2002. Perception of Risk Posed by Extreme Events.

SUPPES, P. 1969. The role of subjective probability and utility in decision-making. *Studies in the Methodology and Foundations of Science.* Springer.

TALEBPOUR, A., MAHMASSANI, H. & HAMDAR, S. 2011. Multiregime Sequential Risk-Taking Model of Car-Following Behavior: Specification, Calibration, and Sensitivity Analysis. *Transportation Research Record: Journal of the Transportation Research Board***,** 60-66.

TARKO, A. P. 2009. Modeling drivers' speed selection as a trade-off behavior. *Accident Analysis & Prevention,* 41**,** 608-616.

TAYLOR, D. 1964. Drivers' galvanic skin response and the risk of accident. *Ergonomics,* 7**,** 439-451.

THIEMANN, C., TREIBER, M. & KESTING, A. 2008. Estimating acceleration and lane-changing dynamics from next generation simulation trajectory data. *Transportation Research Record: Journal of the Transportation Research Board***,** 90-101.

THOMAS, J. A. & WALTON, D. 2007. Measuring perceived risk: Self-reported and actual hand positions of SUV and car drivers. *Transportation research part F: traffic psychology and behaviour,* 10**,** 201-207.

TRANSPORT FOR NSW 2017. Road traffic casualty crashes in New South Wales. [ONLINE] Available at: http://roadsafety.transport.nsw.gov.au /downloads/crashstats2016.pdf. [Accessed 6 March 2018].

TRIMPOP, R. M. 1996. Risk homeostasis theory: problems of the past and promises for the future. *Safety Science,* 22**,** 119-130.

TVERSKY, A. & KAHNEMAN, D. 1986. Rational choice and the framing of decisions. *Journal of business***,** S251-S278.

TVERSKY, A. & KAHNEMAN, D. 1992. Advances in prospect theory: Cumulative representation of uncertainty. *Journal of Risk and uncertainty,* 5**,** 297-323.

ULLEBERG, P. & RUNDMO, T. 2003. Personality, attitudes and risk perception as predictors of risky driving behaviour among young drivers. *Safety science,* 41**,** 427-443.

VISCUSI, W. K. & EVANS, W. N. 1990. Utility functions that depend on health status: estimates and economic implications. *The American Economic Review***,** 353-374.

VO, P., MATTINGLY, S., ARDEKANI, S. & DILSHAD, Y. 2007. Comparison of quality of service in two central business districts: two-fluid model approach in Texas. *Transportation Research Record: Journal of the Transportation Research Board***,** 180-188.

VON NEUMANN, J. & MORGENSTERN, O. 1947. Theory of games and economic behavior, 2nd rev.

VROLIX, K. 2006. Behavioural adaptation, risk compensation, risk homeostasis and moral hazard in traffic safety. literature review. No. RA-2006-95.

WAKKER, P. P. 2008. Explaining the characteristics of the power (CRRA) utility family. *Health economics,* 17**,** 1329-1344.

WAKKER, P. P. & ZANK, H. 1999. State dependent expected utility for Savage's state space. *Mathematics of Operations Research,* 24**,** 8-34.

WARD, H., ROBERTSON, S. & ALLSOP, R. Managing speeds of traffic on European roads: Non-accident external and internal effects of vehicle use and how these depend on speed. Proceedings of the 9th International Conference on Road Safety in Europe, 1998. 21-23.

WEINBLATT, H., MINGE, E. & PETERSEN, S. 2013. Length-Based Vehicle Classification Schemes and Length Bin Boundaries. *Transportation Research Record: Journal of the Transportation Research Board***,** 19-29.

WIEDEMANN, R. 1994. Simulation des Straßenverkehrsflusses. Schriftenreihe Heft 8. *Institute for Transportation Science, University of Karlsruhe, Germany*.

WILDE, G. J. 1982a. Critical issues in risk homeostasis theory. *Risk Analysis,* 2**,** 249-258.

WILDE, G. J. 1982b. The theory of risk homeostasis: implications for safety and health. *Risk analysis,* 2**,** 209-225.

APPENDIX A: DETAILED MICROSCOPIC FORMULATION

$$SH_n(t+\tau) \leq L_{n-1}$$

$$SH_n(t+\tau) = SH_n(t) + v_{n-1}(t) * \tau$$
$$-\left(v_n(t) * \tau + \frac{1}{2} * \left(\frac{v_n(t+\tau) - v_n(t)}{\tau}\right) * \tau^2\right)$$

$$SH_n(t) + v_{n-1}(t) * \tau - \left(v_n(t) * \tau + \frac{1}{2} * \left(\frac{v_n(t+\tau) - v_n(t)}{\tau}\right) * \tau^2\right) \leq L_{n-1}$$

$$v_n(t) \neq 0$$

$$\frac{SH_n(t) + v_{n-1}(t) * \tau - \left(v_n(t) * \tau + \frac{1}{2} * \left(\frac{v_n(t+\tau) - v_n(t)}{\tau}\right) * \tau^2\right)}{v_n(t)} \leq \frac{L_{n-1}}{v_n(t)}$$

$$\frac{SH_n(t)}{v_n(t)} \leq \frac{L_{n-1} - v_{n-1}(t) * \tau + \left(v_n(t) * \tau + \frac{1}{2} * \left(\frac{v_n(t+\tau) - v_n(t)}{\tau}\right) * \tau^2\right)}{v_n(t)}$$

$$TH_n(t) = \frac{SH_n(t)}{v_n(t)}$$

$$\leq \frac{L_{n-1} - v_{n-1}(t) * \tau + \left(v_n(t) * \tau + \frac{1}{2} * \left(\frac{v_n(t+\tau) - v_n(t)}{\tau}\right) * \tau^2\right)}{v_n(t)}$$

$$= TH_n^{critical}(t)$$

$$TH_n^*(t) \leq TH_n^{critical}(t)$$

$$P_c = P\left(TH_n^*(t) \leq TH_n^{critical}(t)\right)$$

$$TH_n^*(t) \backsim N(TH_n(t), \sigma^2)$$

$$TH_n^*(t) = TH_n(t) + \sigma Z$$

$$P\left(TH_n^*(t) \leq TH_n^{critical}(t)\right) = P\left(TH_n(t) + \sigma Z \leq TH_n^{critical}(t)\right)$$

$$= P\left(Z \leq \frac{TH_n^{critical}(t) - TH_n(t)}{\sigma}\right)$$

$$P\left(Z \leq \frac{TH_n^{critical}(t) - TH_n(t)}{\sigma}\right) = \Phi\left(\frac{TH_n^{critical}(t) - TH_n(t)}{\sigma}\right)$$

$$P_s = 1 - P_c = 1 - \Phi\left(\frac{TH_n^{critical}(t) - TH_n(t)}{\sigma}\right)$$

$$U_s = \frac{v_n(t+\tau)^{1-\gamma}}{1-\gamma}$$

$$U_c = -\omega * \frac{v_n(t)^{2*(1-\gamma)}}{1-\gamma}$$

$$EU = P_s U_s + P_c U_c$$

$$EU = \frac{v_n(t+\tau)^{1-\gamma}}{1-\gamma} * \left(1 - \Phi\left(\frac{TH_n^{critical}(t) - TH_n(t)}{\sigma}\right)\right)$$

$$+\Phi\left(\frac{TH_n^{critical}(t) - TH_n(t)}{\sigma}\right) * \left(-\omega * \frac{v_n(t)^{2*(1-\gamma)}}{1-\gamma}\right)$$

$$\Phi\left(\frac{TH_n^{critical}(t) - TH_n(t)}{\sigma}\right) = \frac{1}{\sqrt{2*\pi}} * \int_{-\infty}^{\frac{TH_n^{critical}(t) - TH_n(t)}{\sigma}} e^{-\frac{t^2}{2}} dt$$

$$\frac{d\left(\frac{TH_n^{critical}(t) - TH_n(t)}{\sigma}\right)}{dv_n(t+\tau)}$$

$$= \frac{d\left(\frac{L_{n-1} - v_{n-1}(t)*\tau + \left(v_n(t)*\tau + \frac{1}{2}*\left(\frac{v_n(t+\tau) - v_n(t)}{\tau}\right)*\tau^2\right) - SH_n(t)}{v_n(t)*\sigma}\right)}{dv_n(t+\tau)}$$

$$= \frac{\tau}{2*v_n(t)*\sigma}$$

Leibniz's rule for differentiation under the integral sign

$$\frac{d\Phi\left(\frac{TH_n^{critical}(t)-TH_n(t)}{\sigma}\right)}{dv_n(t+\tau)}=\frac{e^{-\frac{\left(\frac{TH_n^{critical}(t)-TH_n(t)}{\sigma}\right)^2}{2}}*\frac{\tau}{2*v_n(t)*\sigma}}{\sqrt{2*\pi}}$$

$$=\frac{\tau*e^{-\frac{\left(\frac{TH_n^{critical}(t)-TH_n(t)}{\sigma}\right)^2}{2}}}{2*v_n(t)*\sqrt{2*\pi}*\sigma}$$

$$\frac{dEU}{dv_n(t+\tau)}=v_n(t+\tau)^{-\gamma}*\left(1-\ \Phi\left(\frac{TH_n^{critical}(t)-TH_n(t)}{\sigma}\right)\right)$$

$$+\frac{v_n(t+\tau)^{1-\gamma}}{1-\gamma}*\left(-\frac{\tau*e^{-\frac{\left(\frac{TH_n^{critical}(t)-TH_n(t)}{\sigma}\right)^2}{2}}}{2*v_n(t)*\sqrt{2*\pi}*\sigma}\right)$$

$$+\frac{\tau*e^{-\frac{\left(\frac{TH_n^{critical}(t)-TH_n(t)}{\sigma}\right)^2}{2}}}{2*v_n(t)*\sqrt{2*\pi}*\sigma}*\left(-\omega*\frac{v_n(t)^{2*(1-\gamma)}}{1-\gamma}\right)=0$$

$$v_n(t+\tau)^{-\gamma}*\left(1-\ \Phi\left(\frac{TH_n^{critical}(t)-TH_n(t)}{\sigma}\right)\right)$$

$$=\frac{v_n(t+\tau)^{1-\gamma}}{1-\gamma}*\frac{\tau*e^{-\frac{\left(\frac{TH_n^{critical}(t)-TH_n(t)}{\sigma}\right)^2}{2}}}{2*v_n(t)*\sqrt{2*\pi}*\sigma}$$

$$+\frac{\tau*e^{-\frac{\left(\frac{TH_n^{critical}(t)-TH_n(t)}{\sigma}\right)^2}{2}}}{2*v_n(t)*\sqrt{2*\pi}*\sigma}*\omega*\frac{v_n(t)^{2*(1-\gamma)}}{1-\gamma}$$

$$v_n(t+\tau)^{-\gamma} * \left(1 - \Phi\left(\frac{TH_n^{critical}(t) - TH_n(t)}{\sigma}\right)\right)$$

$$= \left(\frac{v_n(t+\tau)^{1-\gamma}}{1-\gamma} + \omega * \frac{v_n(t)^{2*(1-\gamma)}}{1-\gamma}\right) * \frac{\tau * e^{-\frac{\left(\frac{TH_n^{critical}(t) - TH_n(t)}{\sigma}\right)^2}{2}}}{2 * v_n(t) * \sqrt{2 * \pi} * \sigma}$$

$$\frac{v_n(t+\tau)^{-\gamma} * \left(1 - \Phi\left(\frac{TH_n^{critical}(t) - TH_n(t)}{\sigma}\right)\right) * (1-\gamma)}{v_n(t+\tau)^{1-\gamma} + \omega * v_n(t)^{2*(1-\gamma)}}$$

$$= \frac{\tau * e^{-\frac{\left(\frac{TH_n^{critical}(t) - TH_n(t)}{\sigma}\right)^2}{2}}}{2 * v_n(t) * \sqrt{2 * \pi} * \sigma}$$

$$\tau > 0$$

$$\frac{2 * v_n(t) * \sqrt{2 * \pi} * \sigma * v_n(t+\tau)^{-\gamma} * \left(1 - \Phi\left(\frac{TH_n^{critical}(t) - TH_n(t)}{\sigma}\right)\right) * (1-\gamma)}{\left(v_n(t+\tau)^{1-\gamma} + \omega * v_n(t)^{2*(1-\gamma)}\right) * \tau}$$

$$= e^{-\frac{\left(\frac{TH_n^{critical}(t) - TH_n(t)}{\sigma}\right)^2}{2}}$$

Suppose $v_n(t+\tau) = 0$,

1) $\gamma = 0$, $v_n(t+\tau)^{-\gamma}$ becomes 0^0, and it is undefined.

2) $\gamma > 0$, $v_n(t+\tau)^{-\gamma}$ is infinity

3) $\gamma < 0$, $v_n(t+\tau)^{-\gamma} = 0$, thus

$$\frac{2 * v_n(t) * \sqrt{2 * \pi} * v_n(t+\tau)^{-\gamma} * \left(1 - \Phi\left(\frac{TH_n^{critical}(t) - TH_n(t)}{\sigma}\right)\right) * (1-\gamma)}{\left(v_n(t+\tau)^{1-\gamma} + \omega * v_n(t)^{2*(1-\gamma)}\right) * \tau} = 0,$$ which conflicts with

$$e^{-\frac{\left(\frac{TH_n^{critical}(t) - TH_n(t)}{\sigma}\right)^2}{2}} > 0.$$

Hence, $v_n(t+\tau) \neq 0$.

$$ln\left(\frac{2 * v_n(t) * \sqrt{2 * \pi} * \sigma * v_n(t+\tau)^{-\gamma} * \left(1 - \Phi\left(\frac{TH_n^{critical}(t) - TH_n(t)}{\sigma}\right)\right) * (1-\gamma)}{\left(v_n(t+\tau)^{1-\gamma} + \omega * v_n(t)^{2*(1-\gamma)}\right) * \tau}\right)$$

$$= -\frac{\left(\frac{TH_n^{critical}(t) - TH_n(t)}{\sigma}\right)^2}{2}$$

$$-2 * ln\left(\frac{2 * v_n(t) * \sqrt{2 * \pi} * \sigma * v_n(t+\tau)^{-\gamma} * \left(1 - \Phi\left(\frac{TH_n^{critical}(t) - TH_n(t)}{\sigma}\right)\right) * (1-\gamma)}{\left(v_n(t+\tau)^{1-\gamma} + \omega * v_n(t)^{2*(1-\gamma)}\right) * \tau}\right)$$

$$= \left(\frac{TH_n^{critical}(t) - TH_n(t)}{\sigma}\right)^2$$

$$1 - \Phi\left(\frac{TH_n^{critical}(t) - TH_n(t)}{\sigma}\right) \cong 1$$

$$\Phi\left(\frac{TH_n^{critical}(t) - TH_n(t)}{\sigma}\right) < 0.5$$

$$\frac{TH_n^{critical}(t) - TH_n(t)}{\sigma} < 0$$

$$-\sqrt{-2 * ln\left(\frac{2 * v_n(t) * \sqrt{2 * \pi} * \sigma * v_n(t+\tau)^{-\gamma} * (1-\gamma)}{(v_n(t+\tau)^{1-\gamma} + \omega * v_n(t)^{2*(1-\gamma)}) * \tau}\right)}$$

$$= \frac{TH_n^{critical}(t) - TH_n(t)}{\sigma}$$

$$-\sqrt{-2 * ln\left(\frac{2 * v_n(t) * \sqrt{2 * \pi} * \sigma * v_n(t+\tau)^{-\gamma} * (1-\gamma)}{(v_n(t+\tau)^{1-\gamma} + \omega * v_n(t)^{2*(1-\gamma)}) * \tau}\right)}$$

$$= \frac{L_{n-1} - v_{n-1}(t) * \tau + \left(v_n(t) * \tau + \frac{1}{2} * \left(\frac{v_n(t+\tau) - v_n(t)}{\tau}\right) * \tau^2\right) - SH_n(t)}{v_n(t) * \sigma}$$

$$-v_n(t) * \sigma * \sqrt{-2 * ln\left(\frac{2 * v_n(t) * \sqrt{2 * \pi} * \sigma * v_n(t+\tau)^{-\gamma} * (1-\gamma)}{(v_n(t+\tau)^{1-\gamma} + \omega * v_n(t)^{2*(1-\gamma)}) * \tau}\right)}$$

$$= L_{n-1} - v_{n-1}(t) * \tau + \left(v_n(t) * \tau + \frac{1}{2} * \left(\frac{v_n(t+\tau) - v_n(t)}{\tau}\right) * \tau^2\right) - SH_n(t)$$

$$SH_n(t) = L_{n-1} - v_{n-1}(t) * \tau + \left(v_n(t) * \tau + \frac{1}{2} * \left(\frac{v_n(t+\tau) - v_n(t)}{\tau}\right) * \tau^2\right)$$

$$+v_n(t) * \sigma * \sqrt{-2 * ln\left(\frac{2 * v_n(t) * \sqrt{2 * \pi} * \sigma * v_n(t+\tau)^{-\gamma} * (1-\gamma)}{(v_n(t+\tau)^{1-\gamma} + \omega * v_n(t)^{2*(1-\gamma)}) * \tau}\right)}$$

$$SH_n(t) = L_{n-1} - v_{n-1}(t) * \tau + v_n(t) * \tau + \frac{\tau}{2} * \left(v_n(t+\tau) - v_n(t)\right) + v_n(t) * \sigma$$

$$* \sqrt{-2 * ln\left(\frac{2 * v_n(t) * \sqrt{2 * \pi} * \sigma * v_n(t+\tau)^{-\gamma} * (1-\gamma)}{(v_n(t+\tau)^{1-\gamma} + \omega * v_n(t)^{2*(1-\gamma)}) * \tau}\right)}$$

$$SH_n(t) = L_{n-1} - v_{n-1}(t) * \tau + \frac{\tau}{2} * \left(v_n(t+\tau) + v_n(t)\right) + v_n(t) * \sigma$$

$$* \sqrt{-2 * ln\left(\frac{2 * v_n(t) * \sqrt{2 * \pi} * \sigma * v_n(t+\tau)^{-\gamma} * (1-\gamma)}{(v_n(t+\tau)^{1-\gamma} + \omega * v_n(t)^{2*(1-\gamma)}) * \tau}\right)}$$

APPENDIX B: STATA CODE FOR DATA PROCESSING

```
set more off
gen dvelocitym=.
local N=_N-1
forvalues I=2/`N'{
 if id[`I']==id[`I'+1]&id[`I']==id[`I'1]&time[`I']==time[`I'1]+1
    &time[`I']==time[`I'+1]-1{
    replace dvelocitym=(localym[`I'+1]-localym[`I'-1])/0.2 if _n==`I'
    }
}

merge m:1 leader time using C:\THESIS\Estimation\Micro\0.1-
2secondsdifferenciatefromlocationthensmooth\Method\1Differenciatefromlocatio
n\3-3leaderinformationformergeusing.dta
drop if _merge==2
drop _merge
sort id time

gen dspacingm=.
replace dspacingm=llocalym-localym

set more off
```

```
gen reactiontime=.
forvalues i=1/20{
   replace reactiontime=time+`i'  //anticipated velocity
   merge m:1 id reactiontime using C:\THESIS\Estimation\Micro\0.1-
   2secondsdifferenciatefromlocationthensmooth\Method\1Differenciatefromloca
   tion\3-5anticipatedvelocityformergeusing.dta
   rename dvelocitym dvelocitym`i'
   drop if _merge==2
   drop _merge
   sort id time
}

merge m:1 leader time using C:\THESIS\Estimation\Micro\0.1-
2secondsdifferenciatefromlocationthensmoothseparately-
supportedbypaper\2Smoothseparately\Method\3-3-2-
1leaderinformationformergeusing.dta
drop if _merge==2
drop _merge
sort id time

set more off
gen reactiontime=.
forvalues i=1/20{
```

```
    replace reactiontime=time+`i'  //anticipated velocity
    merge m:1 id reactiontime using C:\THESIS\Estimation\Micro\0.1-2secondsdifferenciatefromlocationthensmoothseparately-supportedbypaper\2Smoothseparately\Method\3-3-2-2anticipatedvelocityformergeusingforeachvehicle.dta
    rename sdvelocitym sdvelocitym`i'
    drop if _merge==2
    drop _merge
    sort id time
}

set more off
gen sdvelocitym=.
local M=0   //the last row of previous vehicle group
local T=_N  // total rows of all vehicle groups
local L=1   // the first row of current vehicle group
local H=0   // the last row of current vehicle group
while `H'!=`T'{
    local N=1  // counter of rows of current vehicle group
    while id[`M'+`N']==id[`M'+`N'+1]&time[`M'+`N']==time[`M'+`N'+1]-1
    {   //smooth for each vehicle in consecutive time supported by the paper
        local N=`N'+1
    }
```

```
    local H=`M'+`N'
    forvalues I=`L'/`H'{
        local D=min(30,`I'-`M'-1,`H'-`I')
        //30=3*10(delta=smoothing width)
        //10=1(T=smoothingtimes)/0.1(dt=time interval)
        scalar nu=0
        scalar de=0
        local X=`I'-`D'
        local Y=`I'+`D'
        forvalues J=`X'/`Y'{
            scalar nu=nu+dvelocitym[`J']*exp(-abs(`I'-`J')/10)  //delta=10
            scalar de=de+exp(-abs(`I'-`J')/10)   //delta=10
        }
        replace sdvelocitym=nu/de if _n==`I'
    }
    local M=`H'   // update the last row
    local L=`M'+1  // update the first row
}

set more off
gen slocalym=.
local M=0   //the last row of previous vehicle group
local T=_N  // total rows of all vehicle groups
```

```
local L=1   // the first row of current vehicle group
local H=0   // the last row of current vehicle group
while `H'!=`T'{
   local N=1  // counter of rows of current vehicle group
   while id[`M'+`N']==id[`M'+`N'+1]&time[`M'+`N']==time[`M'+`N'+1]-1{
   //smoothen for each vehicle and consecutive time
      local N=`N'+1
   }
   local H=`M'+`N'
   forvalues I=`L'/`H'{
      local D=min(15,`I'-`M'-1,`H'-`I')  //delta=0.5/dt=5
      scalar nu=0
      scalar de=0
      local X=`I'-`D'
      local Y=`I'+`D'
      forvalues J=`X'/`Y'{
         scalar nu=nu+localym[`J']*exp(-abs(`I'-`J')/5)   //delta=5
         scalar de=de+exp(-abs(`I'-`J')/5)   //delta=5
      }
      replace slocalym=nu/de if _n==`I'   //1second smoothing width
   }
   local M=`H'   // update the last row
   local L=`M'+1  // update the first row
```

```
}

merge 1:1 id time using 3-4-2lengthinformation.dta

keep if sdspacingm>llengthm
```

APPENDIX C: STATA CODE FOR MODEL CALIBRATION

```
set more off
gen nclass=.
gen nlclass=.
replace nclass=1 if lengthm>2.0574&lengthm<=6.7056
replace nclass=2 if lengthm>6.7056
replace nlclass=1 if llengthm>2.0574&llengthm<=6.7056
replace nlclass=2 if llengthm>6.7056
gen headway=sdspacingm/sdvelocitym
gen I=.
gen Obs=.
gen R2=.
gen RMSE=.
gen Sigma_iv=.
gen Sigma=.
gen Sigma_se=.
gen Sigma_t=.
gen Sigma_pvalue=.
gen Gamma_iv=.
gen Gamma=.
gen Gamma_se=.
```

```
gen Gamma_t=.
gen Gamma_pvalue=.
gen W_iv=.
gen W=.
gen W_se=.
gen W_t=.
gen W_pvalue=.
keep if nclass==1&nlclass==1&sdvelocitym!=0&headway>=1&headway<=3
forvalues i=1/20 {
   preserve
   keep if sdvelocitym`i'!=.&sdvelocitym`i'!=0
   local N=_N
   set obs `N'
   set seed 1234
   gen rn=runiform()
   keep if rn>0.3
   local n=`i'
   local t=`i'/10
   local rmse=10
   local Sigma=1
   local Gamma=0.5
   forvalues W=500(500)15000 {
      capture nl(sdspacingm=0.5*(sdvelocitym`i'-sdvelocitym)*`t'+llengthm-
```

```
(lsdvelocitym-sdvelocitym)*`t'+sdvelocitym*{sigma}*sqrt(-
2*ln(sdvelocitym`i'^(-{gamma})*(1-
{gamma})*sqrt(2*3.1415926)*2*sdvelocitym*{sigma}/((sdvelocitym`i'^(1-
{gamma})+{w}*sdvelocitym^(2-2*{gamma}))*`t')))), iter(100) in(sigma
`Sigma' gamma `Gamma' w `W')
if e(converge)==1&_rc!=480 {
    if e(rmse)<`rmse' {
        local obs=e(N)
        local r2=e(r2)
        local rmse=e(rmse)
        local sigmaiv=`Sigma'
        local gammaiv=`Gamma'
        local wiv=`W'
        local sigma=_b[/sigma]
        local gamma=_b[/gamma]
        local w=_b[/w]
        local sigmase=_se[/sigma]
        local sigmat=`sigma'/_se[/sigma]
        local sigmapvalue=2*ttail(e(df_r),abs(`sigma'/_se[/sigma]))
        local gammase=_se[/gamma]
        local gammat=`gamma'/_se[/gamma]
        local gammapvalue=2*ttail(e(df_r),abs(`gamma'/_se[/gamma]))
        local wse=_se[/w]
```

```
            local wt=`w'/_se[/w]

            local wpvalue=2*ttail(e(df_r),abs(`w'/_se[/w]))

        }

    }

}

restore

capture {

    replace I=`i' in `n'

    replace Obs=`obs' in `n'

    replace R2=`r2' in `n'

    replace RMSE=`rmse' in `n'

    replace Sigma_iv=`sigmaiv' in `n'

    replace Sigma=`sigma' in `n'

    replace Sigma_se=`sigmase' in `n'

    replace Sigma_t=`sigmat' in `n'

    replace Sigma_pvalue=`sigmapvalue' in `n'

    replace Gamma_iv=`gammaiv' in `n'

    replace Gamma=`gamma' in `n'

    replace Gamma_se=`gammase' in `n'

    replace Gamma_t=`gammat' in `n'

    replace Gamma_pvalue=`gammapvalue' in `n'

    replace W_iv=`wiv' in `n'

    replace W=`w' in `n'
```

```
        replace W_se=`wse' in `n'
        replace W_t=`wt' in `n'
        replace W_pvalue=`wpvalue' in `n'
    }
}
```

APPENDIX D: STATA CODE FOR MODEL VALIDATION

```
set more off
gen nclass=.
gen nlclass=.
replace nclass=1 if lengthm>2.0574&lengthm<=6.7056
replace nclass=2 if lengthm>6.7056
replace nlclass=1 if llengthm>2.0574&llengthm<=6.7056
replace nlclass=2 if llengthm>6.7056
gen headway=sdspacingm/sdvelocitym
gen RMSE=.
gen R2=.
keep if nclass==2&nlclass==2&sdvelocitym!=0&headway>=1&headway<=5
local i=6
keep if sdvelocitym`i'!=.&sdvelocitym`i'!=0
local N=_N
set obs `N'
set seed 1234
gen rn=runiform()
keep if rn<=0.3
local t=`i'/10
local sigma=1.412753
local gamma=.67014921
```

```
local w=2.665385
gen espacingm=0.5*(sdvelocitym`i'-sdvelocitym)*`t'+llengthm-(lsdvelocitym-sdvelocitym)*`t'+sdvelocitym*`sigma'*sqrt(-2*ln(sdvelocitym`i'^(-`gamma')*(1-`gamma')*sqrt(2*3.1415926)*2*sdvelocitym*`sigma'/((sdvelocitym`i'^(1-`gamma')+`w'*sdvelocitym^(2-2*`gamma'))*`t')))
egen Mean=mean(sdspacingm)
egen SSM=total((espacingm-Mean)^2)
egen SST=total((sdspacingm-Mean)^2)
egen SSR=total((espacingm-sdspacingm)^2)
count if rn<=0.3
local RN=r(N)
replace RMSE=sqrt(SSR/`RN')
replace R2=SSM/SST
```

APPENDIX E: C++ CODE FOR MODEL SIMULATION

```
//My CF model
bool behavioralModelParticular::evaluateCarFollowing(A2SimVehicle *vehicle,
double &newpos, double &newspeed)
{
   double speed = vehicle->getSpeed(vehicle->isUpdated());
   double offset = -1;
   A2SimVehicle *vleader = vehicle->getLeader(offset);
   double leaderlength = vleader->getLength();
   double length = vehicle->getLength();
   double leaderspeed = vleader->getSpeed(vleader->isUpdated());
   double spacing = vleader->getPosition(vleader->isUpdated()) –
                      vehicle->getPosition(vehicle->isUpdated());
   double gap = spacing - leaderlength;
   newspeed = vehicle->getAimsunCarFollowingSpeed();
   if (gap >= 3 && gap <= 50 && leaderspeed >= 1 && leaderspeed <= 20
   && speed >= 1 && speed <= 20) {
      if (length >= 2.0574&&length <= 6.7056) {
         if (leaderlength >= 2.0574&&leaderlength <= 6.7056 && 5 * gap + 3 *
         leaderspeed + 5 - 10 * speed > 0 && 0.532*gap + 0.319*leaderspeed –
         2.107 - speed < 0) {
            double t = 0.6;
```

```
        double s = 1.047;
        double r = 0.725;
        double w = 3.476;
        newspeed = (2 / t)*(spacing - speed * s*sqrt(-2 * log(5.01326*s*(1 - r)
        / ((1 + w * pow(speed, 1 – r))*t))) - leaderlength) + 2 * leaderspeed –
        speed;
    }
    if (leaderlength > 6.7056&&0.44*gap + 0.22*leaderspeed + 0.92 –
    speed > 0 && 2 * gap + leaderspeed - 5 - 4 * speed < 0) {
        double t = 0.5;
        double s = 1.538;
        double r = 0.65;
        double w = 4.559;
        newspeed = (2 / t)*(spacing - speed * s*sqrt(-2 * log(5.01326*s*(1 - r)
        / ((1 + w * pow(speed, 1 - r))*t))) - leaderlength) + 2 * leaderspeed –
        speed;
    }
}
if (length > 6.7056) {
    if (leaderlength >= 2.0574&&leaderlength <= 6.7056&&0.476*gap +
    0.238*leaderspeed + 0.954 - speed > 0 && 0.495*gap +
    0.2475*leaderspeed - 0.96 - speed < 0 && speed >= 1.1) {
        double t = 0.5;
```

```
            double s = 1.217;
            double r = 0.512;
            double w = 4.929;
            newspeed = (2 / t)*(spacing - speed * s*sqrt(-2 * log(5.01326*s*(1 - r)
            / ((1 + w * pow(speed, 1 - r))*t))) - leaderlength) + 2 * leaderspeed –
            speed;
        }
        if (leaderlength > 6.7056&&0.526*gap + 0.3156*leaderspeed + 1.0024 –
        speed > 0 && 0.476*gap + 0.238*leaderspeed - 0.236 - speed < 0) {
            double t = 0.6;
            double s = 1.413;
            double r = 0.67;
            double w = 2.665;
            newspeed = (2 / t)*(spacing - speed * s*sqrt(-2 * log(5.01326*s*(1 - r)
/ ((1 + w * pow(speed, 1 - r))*t))) - leaderlength) + 2 * leaderspeed - speed;
        }
      }
    }
    newpos = vehicle->getPosition(vehicle->isUpdated()) + newspeed *
    getSimStep();
    return true;
}
```